The Dissertation Committee for Rebecca Elizabeth Morrison
certifies that this is the approved version of the following dissertation:

On the Representation of Model Inadequacy: A Stochastic Operator Approach

Committee:

Robert D. Moser, Supervisor

J. Tinsley Oden

Omar Ghattas

Graeme Henkelman

Todd A. Oliver

Christopher S. Simmons

On the Representation of Model Inadequacy: A Stochastic Operator Approach

by

Rebecca Elizabeth Morrison, B.A.; M.S.C.A.M.

DISSERTATION

Presented to the Faculty of the Graduate School of

The University of Texas at Austin

in Partial Fulfillment

of the Requirements

for the Degree of

DOCTOR OF PHILOSOPHY

THE UNIVERSITY OF TEXAS AT AUSTIN

May 2016

To my parents, Kent and Estelle

Acknowledgments

I would first like to thank the Institute of Computational Sciences and Engineering and especially the Center for Predictive Engineering and Computational Science (PECOS) at The University of Texas at Austin. They provided an excellent graduate program with committed professors, outstanding research, and a warm and encouraging environment. In particular, this work was supported by DiaMonD: An Integrated Multifaceted Approach to Mathematics at the Interfaces of Data, Models, and Decisions. DiaMonD is a U.S. Department of Energy Mathematical Multifaceted Integrated Capabilities Center (MMICC).

I would like to thank my advisor, Dr. Robert Moser, for all of the discussions, insights, and encouragement that made this work possible. The road ahead always seemed a little clearer after our meetings. Dr. J. Tinsley Oden was incredibly influential and supportive of forging through the still murky world of validation and uncertainty quantification (UQ). I'd also like to thank Drs. Omar Ghattas and Graeme Henkelman for helpful suggestions about optimization and chemistry, respectively. Drs. Todd Oliver and Chris Simmons were particularly helpful in setting up the framework of the research problem and understanding combustion, numerics, and the long term goals of the project from the beginning.

Much of this thesis relied on work done by the PECOS team. I'd like to thank Dr. Damon McDougall for his frequent help with the statistical inversion library

QUESO, and Drs. Sylvain Plessis, Paul Bauman, and Varis Carey for immediate responses about the chemistry library ANTIOCH. Although not directly related to this thesis, the time spent working with Dr. Serge Prudhomme was valuable and formative for my graduate career.

Thanks are extended to Dr. Corey Bryant for always enjoying a good argument about anything in UQ, to Dr. Rhys Ulerich for the C++ help I didn't even know I needed, to Dr. Andrea Hawkins-Daarud for just about everything, and to Dr. Myoungkyu Lee for remembering that the physics is as important as the mathematics, sometimes. I'd also like to thank Prakash Mohan for countless discussions about programming best-practices, debugging, and staying calm under pressure. Thanks to Dr. Omar Al-Hinai for keeping me and the other graduate students smiling and well-fed.

And finally, thank you to my family and friends, if not already mentioned above. Elizabeth, Hannah, Mesh, Peter, Sally, Silver, Sofia: you're the best.

On the Representation of Model Inadequacy: A Stochastic Operator Approach

Rebecca Elizabeth Morrison, Ph.D.
The University of Texas at Austin, 2016

Supervisor: Robert D. Moser

Mathematical models of physical systems are subject to many sources of uncertainty such as measurement errors and uncertain initial and boundary conditions. After accounting for these uncertainties, it is often revealed that there remains some discrepancy between the model output and the observations; if so, the model is said to be inadequate. In practice, the inadequate model may be the best that is available or tractable, and so despite its inadequacy the model may be used to make predictions of unobserved quantities. In this case, a representation of the inadequacy is necessary, so the impact of the observed discrepancy can be determined. We investigate this problem in the context of chemical kinetics and propose a new technique to account for model inadequacy that is both probabilistic and physically meaningful. Chemical reactions are generally modeled by a set of nonlinear ordinary differential equations (ODEs) for the concentrations of the species and temperature. In this work, a stochastic inadequacy operator $\mathcal{S}$ is introduced which includes three parts. The first is represented by a random matrix S which is embedded within the ODEs of the concentrations. The matrix is required to satisfy several physical constraints,

and its most general form exhibits some useful properties, such as having only non-positive eigenvalues. The second is a smaller but specific set of nonlinear terms that also modifies the species' concentrations, and the third is an operator that properly accounts for changes to the energy equation due to the previous changes. The entries of $\mathcal{S}$ are governed by probability distributions, which in turn are characterized by a set of hyperparameters. The model parameters and hyperparameters are calibrated using high-dimensional hierarchical Bayesian inference, with data from a range of initial conditions. This allows the use of the inadequacy operator on a wide range of scenarios, rather than correcting any particular realization of the model with a corresponding data set. We apply the method to typical problems in chemical kinetics including the reaction mechanisms of hydrogen and methane combustion. We also study how the inadequacy representation affects an unobserved quantity of interest—the flamespeed of a one-dimensional hydrogen laminar flame.

Table of Contents

Glossary

- n: number of species in a chemical mechansim
- m: number of reactions in a chemical mechansim
- A: prefactor constant in an Arrhenius type expression
- E: energy constant in an Arrhenius type expression
- b: temperature exponent in a modified Arrhenius expression
- R°: universal gas constant
- k_i^f: forward rate coefficient of ith reaction, $k(T) = AT^b \exp\left(-E/R^{\circ}T\right)$
- k_i^b: backward rate coefficient of ith reaction
- x_i: concentraton of ith species
- $\mathbb{X}_i$: the ith species
- $\boldsymbol{x}$: vector of species' molar concentrations
- $\boldsymbol{y}$: vector of species' atomic concentrations
- T: temperature [K]
- $\mathfrak{D}$: detailed model
- $\mathfrak{R}$: reduced model
- C: conservation matrix
- P: probabilistic matrix
- S: stochastic atom matrix, $S = CP$
- L: concentration to atom map

- $\hat{S}$: stochastic concentration matrix, $\hat{S} = L^{-1}SL$
- W: stochastic temperature matrix
- $\mathcal{A}$: stochastic nonlinear catchall operator
- $\mathcal{S}$: stochastic inadequacy operator, $\mathcal{S} = \hat{S} + \mathcal{A} + W$
- $\mathcal{O}$: operator model, $\mathcal{O} = \mathcal{R}^S + \mathcal{S}$
- $\rho_{\mathbb{X}_i}$: modified prime number representation of species $\mathbb{X}_i$
- λ_i: number of species $\mathbb{X}_j$ such that $\gcd(\rho_{\mathbb{X}_i}, \rho_{\mathbb{X}_j}) < \rho_{\mathbb{X}_i}$
- Ω: number of zeros in S
- $\boldsymbol{k}$: set of model parameters $\boldsymbol{k} = \{\boldsymbol{A}, \boldsymbol{b}, \boldsymbol{E}\}$
- $\boldsymbol{\xi}$: transformed random variables (from matrix P)
- $\boldsymbol{\kappa}$: catchall reaction rate coefficients
- $\boldsymbol{\alpha}$: thermodynamic parameters
- $\boldsymbol{\psi}$: set of all inadequacy parameters $\boldsymbol{\psi} = \{\boldsymbol{\xi}, \boldsymbol{\kappa}, \boldsymbol{\alpha}\}$
- $\boldsymbol{\zeta}$: set of all hyperparameters
- $\boldsymbol{d}$: data set

Chapter 1

Introduction

Model inadequacy is a complex and critical issue that affects nearly all realms of computational science and engineering. In general, models of physical systems are imperfect: they rely on abstractions and simplifications which do not perfectly represent the modeled system. Sometimes the imperfections are small enough that any discrepancy between the model and observations is overshadowed by measurement error. In contrast, a model is demonstrably inadequate when the imperfections lead to a detectable inconsistency between the model and observations. It is the role of validation to detect such discrepancies: validation is the process of checking that the mathematical model and quantified uncertainties are consistent with our knowledge of the physical system [5, 6, 45]. Moreover, mathematical models are used to make predictions of unobserved quantities. To make predictions with confidence, one must first account for any inconsistency, or inadequacy, of the model. One would generally prefer to improve the model to remove the discrepancy but this is often not feasible. In this case, a representation of the inadequacy is needed, but the formulation of such a representation is very much an open problem. In this work, we propose a new technique to account for model inadequacy that is both probabilistic and physically meaningful. The method is applied to typical problems in chemical kinetics, namely the reaction mechanism models for hydrogen and methane combustion.

Chemical mechanisms and kinetics models describe the process and rates of chemical reactions [55, 61]. In general, a reaction mechanism is extraordinarily complex, even when there are only two or three initial reactants. An accurate description of the chemical processes involved in the oxidation of hydrocarbons, for example, may include hundreds or thousands of reactions and fifty or more chemical species [52, 59]. At the same time, there is significant uncertainty in the reaction rates for these reactions; recent efforts to address this include [36, 42]. Furthermore, kinetics models of these chemical mechanisms are commonly embedded within a larger fluids calculation to represent combustion. The chemical dynamics must then be solved at every point in space and time. Because the computational cost of such detailed mechanisms is so high, it is common practice to use drastically reduced mechanisms. However, errors introduced by the reduced models may render the model inadequate even if the detailed model it is based on is not. This work is concerned with quantifying the uncertainty and accounting for the inadequacy resulting from the use of a reduced model.

Therefore, in using a reduced kinetics model, several sources of uncertainty arise: uncertain kinetics parameters, uncertainty introduced by the use of a reduced model, and measurement errors. A natural framework to deal with multiple uncertainties is Bayesian probability [33, 47]. The Bayesian interpretation of probability determines the probability of an event based on the degree of knowledge about the system in question. In contrast to the frequentist approach, this interpretation does not rely on historical or repeatable events to calculate probabilities. This interpretation also provides a natural framework to calibrate a set of parameters given a

set of observations, called Bayesian inference. There are many good references on Bayesian inference such as [13, 33, 51]. For two random variables x and y, and their probability distributions $p(x)$ and $p(y)$, Bayes' Theorem is: $p(x|y) = \frac{p(y|x)p(x)}{p(y)}$. This can be used for calibration by interpreting x to represent the parameter to be calibrated and y as an observation. Thus, Bayes' Theorem provides the probabilistic connection between the observations and the parameters. The term $p(x|y)$ is called the posterior distribution, which is the conditional distribution of the parameter x given the observed value y, and is therefore the sought result of the calibration.

As mentioned above, if a chemical kinetics model is inadequate, it would be best to improve the kinetics model directly to eliminate the inadequacy. Indeed, refinement of chemical mechanisms in combustion is an active topic of research; for a small sample focused on H_2/O_2 reactions, see [11, 12, 15, 46]. However, as mentioned above, this type of refinement is commonly not an option. Instead, we seek to develop a mathematical representation to account for the discrepancy between the model and the observations, i.e. the model inadequacy. A common approach is to pose a purely statistical model of the discrepancy. The classical framework for this approach was developed by Kennedy and O'Hagan in 2001 [35]. Although this method is widely applicable and often successful (see for example [6, 31, 32, 56]), the structure of the Kennedy and O'Hagan representation precludes its use to characterize the impact of inadequacy on predictions of an unobserved quantity.

In this work, inadequacy representations will be developed for use with a general class of reaction mechanism models. A reaction is modeled by describing the time derivative of the species' concentrations and temperature. In short, the

model consists of a set of nonlinear ordinary differential equations. The complexity of each differential equation depends on the number and type of the elementary reactions included in the detailed reaction mechanism. In this work, a reduced model is adopted that models a subset of the species with a reduced number of elementary or global (aggregate) reactions. Such reduced models are commonly found in the combustion literature [12, 59, 62].

We generally have qualitative and quantitative information about the phenomena being modeled which impose constraints on the inadequacy representation. Exploiting this information should lead to a more reliable formulation, especially for making predictions. Imposing these physical constraints requires that the representation of inadequacy depends on the physical problem. In the context of chemical kinetics, the appropriate constraints are conservation of atoms, conservation of energy, and nonnegativity of concentrations. In this work, these constraints are built into the inadequacy formulation and, thus, are always held true. Moreover, the inadequacy representation is introduced where the actual inadequacy occurs. That is, it is embedded within the existing reduced model and the two are linked together. The implication of this for the Bayesian inference is that the reduced model and the inadequacy representation must be calibrated simulataneously. This is in contrast to calibrating the reduced model first, calibrating an inadequacy model later, and then stitching the two together.

The method proposed here is a stochastic representation of the inadequacy, formulated as an operator $\mathcal{S}$. The main component of this operator is additive, linear, and probabilistic, encoded in the random matrix S. The use of the term *random*

matrix implies that each entry is characterized by a probability distribution. This is consistent with the definition of random matrices from random matrix theory (see [18, 41]), although in that field a random matrix is usually much less constrained than in the present case, and its properties (such as the distributions of the eigenvalues) are found in the limit as the size of the matrix goes to infinity. A few applications of random matrices to engineering problems are presented by Soize [53, 54]. However, this work also differs from our approach in that the probability of a given matrix is characterized by properties of the entire matrix, such as the determinant, whereas we consider the independent distributions of each nonzero entry. Moreover, the inadequacy operator $\mathcal{S}$ may include more general effects in addition to or instead of the random matrix, such as nonlinearities or multiple matrices.

The parameters in the stochastic inadequacy operator $\mathcal{S}$ are uncertain because the exact form of the inadequacy is unknown. Because of this, the inadequacy parameters of the inadequacy representation are in fact characterized as distributions, yielding a stochastic forward problem. Each distribution is characterized by a corresponding set of hyperparameters. Thus, to fully describe the inadequacy model, it is necessary to calibrate these hyperparameters. And, since the inadequacy model is calibrated simultaneously with the reduced model, the task is now to infer the reduced model kinetics parameters and the hyperparameters of the inadequacy model. The method used to do this is called Hierarchical Bayesian Modeling (HBM). In [8], Berliner describes this method as a form of Bayesian inference in which one works directly with conditional distributions, which is advantageous because it is often easier to understand and to sample from conditional distributions (as opposed to a

full joint distribution). This method has been reinterpreted to apply to the stochastic forward problem at hand, i.e. to simultaneously calibrate the reduced model and the stochastic inadequacy operator. The conditional distributions of Berliner's work appear here as the conditional distributions of the inadequacy parameters given their hyperparameters.

After calibration, the process of validation checks that the model output is consistent with the observations. In this work, the validation must account for any sources of uncertainty, including the stochastic forward problem, uncertain model parameters, and measurement error. The approach used here, called posterior predictive assessment [24, 49], calculates how plausible it is that the value of an observation is output of the calibrated, albeit uncertain, model.

The rest of the thesis is organized as follows. In chapter 2, we describe the basics of kinetics modeling. In chapter 3, the general formulation and properties of the stochastic operator are presented. Chapter 4 describes the Bayesian framework for calibration and validation of the various models, including hierarchical Bayesian modeling and validation under uncertainty. In chapter 5, the above is applied to the specific cases of hydrogen and methane combustion. This chapter also includes the description of the flame problem and the flamespeed prediction. Concluding remarks are given in chapter 6.

Chapter 2

Chemical Kinetics

Chemical mechanisms and kinetics models describe the process and rates of chemical reactions. In a typical chemical reaction, there is a set of reactant species which, after a complex series of intermediate reactions, ultimately form the chemical products. These intermediate steps, in which chemical species react directly with each other, are called elementary reactions. The set of elementary reactions is called the reaction mechanism, and a typical combustion problem may include tens to thousands of elementary reactions. The following section presents common variations of a generalized chemical mechanism model and derives the corresponding mathematical models.

2.1 A general chemical mechanism model

First we consider a general chemical mechanism including n species and m reactions. For references, a useful text on general chemical kinetics is [55], while [61] provides a more detailed overview of combustion. The molar concentrations of the species are denoted x_1, x_2, ..., x_n; the set of these is $\boldsymbol{x}$.

2.1.1 Elementary reactions

Consider the following mechanism with four species and two elementary reactions:

$$\mathrm{A} + \mathrm{B} \xrightarrow{k_1} \mathrm{C} \tag{2.1}$$

$$\mathrm{A} + \mathrm{C} \xrightarrow{k_2} \mathrm{D}, \tag{2.2}$$

where k_1 and k_2 are called the rate coefficients. Let $\boldsymbol{x} = [x_1, x_2, x_3, x_4]^T$ be the vector of molar concentrations corresponding to species A, B, C, D. In the differential equation describing the evolution of the species' concentrations, each elementary reaction is a sink for the reactant species and a sources for the product species. The rate of each reaction is often modeled as linear in the concentration of the reactants, although this power, or order, associated with a given species may be non-unity. With the assumption that it is linear in each species, the forward rate expressions of the two reactions are thus

$$r_1 = k_1 x_1 x_2 \tag{2.3}$$

$$r_2 = k_2 x_1 x_3, \tag{2.4}$$

and the ODE's describing the time derivatives of the species' molar concentrations are:

$$\dot{x}_1 = -r_1 - r_2 \tag{2.5}$$

$$\dot{x}_2 = -r_1 \tag{2.6}$$

$$\dot{x}_3 = +r_1 - r_2 \tag{2.7}$$

$$\dot{x}_4 = +r_1. \tag{2.8}$$

Note that, for a general variable a, the notation $\dot{a} = \frac{da}{dt}$ is used.

2.1.2 Global reactions

Although a true chemical reaction proceeds in terms of elementary reactions, it is common to reduce the number of reactions by using a global reaction, i.e. an aggregate reaction that in fact represents multiple elementary reactions. For example, consider the the net effect of the two elementary reactions (2.1) and (2.2). Species C is created but then used up (it "cancels" when combining equations) and the net effect is represented by the global reaction:

$$2\,\mathrm{A} + \mathrm{B} \xrightarrow{k} \mathrm{D}. \tag{2.9}$$

To model this global reaction, the global rate is $r = kx_1x_2$; the ODEs reflect the factor of two:

$$\dot{x}_1 = -2r \tag{2.10}$$

$$\dot{x}_2 = -r \tag{2.11}$$

$$\dot{x}_4 = +r. \tag{2.12}$$

Since two molecules of A react with every one of B, the rate at which A is used up is twice as fast. In chapter 5, two types of reduced models are investigated. In the first example on hydrogen combustion, the reduced mechanism is a subset of the elementary reactions of the detailed model. In the second example on methane combustion, the reduced model is made up of a small number of global reactions, each of which represents many elementary ones. Although the method of reduction

is different, the overall structure of the reduced model is still essentially the same—a collection of reactions which yield a set of nonlinear ODEs.

2.1.3 Stoichiometry

The stoichiometry of a chemical reaction describes the quantitative relation between reactants and products.[1] For a general reaction,

$$\mathrm{n_A A} + \mathrm{n_B B} \xrightarrow{k_1} \mathrm{n_S S} + \mathrm{n_T T}, \tag{2.13}$$

where A and B are the chemical reactants, S and T are the chemical products, and n_A, n_B, n_S, n_T are called the stoichiometric coefficients. This work will mostly be concerned with the stoichiometric ratio in a reaction between a fuel (hydrogen, methane) and an oxidizer (oxygen, air). Then the stochiometric ratio is the ratio of initial concentrations of fuel to oxidizer in which all the fuel is consumed and there is no deficiency of fuel.

Let $x_{f_{STO}}$ and $x_{f_{STO}}$ be the stoichiometric concentrations of fuel and oxidizer at time $t = 0$, and for a given reaction, let x_f and x_o be the initial concentrations of fuel and oxidizer. The initial condition of the reaction is then characterized by the equivalence ratio ϕ which measures how far the ratio of fuel to oxidizer deviates from the stoichiometric case:

$$\phi = \frac{x_f/x_o}{x_{f_{STO}}/x_{o_{STO}}}. \tag{2.14}$$

[1]The term stoichiometry also refers to the branch of chemistry which involves calculating quantities of the chemical elements involved in a reaction.

Note that $\phi = 1$ is the stoichiometric case, $\phi < 1$ indicates a fuel-lean system, while $\phi > 1$ indicates a fuel-rich system.

2.1.4 Reversible reactions

In all the examples above, the reaction only proceeds in one direction (the arrow only points to the right) and so only a forward rate is given. This type of reaction is called irreversible. However, many reactions are in fact reversible, in which case the product species may also react to form the reactants. The example mechanism with reversible reactions is written as:

$$\mathrm{A} + \mathrm{B} \underset{k_1^b}{\overset{k_1^f}{\rightleftharpoons}} \mathrm{C} \tag{2.15}$$

$$\mathrm{A} + \mathrm{C} \underset{k_2^b}{\overset{k_2^f}{\rightleftharpoons}} \mathrm{D}, \tag{2.16}$$

where the f and b stand for forward and backward, respectively. The forward rates are the same as before (except r_i and k_i are now written r_i^f and k_i^f). The backward rates are then

$$r_1^b = k_1^b x_3 \tag{2.17}$$

$$r_2^b = k_2^b x_4, \tag{2.18}$$

and the ODEs for the molar concentrations become

$$\dot{x}_1 = -r_1^f + r_1^b - r_2^f + r_2^b \tag{2.19}$$

$$\dot{x}_2 = -r_1^f + r_1^b \tag{2.20}$$

$$\dot{x}_3 = +r_1^f - r_1^b - r_2^f + r_2^b \tag{2.21}$$

$$\dot{x}_4 = +r_2^f - r_2^b. \tag{2.22}$$

2.1.5 Nonlinear rates

So far, it has been assumed that each rate depends linearly on each reactant and product species. However, it may be that another order is specified. Suppose the mechanism structure is the same as above, but the forward orders for A and B are 3/2 and 1/4, while the backward order for C is 2. The order of a species for a given reaction is often assumed to be the same as the stoichiometric coefficient. However, this is not true in general; in this work, the order and stoichiometric coefficients will always be specified separately. For the forward and backward orders of the two reactions, we write

$$\boldsymbol{o}_1^f = [3/2, 1/4, 0, 0] \tag{2.23}$$

$$\boldsymbol{o}_1^b = [0, 0, 2, 0] \tag{2.24}$$

$$\boldsymbol{o}_1^f = [1, 1, 0, 0] \tag{2.25}$$

$$\boldsymbol{o}_1^b = [0, 0, 0, 1]. \tag{2.26}$$

It is often convenient to combine these into a vector $\boldsymbol{\nu}_r$ for each reaction r: $\boldsymbol{\nu}_r = \boldsymbol{o}_r^f - \boldsymbol{o}_r^b$. Now the rates take the form

$$r_1^f = k_1^f x_1^{3/2} x_2^{1/4} \tag{2.27}$$

$$r_1^b = k_1^b x_3^2 \tag{2.28}$$

$$r_2^f = k_2^f x_1 x_2 \tag{2.29}$$

$$r_2^b = k_2^b x_4. \tag{2.30}$$

This concludes the kinetics mechanism modeling. The next sections cover the empirical rate laws and thermodynamics.

2.2 Rate coefficient models $k(T)$

In general, the rate coefficient k is a function of temperature, and it may follow a given empirical form depending on the specific reaction. A common form is the Arrhenius Law,

$$k(T) = Ae^{-E/R^\circ T}, \tag{2.31}$$

for some prefactor A, energy coefficient E, and universal gas constant R°. Another common form is the modified Arrhenius,

$$k(T) = AT^b e^{-E/R^\circ T}, \tag{2.32}$$

with the additional constant b.

The Arrhenius or modified Arrhenius forms are often found in the literature to describe the forward rate coefficient, and this is the case in all examples considered in this work. However, the backwards rate coefficients are usually not specified. Instead, these can be computed using thermodynamic information. This is presented at the end of the following section.

2.3 Thermodynamics

In most of the reactions considered here, volume is held fixed, while pressure and temperature are not. (This is true for all reactions except that of the flame problem in § 5.3.) The evolution of the temperature must be modeled through an energy conservation equation. Indeed, combustion is characterized by a large release of heat and we want to be able to model this. To do so, it is necessary to introduce some thermodynamic quantities:

- p: Pressure [J/m^3]
- v: Volume [m^3]
- T: Temperature [K]
- R°: Universal gas constant [J/K/mol]
- C_v: Specific heat of the system at constant volume [J/K]
- C_p: Specific heat of the system at constant pressure [J/K]
- c_{v_i}: Specific heat of species i at constant volume [J/K/mol]
- c_{p_i}: Specific heat of species i at constant pressure [J/K/mol]
- U: Total heat of the system [J]
- H: Enthalpy [J]
- S: Entropy [J]
- $\Delta_r G$: Gibbs free energy of reaction r [J/mol]
- u_i: Internal energy of species i [J/mol]
- h_i: Enthalpy of species i [J/mol]
- s_i: Entropy of species i [J/mol]
- g_i: Gibbs free energy of species i [J/mol].

2.3.1 Energy equation

Temperature changes occur due to the difference in chemical energy between the reactants and products. To model this, we start by describing the internal energy U of an ideal gas. In an ideal gas, the internal energy depends only on temperature (not v or p) and the species' concentrations:

$$U(T, \boldsymbol{x}) = \sum_i u_i(T) x_i, \tag{2.33}$$

and so

$$\frac{dU}{dt} = \sum_i \frac{\partial u_i}{\partial t} x_i + u_i \frac{\partial x_i}{\partial t} \tag{2.34}$$

$$= \sum_i c_{v_i} \frac{\partial T}{\partial t} x_i + u_i \frac{\partial x_i}{\partial t} \tag{2.35}$$

$$= \frac{\partial T}{\partial t} \sum_i c_{v_i} x_i + u_i \frac{\partial x_i}{\partial t}. \tag{2.36}$$

But since volume is constant, no work is done on the system, and the change in energy U is zero. Setting dU/dt to zero and solving for dT/dt yields

$$\frac{dT}{dt} = -\left(\frac{1}{\sum_i c_{v_i} x_i}\right)\left(\sum_i u_i \dot{x}_i\right). \tag{2.37}$$

Note that $\frac{dT}{dt}$ is a function of both the molar concentrations and their time derivatives. The remaining quantities c_v (or c_p) and u (or h) are found in the literature along with entropy s. Usually, a set of seven to nine constants are given which specify each quantity as a function of temperature. For example, the so-called NASA polynomials

have the following form [40]:

$$c_p/R^\circ = a_1 + a_2T + a_3T^2 + a_4T^3 + a_5T^4 \tag{2.38}$$

$$h/R^\circ T = a_1 + \frac{a_2}{2}T + \frac{a_3}{3}T^2 + \frac{a_4}{4}T^3 + \frac{a_5}{5}T^4 + \frac{a_6}{T} \tag{2.39}$$

$$s/R^\circ T = a_1 \ln T + a_2T + \frac{a_3}{2}T^2 + \frac{a_4}{3}T^3 + \frac{a_5}{4}T^4 + a_7, \tag{2.40}$$

for some constants a_1, a_2, a_3, a_4, a_5, a_6, a_7. In the expression above, h includes the enthalpy of formation. The value of u can be found from h as $u/R^\circ T = h/R^\circ T - 1$.

2.3.2 Reverse rates

The reverse rate of a reaction can be determined using the forward rate and thermodynamic information. After sufficient time, a reaction approaches chemical equilibrium— a state in which the concentrations of the reactants and products have no tendency to change with time. Hence, the forward and reverse rates are equal. Consider a general reversible reaction:

$$\mathrm{A} + \mathrm{B} \underset{k^b}{\overset{k^f}{\rightleftharpoons}} \mathrm{S} + \mathrm{T} \tag{2.41}$$

where α, β, σ, τ are the forward and reverse orders of species A, B, S, T. Then the forward reaction rate r^f is

$$r^f = k^f A^\alpha B^\beta \tag{2.42}$$

and the reverse reaction rate r^b is

$$r^b = k^b S^\sigma T^\tau. \tag{2.43}$$

At equilibrium, these rates are equal:

$$k^f A^\alpha B^\beta = k^b S^\sigma T^\tau, \tag{2.44}$$

and the concentrations of each species are constant. Thus, the ratio of the forward to backward rate coefficients is also constant. This ratio is denoted the equilibrium constant:

$$K_{eq} = \frac{k^f}{k^b} = \frac{A^\alpha B^\beta}{S^\sigma T^\tau}. \tag{2.45}$$

Next, we want to find K_{eq} in terms of thermodynamic information. Recall $\boldsymbol{o}^f$ is the vector of forward orders, $\boldsymbol{o}^b$ that of backwards, and $\boldsymbol{\nu} = \boldsymbol{o}^f - \boldsymbol{o}^b$. In the current example,

$$\boldsymbol{\nu} = [\alpha, \beta, -\sigma, -\tau]. \tag{2.46}$$

Denote the sum of these as $\gamma = \sum_i \nu_i$. Here the equation for K_{eq} is given directly (see e.g. [1] for the full derivation):

$$K_{eq} = \left(\frac{p^0}{R^\circ T}\right)^\gamma \exp\left(-\frac{\Delta G^0(T)}{R^\circ T}\right), \tag{2.47}$$

where p^0 and $\Delta G^0(T)$ are the pressure and Gibbs free energy of the reaction at the initial state. Finally,

$$k^b = \frac{k^f}{K_{eq}}. \tag{2.48}$$

With the backward rate coefficients, the mathematical model of the reaction mechanism is complete. To summarize, there is an ODE for the time derivative of each species and also for temperature. These can be written more compactly as

$$\mathcal{F}(\boldsymbol{x}, \dot{\boldsymbol{x}}, T) = [\dot{x}_1, \dot{x}_2, \ldots, \dot{x}_n, \dot{T}]^T \tag{2.49}$$

where $\mathcal{F}$ is a general nonlinear operator consisting of the time derivatives of $\boldsymbol{x}$ and T. Note that $\mathcal{F}$ depends on $\dot{\boldsymbol{x}}$ due to the energy equation.

2.4 The detailed and reduced models

In contrast to the example mechanism in § 2.1, consisting of two elementary reactions, a typical mechanism may be unknown, or include hundreds of reactions. One of the standard references for methane combustion, for example, includes fifty-three species and 325 reactions [52]. Because this may be too computationally expensive to include within larger combustion or fluids problems, a reduced model is often used. The complete mechanism is called the detailed model $\mathcal{D}$, and is written here as $\mathcal{D}(\boldsymbol{x}^D, \dot{\boldsymbol{x}}^D, T)$.

Suppose that the detailed model includes n_D species and m_D reactions. Also, suppose that the reduced model includes n_R species and m_R reactions, where $n_R \leq n_D$ and $m_R < m_D$. The two inequalities above follow because the reduced model contains fewer reactions than the detailed; the number of species included in the reduced model may or may not be smaller (although in practice it is almost always true that $m_R < m_D$). The reduced model is then $\mathcal{R}(\boldsymbol{x}^R, \dot{\boldsymbol{x}}^R, T)$.

2.5 Software

A chemistry software library called Antioch (A New Templated Implementation of Chemistry Hydrodynamics) was used to set up the chemical model, query thermodynamic information, and solve for the reverse reaction rates [1]. Antioch is a C++ library, originally developed at ICES in the PECOS Center (Center for Predictive Engineering and Computational Science). It is designed in particular for use in hypersonic aerodynamics, and built specifically for thread-safety and high performance. However, Antioch does not include a built-in solver for the resulting

set of ODEs; for this, GSL (GNU Scientific Library) was used [22].

Another common chemistry package is Cantera, which is a C++ library for kinetics, thermodynamics, and transport processes [27]. This is in fact the library employed for the flame problem, presented at the end of chapter 5.

To recap, this chapter presents the model structure of the detailed and reduced models. In the case that the reduced model does not adequately represent the detailed (or the real chemical reaction), one has two options: (1) improve the reduced model directly with more chemistry, or (2) incorporate a representation of the model error of the reduced model. How to do the latter is the topic of the next chapter.

Chapter 3

Stochastic Inadequacy Operators

At this point, the detailed model $\mathcal{D}$ and the reduced model $\mathcal{R}$ have been presented. In the case that $\mathcal{R}$ is inadequate, a representation of the inadequacy of $\mathcal{R}$ is needed. This inadequacy is revealed after a process of calibration and validation has been applied to the reduced model. The method of Bayesian calibration and validation will be described in the following chapter. First, this chapter describes a formulation of the stochastic inadequacy operator $\mathcal{S}$ to incorporate into a general reaction mechanism model. Figure 3.1 shows the progression from the detailed model to the proposed stochastic model. The term introduced in the lower right corner, $\mathcal{G}_\omega$ respresents a general stochastic inadequacy model, where ω is a set of random variables. This could be, for example, a Gaussian process. On the other hand, this term could represent an augmentation of the chemical mechanism obtained by incorporating more reactions from the detailed model. In this case, the model inadequacy representation would in fact be deterministic (with $\omega = \{\}$). This approach would necessitate more information about the true chemical reaction than we expect to have or are willing to use. Instead, a hybrid approach is proposed: the formulation should respect certain physical constraints but also remain flexible. Flexibility means the ability to incorporate uncertainty about the true system and to be applicable to a broad class of scenarios. The proposed inadequacy representation in this work

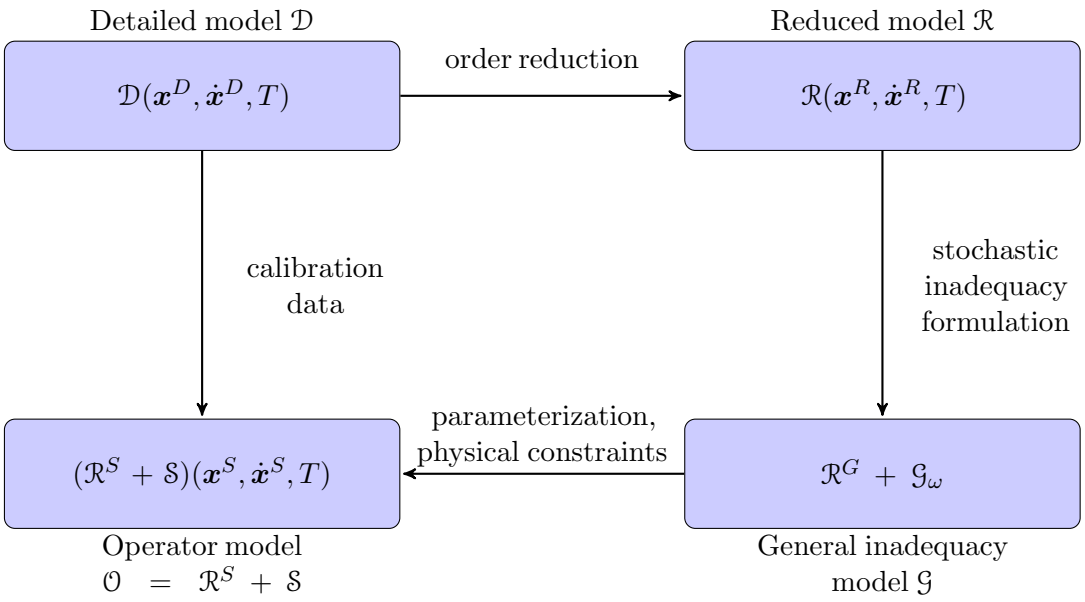

Figure 3.1: Models under consideration.

is a stochastic inadequacy operator, which is shown in the bottom left of figure 3.1. The reduced model plus the stochastic inadequacy operator is called the operator model $\mathcal{O}$. Note that the superscripts (D, R, G S) on either the state vector $\boldsymbol{x}$ or the reduced model $\mathcal{R}$ reflect the model at hand.

3.1 Initial points to note

Here we make a few important points about notation and structure of the various models under consideration.

3.1.1 Actions of the operator

The main action of the inadequacy operator $\mathcal{S}$ is to modify the time derivatives of the species' concentrations. For simplicity the operator is presumed to be linear in the state, that is, a random matrix S. However, to preserve an important property of the solution (see § 3.6), it is necessary to introduce a non-linear modification, expressed as a non-linear operator $\mathcal{A}$.[1] The final role of the operator is to properly account for energy changes by modifying the time derivative of temperature, encoded in the linear operator W.

Note that S and $\mathcal{A}$ act on just the concentrations, while W acts on the concentrations and their derivatives. Moreover, it is convenient to formulate S in terms of atomic concentrations, while $\hat{S}$ denotes the corresponding matrix in terms of molar concentrations. This chapter focuses on S instead of $\hat{S}$ because many of the properties of the matrix (such as non-positivity of eigenvalues) are better expressed in terms of atoms instead of moles (see § 3.5). To map between S and $\hat{S}$, the vector $\boldsymbol{l}$ is used, whose ith entry counts the number of atoms (of all types) in one molecule of the ith species. For example, if the set of species is H_2, O_2, H, O, OH, H_2O, then $\boldsymbol{l} = [2, 2, 1, 1, 2, 3]$. Let $L = \boldsymbol{l} I_{n_S}$, where I_{n_S} is the $n_S \times n_S$ identity matrix. Then $\hat{S} = L^{-1} S L$ applies to molar concentrations. Finally, putting the three pieces

[1] In general, a script letter refers to a nonlinear operator, capital letters to linear operators (matrices), lowercase bold letters to vectors, and lowercase (unbolded) letters to scalars.

together,

$$\mathcal{S} = \hat{S} + \mathcal{A} + W \tag{3.1}$$

$$= L^{-1}SL + \mathcal{A} + W, \quad \text{or more explicitly,} \tag{3.2}$$

$$\mathcal{S}(\boldsymbol{x}^S, \dot{\boldsymbol{x}}^S, T) = L^{-1}SL\boldsymbol{x}^S + \mathcal{A}(\boldsymbol{x}^S) + W(\boldsymbol{x}^S, \dot{\boldsymbol{x}}^S, T). \tag{3.3}$$

3.1.2 Augmentation of the state vector

The reduced model tracks fewer species than the detailed model. It should be possible then, for the inadequacy formulation to represent this difference. However, we do not want to include all the extra (missing) species in the inadequacy representation. Therefore, in order to account for the missing species in the reduced model, the state space is augmented by entries for all types of atoms. These entries act as a sort of pool of each atom type. By doing so, the operator $\mathcal{S}$ can send atoms to and from these pools instead of constraining every atom to one of the species of the reduced model. That is, $\boldsymbol{x}^S$ is of length $n_S = n_R + n_\alpha$, where n_α is the number of atom types. These objects are referred to as catchall species. Thus, $\boldsymbol{x}^S$ is of the form

$$\boldsymbol{x}^S = [x_1, \ldots, x_{n_\alpha}, x_{n_\alpha+1}, \ldots, x_{n_\alpha+n_R}]^T.$$

The catchall species of element $\mathbb{X}$ is denoted $\mathbb{X}'$.

For example, consider a reduced model species that includes H_2, O_2, OH, and H_2O. Then the catchall species are H′ and O′, and

$$\boldsymbol{x}^S = [x_1, x_2, x_3, x_4, x_5, x_6]^T \tag{3.4}$$

where $x_1, \ldots, x_6$ corresponds to H′, O′, H_2, O_2, OH, and H_2O, in that order.

This brings us to an important point about the structure of the reduced model: it takes on a different form when used in conjunction with the stochastic operator $\mathcal{S}$. There are two reasons for this. First, $\mathcal{R}$ now acts on a vector space of dimension n_S, although it has no effect on the first n_α entries of $\boldsymbol{x}^S$. Second, the effect of the catchall species on the energy equation is not additive. Because of this, the differential equation for T is removed from $\mathcal{R}$ and the entire calculation is accounted for with W. These changes are reflected by writing the reduced model as $\mathcal{R}^S$ when used with the stochastic operator $\mathcal{S}$. That is, $\mathcal{R}^S$ only includes the differential equations for the concentrations as in the reduced model, and dT/dt is given entirely by W.

A natural question at this point is: what is the most general form of such a matrix S? We show that the general structure includes many identically zero entries and is the result of enforcing two important constraints: conservation of atoms, and non-negativity of concentrations. The matrix also exhibits some interesting properties, including: 1) the columns sum to zero, 2) the diagonal is negative, 3) the matrix is weakly diagonally dominant, and 4) the eigenvalues are non-positive.

3.2 Physical constraints

There are two non-negotiable constraints that our system must respect: (I) conservation of atoms, and (II) non-negativity of concentrations. This ensures that the inadequacy operator respects physical laws that are expected to always be true.

3.2.1 Conservation of atoms

To enforce (I), first let $E = [e_{ij}]$ be the $n_\alpha \times n_S$ matrix, where e_{ij} is the fraction of atoms of type i in one molecule of species j. Then it must be that $ES = 0$. This ensures that the operator acts on all atoms of a given type without creating or destroying atoms. That is, the ith row of E applied to the jth colomn of S equal to 0 shows that the ith type of atom is conserved as the operator redistributes that atom type from species j among the rest of the species.

To continue the example shown in § 3.1, consider the case with atom types H and O, and species H′, O′, H_2, O_2, OH, H_2O. Then matrix E takes the form:

$$E = \begin{bmatrix} 1 & 0 & 1 & 0 & 1/2 & 2/3 \\ 0 & 1 & 0 & 1 & 1/2 & 1/3 \end{bmatrix}. \tag{3.5}$$

To satisfy the constraint that $ES = 0$, the matrix S is decomposed as:

$$S = CP, \tag{3.6}$$

where C is a deterministic matrix and P is probabilistic. The matrix C ensures conservation of atoms, and P ensures that the concentrations are non-negative. The columns of C span the nullspace of E, i.e. $\text{span}(C) = \text{null}(E)$. Thus,

$$ES = ECP = (EC)P = 0 \cdot P = 0. \tag{3.7}$$

E is of dimension $n_\alpha \times n_S$, so the dimension of the nullspace is $n_S - n_\alpha = n_R$. Thus C is of dimension $n_S \times n_R$ and P is of dimension $n_R \times n_S$.

3.2.2 Non-negativity of concentrations

The second constraint (II) is that the concentrations must not be negative. To see how to enforce this, consider the differential equation for species $\mathbb{X}_i$[2]:

$$\dot{x}_i = (\mathcal{R}^S(\boldsymbol{x}, \boldsymbol{T}))_i + (\mathcal{S}(\boldsymbol{x}))_i \tag{3.8}$$

$$= (\mathcal{R}^S(\boldsymbol{x}, \boldsymbol{T}))_i + (L^{-1}SL\boldsymbol{x})_i + (\mathcal{A}(\boldsymbol{x}))_i. \tag{3.9}$$

We must ensure that $x_i \geq 0$ when $x_i = 0$ for $i = 1, \ldots, n_S$. The first term of the RHS of (3.9) is not a problem, as this is the nonlinear part from the reaction mechanism and is thus already physically consistent [20]. The same argument holds for $\mathcal{A}(\boldsymbol{x})$; more will be said about this in § 3.6. Note the the energy operator W is not written above because it does not modify the derivative of x_i.

Finally, the second term must satisfy the constraint. Although it is in terms of molar concentrations, it is helpful to rephrase this in terms of atomic concentrations. That is, the constraint is satisfied for moles if and only if it is satisfied for atoms:

$$L^{-1}SL\boldsymbol{x} \geq 0 \quad \iff \quad S\boldsymbol{y} \geq 0. \tag{3.10}$$

To prove this, consider the ith entry of $L^{-1}SL\boldsymbol{x}$:

$$(L^{-1}SL\boldsymbol{x})_i = L^{-1} \sum_j s_{ij} l_j x_j \tag{3.11}$$

$$= \frac{1}{l_i} \sum_j s_{ij} l_j x_j \tag{3.12}$$

[2]We drop the superscript S from $\boldsymbol{x}$ here for ease of notation.

but $l_j x_j = y_j$ and all $l_i > 0$, $i = 1, \ldots, n_S$. Thus,

$$\frac{1}{l_i} \sum_j s_{ij} l_j x_j \geq 0 \iff \sum_j s_{ij} y_j \geq 0. \tag{3.13}$$

But the final term is exactly the ith element of $S\boldsymbol{y}$.

To continue in terms of atomic concentrations y_i:

$$(S\boldsymbol{y})_i = s_{ii} y_i + \sum_{j \neq i} s_{ij} y_j. \tag{3.14}$$

The first term from the diagonal, $s_{ii} y_i$, automatically respects the constraint: s_{ii} may be set to be any constant value, since then $s_{ii} y_i \to 0$ as $y_i \to 0$. Finally, it must be that the sum, $\sum_{j \neq i} s_{ij} y_j$, is greater than zero. But this sum does not depend on y_i, so set $s_{ij} \geq 0$ for all $i \neq j$. This could be made less restrictive by incorporating information from the nonlinear system, i.e. set $(\mathcal{R}^S(\boldsymbol{x}))_i + \sum_{j \neq i} \hat{s}_{ij} x_j \geq 0$, but this would be substantially harder to implement, especially computationally. It would also necessitate using information from the reduced model, whereas we aim to constrain the inadequacy operator independently of $\mathcal{R}$.

3.3 Sparsity of S

In practice, many of the entries of S are identically zero. In theory, S could be completely dense if every species included every type of atom. However, this never occurs in practical combustion reactions. The following proves which entries of S are identically zero, using an argument based on the zeros of the matrix E.

Theorem 3.3.1. *Consider the ith row of E. Let $\mathcal{J}_i = \{j | e_{ij} \neq 0\}$ and $\mathcal{J}_i^c = \{j | e_{ij} = 0\}$. Then every element $s_{jk} = 0$ for $j \in \mathcal{J}_i$ and $k \in \mathcal{J}_i^c$.*

Proof. Consider the ith row of E and the kth column of S. We have

$$0 = \sum_j e_{ij} s_{jk} \tag{3.15}$$

$$= \sum_{j \in \mathcal{J}_i} e_{ij} s_{jk} + \sum_{j \in \mathcal{J}_i^c} e_{ij} s_{jk} \tag{3.16}$$

$$= \sum_{j \in \mathcal{J}_i^c} e_{ij} s_{jk} + 0. \tag{3.17}$$

But since j and k are in disjoint sets, the sum in line (3.17) does not include the diagonal term s_{jj}. But the diagonal term is the only negative value in the k column. Thus, all $s_{jk} = 0$, where $j \in \mathcal{J}_i$ and $k \in \mathcal{J}_i^c$. □

There is another way to determine which entries of S are identically zero. This is due to physical restrictions about how different species' concentrations interact with each other. To determine the sparsity in this way, each species $\mathbb{X}$ is characterized by a composite number $\rho_{\mathbb{X}}$. First associate a prime number p_i with each atom type $i = 1, \ldots n_\alpha$. Each species $\mathbb{X}$ is made up of a collection of atom types; let $\rho_{\mathbb{X}}$ be the product of prime numbers corresponding to each type of atom making up species $\mathbb{X}$. For example, if elements H and O correspond to the prime numbers 2 and 3, then $\rho_{\mathrm{H}} = 2$ and $\rho_{\mathrm{H_2O}} = 6$. In effect, this yields a prime number representation of each species where multiplicity is ignored.

Next, the columns of S correspond to chemical reactants and the rows to chemical products. The entry s_{ij} controls how many atoms move from species j- a sort of reactant- to species i- a sort of product. The operator can only move a positive amount of species $\mathbb{X}_j$ to $\mathbb{X}_i$ if the former contains all elements that comprise

the latter. If not, then the $\gcd(\rho_{\mathbb{X}_i}, \rho_{\mathbb{X}_j}) < \rho_{\mathbb{X}_i}$. But in this case there can be no flow of atoms from $\mathbb{X}_j$ to $\mathbb{X}_i$, and thus $s_{ij} \equiv 0$.

This technique can also be used to count the total number of entries that are identically zero in the matrix. Call this total number Ω and, for $i = 1, \ldots, n_S$, let λ_i be the number of species $\mathbb{X}_j$ such that $\gcd(\rho_{\mathbb{X}_i}, \rho_{\mathbb{X}_j}) < \rho_{\mathbb{X}_i}$. By the argument in the previous paragraph, λ_i is the number of zeros in the ith column of S. Then the number of zeros in S is $\Omega = \sum_{i=1}^{n_S} \lambda_i$ because the sum is taken with respect to the different species, and each of these correspond to a different column of S.

3.4 Construction of the matrix S

The structure of S is now clear; the next step is to actually construct it. The challenge here is that both constraints must be simultaneously satisfied by any realization of S. This section presents a method for construction of the operator. To help demonstrate the upcoming matrix decompositions and inequality constraints, the construction will also be shown for the example set of species (H′, O′, H_2, O_2, OH, H_2O). In this case, S has the form

$$S = \begin{bmatrix} s_{1,1} & 0 & s_{1,3} & 0 & s_{1,5} & s_{1,6} \\ 0 & s_{2,2} & 0 & s_{2,4} & s_{2,5} & s_{2,6} \\ s_{3,1} & 0 & s_{3,3} & 0 & s_{3,5} & s_{3,6} \\ 0 & s_{4,2} & 0 & s_{4,4} & s_{4,5} & s_{4,6} \\ 0 & 0 & 0 & 0 & s_{5,5} & s_{5,6} \\ 0 & 0 & 0 & 0 & s_{6,5} & s_{6,6} \end{bmatrix}, \tag{3.18}$$

where the diagonal elements are non-positive and the off-diagonal elements are non-negative. Here, $n_R = 4$, $n_\alpha = 2$.

First, C is formed as follows: let the bottom $n_R \times n_R$ block be the identity matrix I_{n_R}. The remaining top n_α rows will be the negative of the last n_R columns of E. Let this matrix block be denoted E^*. Note that every element of E^* is non-positive. So, C has the form

$$C = \left[\frac{E^*}{I_{n_R}}\right]. \tag{3.19}$$

As seen earlier for this example,

$$E = \begin{bmatrix} 1 & 0 & 1 & 0 & 1/2 & 2/3 \\ 0 & 1 & 0 & 1 & 1/2 & 1/3 \end{bmatrix}, \tag{3.20}$$

so

$$E^* = \begin{bmatrix} -1 & 0 & -1/2 & -2/3 \\ 0 & -1 & -1/2 & -1/3 \end{bmatrix} \tag{3.21}$$

and

$$C = \begin{bmatrix} -1 & 0 & -1/2 & -2/3 \\ 0 & -1 & -1/2 & -1/3 \\ 1 & 0 & 0 & 0 \\ 0 & 1 & 0 & 0 \\ 0 & 0 & 1 & 0 \\ 0 & 0 & 0 & 1 \end{bmatrix}. \tag{3.22}$$

Next, P is an $n_R \times n_S$ random matrix. To construct P, the first step is to specify which entries are non-negative, non-positive, or strictly zero. Then, by taking advantage of the special structure of C, it is possible to transfer the inequalities placed on the entries of S to those of P. Let P_1 contain the first n_α columns of P,

and P_2 the remaining n_R columns. So far we have

$$S = CP \tag{3.23}$$

$$= \left[\frac{E^*}{I_{n_R}}\right] \left[\begin{array}{c|c} P_1 & P_2 \end{array}\right] \tag{3.24}$$

$$= \left[\frac{E^*P_1 \mid E^*P_2}{I_{n_R}P_1 \mid I_{n_R}P_2}\right] \tag{3.25}$$

$$= \left[\frac{E^*P_1 | E^*P_2}{I_{n_R}P}\right]. \tag{3.26}$$

The bottom row of (3.26) shows how to transfer the inequalities from matrix S to P. Since P is left-multiplied by the identity matrix, it must be that the signs match for the corresponding elements of S. In particular, for $1 < i \leq n_R$ and $\forall j$, then

$$p_{i,j} \leq 0 \text{ if } s_{(i+n_\alpha),j} \leq 0 \tag{3.27}$$

$$p_{i,j} \geq 0 \text{ if } s_{(i+n_\alpha),j} \geq 0 \tag{3.28}$$

$$p_{i,j} \equiv 0 \text{ if } s_{(i+n_\alpha),j} \equiv 0. \tag{3.29}$$

Thus, in the example,

$$P = \begin{bmatrix} p_{1,1} & 0 & p_{1,3} & 0 & p_{1,5} & p_{1,6} \\ 0 & p_{2,2} & 0 & p_{2,4} & p_{2,5} & p_{2,6} \\ 0 & 0 & 0 & 0 & p_{3,5} & p_{3,6} \\ 0 & 0 & 0 & 0 & p_{4,5} & p_{4,6} \end{bmatrix}, \tag{3.30}$$

where

$$p_{1,3},\, p_{2,4},\, p_{3,5},\, p_{4,6} \leq 0$$

and

$$p_{1,1},\, p_{1,5},\, p_{1,6},\, p_{2,2},\, p_{2,5},\, p_{2,6},\, p_{3,6},\, p_{4,5} \geq 0.$$

Note that the number of non-zero elements in P is 12.

The three inequalities above (3.27-3.29) are necessary but not sufficient as this only guarantees the inequalitites of the bottom row of (3.26) hold. The top row introduces more restrictive inequalities on a subset of the entries of P. First consider the top left block. The only nonzero elements here are the negative entries on the diagonal. There can be no non-zero off-diagonal elements of S in this block, because each row and column correspond to a catchall species, and atoms can never move from one catchall to another because they are of different types, by definition. But all the entries of E^* are non-positive, and all entries of P_1 are non-negative by (3.28) (these correspond to off-diagonal elements of S). Thus, the diagonal elements of S in this top left block are guaranteed to be non-positive, as required.

Lastly, consider the top right block: E^*P_2. To guarantee that these elements are non-negative, it is necessary that the negative entries of P_2 (on its diagonal) are large enough in magnitude. For these elements $s_{i,k}$ in the top right block, $1 \leq i \leq n_\alpha$ and $n_\alpha < k \leq n_s$. Now

$$0 \leq s_{i,k} = E^*_{(i,\cdot)} P_{(\cdot,2_k)} \tag{3.31}$$

$$= E^*_{(i,\cdot)} P_{(\cdot,k+n_\alpha)} \tag{3.32}$$

$$= E^*_{(i,\cdot)} P_{(\cdot,k')} \tag{3.33}$$

$$= \sum_j e^*_{i,j} p_{j,k'}, \tag{3.34}$$

where $k' = k + n_\alpha$. The only positive term above in the sum is $e^*_{i,k} p_{k,k'}$, so this implies

$$e^*_{i,k} p_{k,k'} \geq \sum_{j \neq k} e^*_{i,j} p_{j,k'}. \tag{3.35}$$

A similar inequality is placed on the each element $p_{k,k'}$ for each type of atom (each row of E^* that multiplies the k'th column of P). Therefore, to complete the set of inequalities on P, it is sufficient that, for $i = 1, \ldots, n_\alpha$ and $k = 1, \ldots, n_R$:

$$-p_{k,k'} \geq \frac{1}{\min_i(e^*_{i,k})} \sum_{j \neq k} \max_i(e^*_{i,j}) p_{j,k'}, \tag{3.36}$$

or, in terms of the matrix C:

$$-p_{k,k'} \geq \frac{1}{\min_i |c_{i,k}|} \sum_{j \neq k} \max_i |c_{i,j}| p_{j,k'}. \tag{3.37}$$

For use in the following development, denote the RHS of (3.37) above as $q_{k'}$.

In the example, the extra constraints from E^*P_2 correspond to the diagonal elements of P: $p_{1,3}$, $p_{2,4}$, $p_{3,5}$, $p_{4,6}$. For example, the constraint $s_{1,5} \geq 0$ implies $E^*_{(1,\cdot)} P_{(\cdot,5)} \geq 0$ and $s_{2,5} \geq 0$ implies $E^*_{(2,\cdot)} P_{(\cdot,5)} \geq 0$. These two constraints are then

$$-1p_{1,5} - 0p_{2,5} - \frac{1}{2}p_{3,5} - \frac{2}{3}p_{4,5} \geq 0 \tag{3.38}$$

$$-0p_{1,5} - 1p_{2,5} - \frac{1}{2}p_{3,5} - \frac{1}{3}p_{4,5} \geq 0. \tag{3.39}$$

The two lines above can be condensed into a single inequality which is stronger than either of the two as:

$$-p_{3,5} \geq 2(p_{1,5} + p_{2,5} + \frac{2}{3}p_{4,5}). \tag{3.40}$$

Similary, the constraints for the other negative elements take the form:

$$-p_{1,3} \geq 0 \tag{3.41}$$

$$-p_{2,4} \geq 0 \tag{3.42}$$

$$-p_{4,6} \geq 3(p_{1,6} + p_{2,6} + \frac{1}{2}p_{3,6}). \tag{3.43}$$

3.4.1 Transform from P to ξ

Now each element of P is of one of the following forms:

$$p_{i,k} \equiv 0 \tag{3.44}$$

$$p_{i,k} \geq 0 \tag{3.45}$$

$$-p_{i,k} \geq q_k, \quad k = i + n_\alpha. \tag{3.46}$$

These variables can be transformed and reindexed to a new set $\{\xi_l\}_{l=1}^{n_\xi}$ such that the inequalities take the simple form $\xi_l \geq 0$ for each l. This mapping also changes from a double-indexed system $(p_{i,j})$ to a single index (ξ_l). The index l is introduced because the zero elements of P are not mapped to $\boldsymbol{\xi}$, so the mapping is unique to every matrix. For n_ξ sets $\{l, i, k\}$, each ξ_l is of one of the following two forms:

$$\xi_l = p_{i,k}, \quad k \neq i + n_\alpha \tag{3.47}$$

$$\xi_l = -(p_{i,k} + q_k), \quad k = i + n_\alpha. \tag{3.48}$$

Note that the second set is of size n_R and thus the size of the first set is $n_\xi - n_R$.

For the example, $n_\xi = 12$ since there are 12 non-zero elements of P. There are $n_R = 4$ variables whose transform depends on q_k, and thus $n_\xi - n_R = 8$ variables whose transform does not. The total transform is given in table 3.1.

To complete the construction, it remains to specify the probability distribution that governs each variable ξ_l. Since $\xi_l \geq 0, l = 1, \ldots, n_\xi$, let

$$\xi_l \sim \log \mathcal{N}(\mu_l^\xi, \eta_l^\xi). \tag{3.49}$$

ξ_i	$=$	$p_{j,k}$
ξ_1	$=$	$p_{1,1}$
ξ_2	$=$	$-p_{1,3}$
ξ_3	$=$	$p_{1,5}$
ξ_4	$=$	$p_{1,6}$
ξ_5	$=$	$p_{2,2}$
ξ_6	$=$	$-p_{2,4}$
ξ_7	$=$	$p_{2,5}$
ξ_8	$=$	$p_{2,6}$
ξ_9	$=$	$-p_{3,5} - \frac{2}{3}(p_{1,5} + p_{3,5} + \frac{2}{3}p_{4,5})$
ξ_{10}	$=$	$p_{3,6}$
ξ_{11}	$=$	$p_{4,5}$
ξ_{12}	$=$	$-p_{4,6} - 3(p_{1,6} + p_{2,6} + \frac{1}{2}p_{3,6})$

Table 3.1: The transformed variables $\boldsymbol{\xi}$ for the example operator.

The role of the hyperparameters μ and η and how to calibrate them will be explained in detail in the next chapter. For ease and generality of notation, let $\boldsymbol{k}$ be the vector of all model parameters (this includes $\boldsymbol{A}$, $\boldsymbol{b}$, $\boldsymbol{E}$), let $\boldsymbol{\psi}$ be the vector of inadequacy parameters (so far, $\boldsymbol{\xi} \in \boldsymbol{\psi}$ and more inadequacy parameters will be introduced in the upcoming sections), and let $\boldsymbol{\zeta}$ be the vector of all hyperparameters.

3.5 Properties of S

Enforcing the two constraints— (I) conservation of atoms and (II) non-negativity of concentrations yields some interesting properties of the random matrix S. The non-positivity of eigenvalues is consistent with the constraints: no species can grow arbitrarily large over time. The proof follows:

Theorem 3.5.1. *Let S be any random matrix such that $ES = 0$ and the off-diagonal elements of S be non-negative. Then (a) the columns sum to zero, (b) the diagonal*

is negative, (c) the matrix is weakly diagonally dominant, and (d) the eigenvalues are non-positive.

Proof. (a) Consider $ES_{(\cdot,j)} = 0$, where $S_{(\cdot,j)}$ is the jth column of S. There are n_α equations:

$$\begin{aligned} e_{1,1}s_{1,j} + e_{1,2}s_{2,j} + \cdots + e_{1,n_S}s_{n_S,j} &= 0 \\ e_{2,1}s_{1,j} + e_{2,2}s_{2,j} + \cdots + e_{2,n_S}s_{n_S,j} &= 0 \\ &\vdots \\ e_{n_\alpha,1}s_{1,j} + e_{n_\alpha,2}s_{2,j} + \cdots + e_{n_\alpha,n_P}s_{n_S,j} &= 0. \end{aligned}$$

Now add the lines together:

$$\sum_i \sum_k e_{k,i}s_{i,j} = 0, \tag{3.50}$$

but $\sum_k e_{k,i} = 1$ by definition. Thus,

$$\sum_i s_{i,j} = 0. \tag{3.51}$$

(b) In equation (3.51), move the diagonal term to the RHS:

$$\sum_{i \neq j} s_{i,j} = -s_{j,j}. \tag{3.52}$$

Since all off-diagonal terms are non-negative, it must be that the diagonal element is negative.

(c) The line above also shows weak diagonal dominance, since

$$|s_{j,j}| = \left| \sum_{i \neq j} s_{i,j} \right| \tag{3.53}$$

$$= \sum_{i \neq j} |s_{i,j}|, \tag{3.54}$$

where the second equality holds because all off-diagonal elements are non-negative.

(d) Since S and S^T have the same eigenvalues, we will show that the claim is true for S^T. Let $B = S^T$ and $B_i = \sum_{j \neq i} |b_{i,j}| = \sum_{j \neq i} b_{i,j}$ be the sum of off-diagonals in the ith row. Now let $D(b_{i,i}, B_i)$ be the closed disc centered at $b_{i,i}$ with radius B_i. Then the Gershgorin theorem states that every eigenvalue of B lies within at least one of the discs [7]. In this case, we have $b_{i,i} = s_{i,i}$ and $B_i = |s_{i,i}|$, so every eigenvalue lies within at least one disc $D(s_{i,i}, |s_{i,i}|)$, where $s_{i,i} \leq 0$. □

This concludes the description of S. Recall that the operator consists of three pieces:

$$\mathcal{S} = \hat{S} + \mathcal{A} + W. \tag{3.55}$$

The next sections continue with formulations of $\mathcal{A}$ and W.

3.6 The catchall reactions $\mathcal{A}$

There is much flexibility in the matrix S with respect to how it can redistribute atoms from certain concentrations to others. In fact, it is the most flexible (or general) linear formulation. That is, at every point in time, a certain species $\mathbb{X}_i$ can

be redistributed among all other species $\mathbb{X}_j$ as long as $\rho_{\mathbb{X}_j} \leq \rho_{\mathbb{X}_i}$. Moreover, the rates at which these processes occur are not set a priori, but are calibrated using the available data. The random matrix S also provides the flexibility of the catchall species— allowing a place for atoms to go that might in fact make up a species not included in $\mathcal{R}$ but present in $\mathcal{D}$.

However, there is one serious limitation of S due entirely to the linearity: while any species can move to the catchall species (i.e. $H_2O \longrightarrow 2\,H' + O'$), a catchall species can only directly move to a species made up of the same type of atom. Therefore, a reaction like the reverse of the previous, namely $2\,H' + O' \longrightarrow H_2O$, is not allowed. This would require a term that depends on the concentrations of both catchall species, but in a linear operator this is not possible. On the one hand, in the example reaction with species H_2, O_2, OH, and H_2O, the catchall species could move back to the reduced set of species since H' could form H_2 and O' could form O_2. In some cases, this might not be such a serious limitation.

On the other hand, consider a reaction that includes the species H_2, O_2, H_2O, CH_4, CO, and CO_2 (this is the species set of the reduced methane mechanism presented in chapter 5). Then the operator model species set is H', O', C', H_2, O_2, H_2O, CH_4, CO, and CO_2. Here, S can send carbon atoms from CH_4, CO, and CO_2 into C'. But then they are stuck: C_n, for any $n = 1, 2, \ldots$, is not in the reduced set of species. To overcome the linearity limitation, there is a straightforward modification to the operator: for any species $\mathbb{X}_i$ that is made up of more than one type of atom, a nonlinear reaction is included in which the product is $\mathbb{X}_i$ and the reactants are the

corresponding catchall species. Continuing with the methane reaction,

$$2\,\mathrm{H}' + \mathrm{O}' \xrightarrow{\kappa_1} \mathrm{H_2O} \tag{3.56}$$

$$4\,\mathrm{H}' + \mathrm{C}' \xrightarrow{\kappa_2} \mathrm{CH_4} \tag{3.57}$$

$$\mathrm{O}' + \mathrm{C}' \xrightarrow{\kappa_3} \mathrm{CO} \tag{3.58}$$

$$2\,\mathrm{O}' + \mathrm{C}' \xrightarrow{\kappa_4} \mathrm{CO_2}. \tag{3.59}$$

This set of reactions is represented by the nonlinear operator $\mathcal{A}$. Note that the form is analogous to a general reaction model. Thus, the constraints (I) and (II) are automatically satisfied.

This modification introduces n_κ reaction rate coefficients κ to be calibrated. Similar to the variables $\boldsymbol{\xi}$, each κ is positive, by design. Thus,

$$\kappa \sim \log \mathcal{N}(\mu^\kappa, \eta^\kappa). \tag{3.60}$$

Then $\boldsymbol{\psi}$ is augmented to include these rate coefficients κ and $\boldsymbol{\zeta}$ is augmented to include the additional hyperparameters μ^κ and η^κ.

3.7 The energy operator W

The third and final component of the operator is the linear stochastic energy operator W. The role of W is to account for temperature changes due to atoms moving into and out of the catchall species. In other words, allowing for the existence of the catchall species endows them with mass; here the catchall formulation is completed by endowing them with thermodynamic properties. Specifically, this includes internal energy and specific heat capacity.

Recall the differential equation for dT/dt:

$$\frac{dT}{dt} = W(\boldsymbol{x}, \dot{\boldsymbol{x}}, T) = -\left(\frac{1}{\sum_i^{n_S} c_{v_i}(T) x_i}\right)\left(\sum_i^{n_S} u_i(T)\dot{x}_i\right). \tag{3.61}$$

For $n_\alpha < i \leq n_S$, $c_{v_i}(T)$ and $u_i(T)$ are known as functions of temperature from the literature on thermodynamic properties of chemical species [40]. The new contribution is to allow for $u_i(T)$ and $c_{v_i}(T)$ for $i = 1, \ldots, n_\alpha$, that is, allow for catchall energies and specific heats and then incorporate these into the calculation of the time derivative of temperature. For actual chemical species, these properties are always given as a function of temperature. Thus, each new coefficient will also be allowed to have a simple temperature-dependence. Consider a catchall species $\mathbb{X}'_i$, $i = 1, \ldots, n_\alpha$. For the internal energy, we pose the following form:

$$u_i(T) = \alpha_{0_i} + \alpha_{1_i} T + \alpha_{2_i} T^2, \tag{3.62}$$

and, since c_v is its derivative with respect to temperature,

$$c_{v_i}(T) = \alpha_{1_i} + 2\alpha_{2_i} T. \tag{3.63}$$

Then α_0, α_1, and α_2 are additional parameters to be calibrated. Furthermore, like all the other random variables introduced during the modeling of the inadequacy operator, each will in fact be represented by a probability distribution. This is appropriate since we have incorporated some physical information (temperature-dependence), but the true functional form is uncertain. It is known that α_1 and α_2 are positive, while α_0 could be positive or negative. These properties are exhibited

in pdf's of the form

$$\alpha_0 \sim \mathcal{N}(\mu_0^\alpha, \eta_0^\alpha) \tag{3.64}$$

$$\alpha_l \sim \log \mathcal{N}(\mu_l^\alpha, \eta_l^\alpha), \quad l = 1, 2. \tag{3.65}$$

Since the above applies to the n_α catchall species, there are $3n_\alpha$ new variables. Of course, $\boldsymbol{\psi}$ and $\boldsymbol{\zeta}$ are again augmented to include the new (and final) inadequacy parameters and hyperparameters. Thus, the sets are the model parameters $\boldsymbol{k} = \{\boldsymbol{A}, \boldsymbol{b}, \boldsymbol{E}\}$, the inadequacy parameters $\boldsymbol{\psi} = \{\boldsymbol{\xi}, \boldsymbol{\kappa}, \boldsymbol{\alpha}\}$, and the hyperparameters $\boldsymbol{\zeta} = \{\boldsymbol{\mu}^{\boldsymbol{\xi}}, \boldsymbol{\eta}^{\boldsymbol{\xi}}, \boldsymbol{\mu}^{\boldsymbol{\kappa}}, \boldsymbol{\eta}^{\boldsymbol{\kappa}}, \boldsymbol{\mu}^{\boldsymbol{\alpha}}, \boldsymbol{\eta}^{\boldsymbol{\alpha}}\}$.

This concludes the description of the stochastic operator $\mathcal{S}$. Many model parameters and hyperparameters have been introduced for the formulation of the reduced and stochastic operator models; the calibration of these parameters and validation of the models is the subject of the next chapter.

3.8 Mapping from the operator to typical reaction form

Before presenting the calibration and validation of the models, there is a final detail to consider regarding the formulation of the operator. A natural question after inspection of the operator is: What does this look like in terms of typical chemical reactions? The answer connects the action of the operator $\hat{S}$ to the physical interpretation of chemical reactions. Also, on a more practical level, it may be necessary to write the operator in this form. For example, when solving for the flamespeed of a hydrogen flame in § 5.3, the operator was incorporated into an existing program by encoding it in a chemical reaction input file, which must written in the typical

reaction form. It is now demonstrated that the random matrix $\hat{S} = L^{-1}SL$ can be mapped to a typical chemical reaction of the form $\mathrm{A} \xrightarrow{k} \sum \beta B$.

Theorem 3.8.1. *For every $j = 1, \ldots, n_S$, the jth column of $\hat{S}$ corresponds to the reaction*

$$\mathrm{X}_j \xrightarrow{k_j} \sum_{p \neq j} \beta_{jp} \mathrm{X}_p, \tag{3.66}$$

where $k_j = \left|\hat{s}_{jj}\right|$ and $\beta_{jp} = \frac{\hat{s}_{jp}}{\left|\hat{s}_{jj}\right|}$.

Proof. Let $\boldsymbol{x}$ be the vector of concentrations of length n (drop the subscript S for ease of notation). Let the set of reactions above be denoted $\mathcal{L}(\boldsymbol{x})$ (in the same way that the reduced mechanism model is written $\mathcal{R}(\boldsymbol{x})$). We will show $\hat{S}\boldsymbol{x} = \mathcal{L}(\boldsymbol{x})$, element-wise.

First,

$$\hat{S}\boldsymbol{x} = \begin{pmatrix} \hat{s}_{1,1}x_1 + \hat{s}_{1,2}x_2 + \cdots + \hat{s}_{1,n}x_n \\ \hat{s}_{2,1}x_1 + \hat{s}_{2,2}x_2 + \cdots + \hat{s}_{2,n}x_n \\ \vdots \\ \hat{s}_{n,1}x_1 + \hat{s}_{n,2}x_2 + \cdots + \hat{s}_{n,n}x_n \end{pmatrix}, \tag{3.67}$$

and for a single species $\mathbb{X}_i$,

$$(\hat{S}\boldsymbol{x})_i = \sum_j \hat{s}_{ij}x_j. \tag{3.68}$$

Now consider $\mathcal{L}(\boldsymbol{x})$. The rate for a particular $\mathbb{X}_i$ consists of multiple terms: one in which $\mathbb{X}_i$ is the chemical reactant, and $n-1$ terms in which $\mathbb{X}_i$ is the chemical product. When $\mathbb{X}_i$ is a reactant, the corresponding rate is $-k_i x_i = \hat{s}_{ii}x_i$. When $\mathbb{X}_i$ is a product (and $\mathbb{X}_j$ is the reactant, $j \neq i$), the rates from each reaction are

$$+ k_j\beta_{ij}x_j = \left|\hat{s}_{jj}\right| \left(\frac{\hat{s}_{ij}}{\left|\hat{s}_{jj}\right|}\right) x_j = \hat{s}_{ij}x_j, \quad j \neq i. \tag{3.69}$$

Putting the two terms together, we have

$$(\mathcal{L}(\boldsymbol{x}))_i = \hat{s}_{ii}x_i + \sum_{j\neq i} \hat{s}_{ij}x_j \tag{3.70}$$

$$= \sum_j \hat{s}_{ij}x_j \tag{3.71}$$

$$= (\hat{S}\boldsymbol{x})_i. \tag{3.72}$$

□

Chapter 4

Calibration and Validation

This chapter describes the Bayesian approach to model calibration. First the standard method is presented which can be applied to calibrate the reduced model. Then, to calibrate the inadequacy model parameters and hyperparameters of the operator model, an extension called Hierarchical Bayesian Modeling (HBM) is presented. Finally, a compatible method of Bayesian model validation is described to test the performance of the various models.

4.1 Bayesian inverse problems

A mathematical model is usually framed in terms of a *forward problem*; i.e. the model takes some parameter inputs and yields the model output. When this output is an observable quantity, it is called a *parameter-to-observable map* (this map may include the main physics model plus some post-processing or data reduction to arrive at the observable value). Let the parameters be denoted θ and the parameter-to-observable map $\mathcal{M}$. Then the value of $\mathcal{M}(\theta)$ is comparable to some data d, although there is usually some measurement error ϵ associated with the data. In general, then, if $\mathcal{M}$ is an accurate representation of the system, we would expect

$$d = \mathcal{M}(\theta) + \epsilon. \tag{4.1}$$

Here the measurement error is assumed to be additive, although it could take on other forms, such as multiplicative [13, 51].

As an example, consider a model of projectile motion. The input parameters are the initial speed s, angle α, and density ρ of the projectile. Let's call these $\theta = \{s, \alpha, \rho\}$. The output of the model is the maximum height $y_{max} = \mathcal{M}(\theta)$ reached by the projectile. We can run the model and also perform the corresponding experiment to measure the maximum height. Using the given model inputs to predict the projectile's height is the forward problem. To validate the model, we compare how well y_{max} matches the experimental data d.

The flip side of this problem is called the *inverse problem*. That is, suppose we have some experimental data of various trials. The initial angle and density are known, and the maximum heights were measured. But we do not know the initial speed of the projectile. An inverse problem is used to calibrate the parameter s (initial speed) given the model, including the known inputs α and ρ, and the data d (maximum heights).

A common, probabilistic, and very flexible way to do so is to use Bayesian inference based on Bayes' Theorem, which is a one-line manipulation of the relationship between joint and conditional distributions. Let x and y be random variables, and let $p(x, y)$ be their joint probability density function (pdf). The joint density can be expanded in terms of conditionals in two ways:

$$p(x, y) = p(y|x)p(x) \tag{4.2}$$

$$= p(x|y)p(y). \tag{4.3}$$

Equating (4.2) and (4.3) and dividing by $p(y)$ yield Bayes' Theorem:

$$p(x|y) = \frac{p(y|x)p(x)}{p(y)}. \tag{4.4}$$

To see how (4.4) can be used in calibration, interpret x to represent the parameter to be calibrated while y represents an observation. The three terms on the RHS are termed as follows: (1) $p(y|x)$ is the likelihood, which is the probability of seeing the observation y given the value of the parameter x; (2) $p(x)$ is the prior distribution for the random variable x; and (3) $p(y)$ is called the evidence (for y). The term on the LHS is called the posterior, which is the conditional distribution of the parameter x given the observed value y, and is therefore the sought result of the calibration.

The evidence is a constant with respect to the parameters, and can often be ignored in the above computation because it is simply the normalization required to make $p(x|y)$ integrate to 1 with respect to x. That is, the posterior is proportional to the numerator in (4.4),

$$p(x|y) \propto p(y|x)p(x). \tag{4.5}$$

In fact, for most sampling algorithms used for Bayesian inference, the unnormalized posterior is sufficient. The posterior distribution can be sampled using Markov chain Monte Carlo sampling methods [16, 25, 29]. More will be said about these in the following section.

Of course, to calibrate a model in this way (and really in any way), a set of observations is necessary. Consider a given data set:

$$\boldsymbol{d} = \{d_i\}_{i=1}^{n_d}. \tag{4.6}$$

It is commonly assumed that a data point d_i is related to the model output through an additive Gaussian noise term, which represents observation errors:

$$d_i = \mathcal{M}_i(\boldsymbol{\theta}) + \epsilon_i, \tag{4.7}$$

where $\epsilon_i \sim \mathcal{N}(0, \sigma_\epsilon^2)$ for each $i = 1, \ldots, n_d$, though in general the observation error could have any distribution. This is often called the data model, i.e. the model that maps between the model output and a distribution of possible observations. When $\mathcal{M}$ is a model to be calibrated or validated (i.e. $\mathcal{M}^R$ or $\mathcal{R}^S$), then (4.7) provides a predictive distribution for the observed quantities, for a given set of parameters $\boldsymbol{\theta}$. The predictive distribution is used along with the observed values (the data) to determine the likelihood, as discussed in § 4.3.2.

In the current study, the additive Gaussian form above is assumed for all observations. However, instead of experimental data, synthetic data is generated using the detailed model and Gaussian noise is added to simulate measurement error. Therefore, (4.7) also defines how the observational data is generated, with $\mathcal{M}$ being $\mathcal{M}^D$, the parameters $\boldsymbol{\theta}$ fixed at values reported in the literature, and ϵ a sample from the experimental noise distribution. Then the value generated by the detailed model is considered to be the unknown true value, d^t, so that

$$d_i = d_i^t + \epsilon_i \tag{4.8}$$

$$= \mathcal{M}_i^D(\boldsymbol{\theta}) + \epsilon_i. \tag{4.9}$$

4.2 Monte Carlo Sampling algorithms

With the information above, the final step in a standard Bayesian inverse problem is to sample the posterior distribution. The algorithm used here is the Delayed Rejection Adaptive Metroplis (DRAM) algorithm [29]. This technique is a modification of the Metropolis Hastings algorithm, which is a type of Markov chain Monte Carlo (MCMC) algorithm. The Metropolis Hastings algorithm yields samples from the target distribution $\pi(x)$. The ingredients of this algorithm are a starting point x_0, a proposal distribution $q(c|x)$ (with covariance C), a random number generator, and an evaluator for the target distribution $\pi(x)$ given x. The basic steps are shown in algorithm 1.

Algorithm 1: Metropolis-Hastings

input : starting point $x^{(0)}$
output : Markov chain $\{x^{(k)}\}$, $k = 0, 1, \ldots, N$

for $k = 1$ **to** N **do**
  Generate candidate c with probability density $q(c|x^{(k-1)})$
  Compute $a = \frac{\pi(c)}{\pi(x^{(k-1)})} \frac{q(x^{(k-1)}|c)}{q(c|x^{(k-1)})}$
  if $a \geq 1$ **then** $x^{(k)} = c$
  else
    Draw $r \sim \mathcal{U}[0, 1]$
    if $a \geq r$ **then** $x^{(k)} = c$
    else $x^{(k)} = x^{(k-1)}$

DRAM combines two modifications to Metropolis Hastings: Delayed Rejection [28, 44] and Adaptive Metropolis [30]. Delayed Rejection (DR) allows for multiple proposals before rejection. This is done over a number of stages n_s. The acceptance

probability of each stage is computed to maintain reversibility of the chain. Adaptive Metropolis (AM) updates the proposal covariance at given intervals during generation of the chain. Together, DR and AM constitute DRAM which is presented in algorithm 2.

In Adaptive Metropolis, there is an initial non-adapted period of length n_0. For the first n_0 steps of the chain, the covariance is set to C_0, which is chosen according to a priori knowledge. Then, for each step n such that $n > n_0$, the covariance is adapted as

$$C_n = s_d \text{Cov}(x^{(0)}, \ldots, x^{(n-1)}) + s_d \epsilon I_d, \tag{4.10}$$

where ϵ is a regularization factor, s_d is a scaling factor, and d is the dimension of the target distribution. Also, $\text{Cov}(x^{(0)}, \ldots, x^{(k)})$ is the empirical covariance matrix determined by the first k points:

$$\text{Cov}(x^{(0)}, \ldots, x^{(k)}) = \frac{1}{k} \left(\sum_{i=0}^{k} x^{(i)} (x^{(i)})^T - (k+1) \bar{x}^{(k)} (\bar{x}^{(k)})^T \right), \tag{4.11}$$

where $\bar{x}^{(k)} = \frac{1}{k+1} \sum_{i=1}^{k} x^{(i)}$ and the $x^{(i)}$ are column vectors in $\mathbb{R}^d$.

When combined with Delayed Rejection, the covariance at stage i is computed such that $C^{(i)} = \gamma_i C^{(1)}$, for some scalar γ_i and with $C^{(1)}$ as found in (4.10). The algorithm also requires n_p, the total number of positions in the chain and α_i, the ratio computed for each candidate to be compared to the uniform sample.

Algorithm 2: Delayed Rejection Adaptive Metropolis (DRAM)

input : x_0, s_d, ϵ, n_0
output : DRAM chain $\{x^{(k)}\}$, $k = 0, 1, \ldots, n_p$

for $i = 1$ **to** n_s **do**
  Select γ_i

while $k \leq n_p$ **do**
  $ACCEPT = false$
  $i = 1$
  if $k \geq n_0$ **then**
    $C^{(1)} = s_d \mathrm{Cov}(x^{(0)}, \ldots, x^{(k-1)}) + s_d \epsilon I_d$
  while $(ACCEPT = false)$ *and* $(i \leq n_s)$ **do**
    Generate candidate $c^{(i)}$ with probability density
    $q_i(c^{(i)}|x^{(k-1)}, c^{(1)}, \ldots, c^{(i-1)})$
    if $c^{(i)} \notin supp(\pi)$ **then** $i = i + 1$
    if $c^{(i)} \in supp(\pi)$ **then**
      Compute $\alpha_i(x^{(k)}, c^{(1)}, \ldots, c^{(i)})$
      Generate $r \sim \mathcal{U}[0, 1]$
      if $(\alpha_i < r)$ **then** $i = i + 1$
      if $(\alpha_i \geq r)$ **then** $ACCEPT = true$
    $C^{(i)} = \gamma_i C^{(1)}$
    if $(ACCEPT = true)$ **then** $x^{(k)} = c^{(i)}$
    if $(ACCEPT = false)$ **then** $x^{(k)} = x^{(k-1)}$
    $k = k + 1$

4.3 Calibration of the reduced model

This section presents the calibration of the reduced model as a standard Bayesian inverse problem.

4.3.1 The observations

The set of observations are measurements generated by the detailed chemical kinetics model. They are taken of each of the n_R species tracked by the reduced model and temperature, at n_t instances in time, and for n_{IC} initial conditions. The initial condition is given by the set $\{x_f, x_o, T\}|_{t=0}$, that is, the initial concentrations of the fuel x_f, the oxidizer x_o, and the temperature. Recall that the initial ratio of fuel to oxidizer is described by a single number ϕ, called the equivalence ratio. The equivalence ratio shows how far the initial condition deviates from the stoichiometric ratio of fuel to oxidizer: that is,

$$\phi = \frac{x_f/x_o}{x_{f_{STO}}/x_{o_{STO}}}. \tag{4.12}$$

The initial condition is written as the set $IC = \{\phi, T(t=0)\}$. Thus, $\boldsymbol{d} = \{d_{ijl}\}$ where $d_{ijl} = d^t_{ijl} + \epsilon_{ijl}$ and

$$d^t_{ijl} = x_i^D(t_j, IC_l), \quad i = 1, \ldots, n_R; \quad j = 1, \ldots, n_t; \quad l = 1, \ldots, n_{IC}; \tag{4.13}$$

$$d^t_{ijl} = T^D(t_j, IC_l), \quad i = n_R + 1. \tag{4.14}$$

In the calibration of the reduced model, $n_{IC} = 1$. It will be shown that the reduced model cannot be valid even for a single initial condition. Therefore, the reduced model cannot have the flexibility to apply to multiple scenarios. However,

for the calibration of the stochastic operator model, $n_{IC} > 1$. In that case, calibrating against multiple initial conditions is done so that the calibrated inadequacy operator can be used over a range of scenarios, including possible prediction scenarios.

To set up the calibration of $\mathcal{R}$, assume that the reduced model does in fact represent the reaction that generated the data, and that the only error is in the measurements. (Later, validation will show that this is in fact incorrect.) This implies that each observed value, d_{ijl}, is equal to the model output $\mathcal{M}^R_{ijl}(\boldsymbol{\theta})$ plus some measurement error, $\epsilon \sim \mathcal{N}(0, \sigma^2_\epsilon)$. Therefore, the data model is:

$$d_{ijl} = \mathcal{M}^R_{ijl}(\boldsymbol{\theta}) + \epsilon_{ijl}. \tag{4.15}$$

Recall that $\mathcal{M}^R_{ijl}$ denotes the model output corresponding to the data point for species i (or temperature if $i = n_R + 1$), at time j, and for initial condition l. For simplicity of exposition in the following, this can be reindexed:

$$d_i = \mathcal{M}^R_i(\boldsymbol{\theta}) + \epsilon_i, \quad i = 1, \ldots, n_d. \tag{4.16}$$

4.3.2 The Bayesian distributions

The model parameters of the reduced model are the parameters for the Arrhenius reaction rate model for the m_R reaction rates, where each $k = AT^b \exp(-E/R^\circ T)$. The vector $\boldsymbol{k}$ of calibration parameters is then: $\boldsymbol{k} = [A_1, \ldots, A_{m_R}, b_1, \ldots, b_{m_R}, E_1, \ldots, E_{m_R}]^T$. The posterior distribution for the model parameters $\boldsymbol{k}$ given the data $\boldsymbol{d}$ is given by Bayes' Theorem:

$$p(\boldsymbol{k}|\boldsymbol{d}) \propto p(\boldsymbol{d}|\boldsymbol{k})p(\boldsymbol{k}), \tag{4.17}$$

where $p(\boldsymbol{k})$ is a prior distribution of the parameters representing knowledge of $\boldsymbol{k}$ before considering the data.

The prior for A in each reaction rate is taken to be an independent lognormal distribution since this parameter is known to be positive. For b and E, the prior is chosen with an independent Gaussian distribution. For all these, the prior has mean μ equal to the nominal value, i.e. the value given for the corresponding elementary reaction in the detailed model. The variance of each distribution corresponds to a standard deviation between roughly 1 and 10%. Larger values are allowed for less sensitive parameters. These comprise the complete set of model parameters for the reduced model; the joint prior is a product of these:

$$p(\boldsymbol{k}) = p(\boldsymbol{A})p(\boldsymbol{b})p(\boldsymbol{E}), \tag{4.18}$$

where

$$A_i \sim \log \mathcal{N}(\mu_i^A, \eta_i^A) \tag{4.19}$$

$$b_i \sim \mathcal{N}(\mu_i^b, \eta_i^b) \tag{4.20}$$

$$E_i \sim \mathcal{N}(\mu_i^E, \eta_i^E), \tag{4.21}$$

where $i = 1, \ldots, m_R$.

The likelihood function $p(\boldsymbol{d}|\boldsymbol{k})$ represents how "likely" it is that the data $\boldsymbol{d}$ arose from the model with specific values of the parameters $\boldsymbol{k}$. With a Gaussian data model and n_d data points, the likelihood takes the form:

$$p(\boldsymbol{d}|\boldsymbol{k}) = \frac{1}{(2\pi)^{n_d/2}|\Sigma|^{1/2}} \exp\left\{-\frac{1}{2}(\boldsymbol{d} - \mathcal{M}^R(\boldsymbol{k}))^T\Sigma^{-1}(\boldsymbol{d} - \mathcal{M}^R(\boldsymbol{k}))\right\}, \tag{4.22}$$

where Σ is the diagonal matrix of variances corresponding to the measurement error ϵ_i of the n_d observations. Now that the prior and likelihood are determined, the posterior $p(\boldsymbol{k}|\boldsymbol{d})$ is defined by (4.4). Finally, the posterior distribution can be sampled using Markov chain Monte Carlo sampling methods [16, 25, 29]. This concludes the description of the reduced model calibration.

4.4 Hierarchical Bayesian Modeling

As shown is the previous chapter, the entries of S, $\mathcal{A}$, and W are characterized by probability distributions whose hyperparameters must also be calibrated. Note that these hyperparameters $\boldsymbol{\zeta}$ are calibrated in addition to the reaction rate parameters of the reduced model: the aim is now to calibrate the model parameters $\boldsymbol{k}$, the inadequacy parameters $\boldsymbol{\psi}$, and the hyperparameters $\boldsymbol{\zeta}$ given the observations $\boldsymbol{d}$. To do so, we employ a hierarchical Bayesian framework. The rest of this section closely follows the work of Berliner (see [8, 60]), though here the interpretation is somewhat different.

First, a brief explanation of hierarchical Bayesian modeling is given. Let x represent the parameter(s) to be calibrated and y the observations. Then Bayes' Theorem is:

$$p(x|y) = \frac{p(y|x)p(x)}{p(y)}. \tag{4.23}$$

Next, let z be another random variable. The joint distribution of x, y, and z is given by

$$p(y, z, x) = p(y|z, x)p(z|x)p(x). \tag{4.24}$$

Bayes' Theorem can then be written:

$$p(z, x|y) \propto p(y|z, x)p(z|x)p(x). \tag{4.25}$$

Berliner introduces three models: the *parameter model* $p(x)$, the *process model* $p(z|x)$, and the *data model* $p(y|z, x)$. In this work, the parameter model corresponds to the prior distribution on the hyperparameters $\boldsymbol{\zeta}$ and model parameters $\boldsymbol{k}$:

$$p(x) \leftarrow p(\boldsymbol{\zeta}, \boldsymbol{k}) = p(\boldsymbol{\zeta})p(\boldsymbol{k}). \tag{4.26}$$

These are the parameters that do not depend conditionally on any others in the prior. The process model relates the inadequacy parameters $\boldsymbol{\psi} = \{\boldsymbol{\xi}, \boldsymbol{\alpha}, \boldsymbol{\beta}\}$ and their hyperparameters:

$$p(z|x) \leftarrow p(\boldsymbol{\psi}|\boldsymbol{\zeta}, \boldsymbol{k}) = p(\boldsymbol{\psi}|\boldsymbol{\zeta}). \tag{4.27}$$

Note that the above holds as the inadequacy parameters $\boldsymbol{\psi}$ are independent in the prior of the rate constants $\boldsymbol{k}$. Finally, the data model corresponds to the likelihood:

$$p(y|z, x) \leftarrow p(\boldsymbol{d}|\boldsymbol{\psi}, \boldsymbol{\zeta}, \boldsymbol{k}) = p(\boldsymbol{d}|\boldsymbol{\psi}, \boldsymbol{k}). \tag{4.28}$$

The final equality holds because once $\boldsymbol{\psi}$ and $\boldsymbol{k}$ are given, the hyperparameters have no effect on the model. Thus, the posterior distribution is

$$p(\boldsymbol{\psi}, \boldsymbol{\zeta}, \boldsymbol{k}|\boldsymbol{d}) \propto p(\boldsymbol{d}|\boldsymbol{\psi}, \boldsymbol{k})p(\boldsymbol{\psi}|\boldsymbol{\zeta})p(\boldsymbol{\zeta})p(\boldsymbol{k}). \tag{4.29}$$

The posterior has been augmented to include the model parameters $\boldsymbol{k}$, the hyperparameters $\boldsymbol{\zeta}$, and the inadequacy parameters $\boldsymbol{\psi}$. Of course, one can marginalize

as needed. For example, only the joint distribution of the hyperparameters and model parameters given the data will be of interest here:

$$p(\boldsymbol{\zeta}, \boldsymbol{k}|\boldsymbol{d}) = \int p(\boldsymbol{\psi}, \boldsymbol{\zeta}, \boldsymbol{k}|\boldsymbol{d}) d\boldsymbol{\psi}. \tag{4.30}$$

4.5 Calibration of the inadequacy operator model

This section shows the specifics of the calibration of the inadequacy operator.

4.5.1 The observations

The data set is similar to the previous case, but $n_{IC} > 1$. Instead of the parameter-to-observable map for the reduced model $\mathcal{M}^R$ (which is invalidated in the upcoming examples), now consider $\mathcal{M}^S$. The data model is the same and again the dataset is reindexed so that

$$d_i = \mathcal{M}_i^S(\boldsymbol{\theta}) + \epsilon_i, \quad i = 1, \ldots, n_d. \tag{4.31}$$

4.5.2 The hierarchical Bayesian distributions

The prior for the model parameters $p(\boldsymbol{k})$ is the same here as in the previous case (see § 4.3). Following the hierarchical scheme, a conditional prior distribution $p(\boldsymbol{\psi}|\boldsymbol{\zeta})$ for the inadequacy parameters given the hyperparameters is also required. This is inherited from the proposed structure in chapter 3, given in lines (3.49), (3.60), (3.64), (3.65). That is, the conditional prior distribution of each inadequacy

parameter is the following:

$$\xi_i \sim \log \mathcal{N}(\mu_i^{\xi}, \eta_i^{\xi}), \quad i = 1, \ldots, n_\xi \tag{4.32}$$

$$\kappa_i \sim \log \mathcal{N}(\mu_i^{\kappa}, \eta_i^{\kappa}), \quad i = 1, \ldots, n_\kappa \tag{4.33}$$

$$\alpha_{0_i} \sim \mathcal{N}(\mu_{0_i}^{\alpha}, \eta_{0_i}^{\alpha}), \quad i = 1, \ldots, n_\alpha \tag{4.34}$$

$$\alpha_{l_i} \sim \log \mathcal{N}(\mu_{l_i}^{\alpha}, \eta_{l_i}^{\alpha}), \quad l = 1, 2,\ i = 1, \ldots, 2n_\alpha. \tag{4.35}$$

Recall $\boldsymbol{\xi}$ are the inadequacy parameters of S, $\boldsymbol{\kappa}$ are those of $\mathcal{A}$, and $\boldsymbol{\alpha}$ of W.

Then the hyperparameters are calibrated: for the prior distributions $p(\boldsymbol{\zeta})$, set

$$\mu_i^{(\cdot)} \sim \mathcal{N}(\mu_i^{\mu^{(\cdot)}}, \eta_i^{\mu^{(\cdot)}}) \tag{4.36}$$

$$\eta_i^{(\cdot)} \sim \mathcal{J}(0, \infty), \tag{4.37}$$

where $(\cdot)$ represents ξ, κ, or α. In one dimension x, the Jeffreys distribution $p_{\mathcal{J}}(x) \sim \mathcal{J}(0, \infty)$ is given by

$$p_{\mathcal{J}}(x) = \frac{1}{x}, \quad x \in (0, \infty). \tag{4.38}$$

This cannot be normalized (it is an improper distibution), but it can still be used as a prior distribution [17].

Again, taking into account the Gaussian measurement error, the likelihood is given by

$$p(\boldsymbol{d}|\boldsymbol{\psi}, \boldsymbol{\zeta}, \boldsymbol{k}) = p(\boldsymbol{d}|\boldsymbol{\psi}, \boldsymbol{k}) \tag{4.39}$$

$$= \frac{1}{(2\pi)^{n_d/2}|\Sigma|^{1/2}} \exp\left\{-\frac{1}{2}(\boldsymbol{d} - \mathcal{M}^S(\boldsymbol{\psi}, \boldsymbol{k}))^T \Sigma^{-1} (\boldsymbol{d} - \mathcal{M}^S(\boldsymbol{\psi}, \boldsymbol{k}))\right\} \tag{4.40}$$

where $n_d = (n_R + 1) \times n_t \times n_{IC}$ (number of species, times of measurement, initial conditions) is the total number of observations. As described previously, the posterior distribution $p(\boldsymbol{\psi}, \boldsymbol{\zeta}, \boldsymbol{k}|\boldsymbol{d})$ is sampled using Delayed Rejection Adaptive Metroplis (DRAM) [29].

4.6 Software

As seen in the set up for the reduced and operator models, the final step in a standard Bayesian inverse problem is to sample the posterior distribution. For this investigation, the software QUESO (Quantification for Estimation, Simulation, and Optimization) is used[14, 48]. QUESO is a statistical numerical library, and was developed (like Antioch) at ICES within the PECOS Center. It is designed for research on statistical forward and inverse problems, and can be run in multiprocessor environments.

There are other software libraries available to sample posterior distributions. For example, BUGS (Bayesian Inference Using Gibbs Sampling) is a well-developed code project for Bayesian inference with MCMC that began out of medical research [38]. Another commonly used Bayesian inference package is MUQ (MIT Uncertainty Quantification library). In addition to MCMC, MUQ has tools for polynomial chaos and Karhunen-Loeve expansions, Gaussian process regression, and optimal transport maps [3].

4.7 Validation

Once a model has been constructed and calibrated, the next step is validation; that is, the process of checking if data obtained from observations of the modeled system are consistent with the calibrated model, given uncertainties in the model parameters, the model inadequacy and the observational errors. The validation approach used here is that of posterior predictive assessment [24, 49].

Consider a set of observations of the system $\{v_i\}_{i=1}^{n_v}$. This set will in general include the data $\boldsymbol{d}$ used for calibration and may also include additional observations of the same or different quantities not used in calibration. However, there is an observational error ϵ for each observation so that the observed value v_i is related to the unknown true value v_i^t by

$$v_i = v_i^t + \epsilon_i. \tag{4.41}$$

The calibrated model makes a claim about the distribution of plausible values of v_i^t given by $p(v_i^t|\boldsymbol{d})$. The relevant validation question is whether the observations v_i are consistent with the model's claim regarding the observation. This is given by

$$p(v_i|\boldsymbol{d}) = \int_{d_t} p(v_i|v_i^t)p(v_i^t|\boldsymbol{d})\, dv_i^t = \int_{d_t} p_\epsilon(v_i - v_i^t)p(v_i^t|\boldsymbol{d})\, dv_i^t \tag{4.42}$$

where p_ϵ is the probability distribution of the observation errors.

Finally, the posterior distribution of v_i^t is determined from the calibrated distributions of the model parameters $\boldsymbol{\theta}$, yielding

$$p(v_i|\boldsymbol{d}) = \int_{d_t} p_\epsilon(v_i - v_i^t) \left(\int_{\boldsymbol{\theta}} p(v_i^t|\boldsymbol{\theta})p(\boldsymbol{\theta}|\boldsymbol{d})\, d\boldsymbol{\theta} \right) dv_i^t. \tag{4.43}$$

Here, depending on the circumstance, the parameters $\boldsymbol{\theta}$ can include the physical parameters $\boldsymbol{k}$, the hyperparameters $\boldsymbol{\zeta}$ and/or the inadequacy distributions $\boldsymbol{\psi}$.

In the case of the chemical kinetics models considered here, three different validation situations are relevant. First, in testing the reduced model itself (without inadequacy), $\boldsymbol{\theta}$ includes only the kinetic parameters $\boldsymbol{k}$. Second, when testing the form of the inadequacy model to determine whether it is sufficient to represent the observed discrepancy with the calibration data, the question is whether the inadequacy form, considered to be deterministic in $\boldsymbol{\psi}$, can correct the model relative to the calibration data. In this case, $\boldsymbol{\theta}$ includes $\boldsymbol{\psi}$ and $\boldsymbol{k}$ and the posterior of v_i^t is given by

$$p(v_i^t|\boldsymbol{d}) = \int_{\boldsymbol{k}} \int_{\boldsymbol{\psi}} p(v_i^t|\boldsymbol{k}, \boldsymbol{\psi}) p(\boldsymbol{k}, \boldsymbol{\psi}|\boldsymbol{d})\, d\boldsymbol{\psi}\, d\boldsymbol{k}. \tag{4.44}$$

In the third situation, one tests whether the stochastic inadequacy representation can account for model discrepancies over a broad range of conditions, particularly for conditions not included in the calibration. Here, the inadequacy form is stochastic in $\boldsymbol{\psi}$ and this stochasticity is characterized by the hyperparameters $\boldsymbol{\zeta}$. In this case, the posterior of v_i^t is

$$p(v_i^t|\boldsymbol{d}) = \int_{\boldsymbol{k}} \int_{\boldsymbol{\psi}} \int_{\boldsymbol{\zeta}} p(v_i^t|\boldsymbol{k}, \boldsymbol{\psi}, \boldsymbol{\zeta}) p(\boldsymbol{\psi}|\boldsymbol{\zeta}) p(\boldsymbol{k}, \boldsymbol{\zeta}|\boldsymbol{d}) d\boldsymbol{\zeta} d\boldsymbol{\psi} d\boldsymbol{k}. \tag{4.45}$$

The integral (4.43) yields the posterior prediction of the observation v_i which can be used to find the total probability of observing a value less probable than the actual observation. As explained in [47], this probability can be used as a validation metric, which in turn makes use of highest probability density (HPD) credibility regions [10]. In [47], the β-HPD ($0 \leq \beta \leq 1$) credibility region $\mathbb{S}$ is the set for which

the probability of belonging to $\mathbb{S}$ is β and the probability density for any point inside $\mathbb{S}$ is higher than those outside. Define for one observation v_i,

$$\gamma_i = 1 - \beta_{\min_i}, \tag{4.46}$$

where $\beta_{\min_i}$ is the smallest value of β for which $v_i \in \mathbb{S}_i$. Another way to think of γ_i is that it is the integral of $p(v_i^t|\boldsymbol{d})$ over the domain $\mathcal{V}_i = \{v_i^t : p(v_i^t|\boldsymbol{d}) < p(v_i|\boldsymbol{d})\}$. For samples $\{\boldsymbol{v}_{ij}\}_{j=1}^J$ of this distribution $p(v_i^t|\boldsymbol{d})$, we have

$$\gamma_i = \int_{\mathcal{V}_i} p(v_i^t|\boldsymbol{d}) dv_i^t \tag{4.47}$$

$$\simeq \frac{1}{J} \sum_j 1_{\boldsymbol{v}_{ij} \in \mathcal{V}_i}. \tag{4.48}$$

A delicate point here is the choice of tolerance τ: if $\gamma < \tau$, the model has been shown to be inconsistent with the observation(s). A typical value for the tolerance is 0.05, although there is an extensive discussion in the statistics literature about how to interpret this [23, 43, 47]. When comparing multiple observations but treating them as independent, as we will later on, the tolerance should be corrected and set lower because with many observations of a random variable it is more likely to make a low-probability observation. The Bonferroni correction suggests dividing the tolerance by the number of points [9]. Ideally, all data points will be clearly consistent with the model output (the model is not invalidated), or, at least one will be clearly inconsistent (the model is invalid and thus inadequate).

Chapter 5

Examples in Combustion Kinetics

This chapter presents a few examples of the stochastic operator applied to reduced models in combustion kinetics. First hydrogen combustion is examined. Two different formulations of the operator result due to the amount of information we claim to know about the detailed model. Second, methane combustion is investigated, a much more complex mechanism. The implementation of the operator for this problem helped illuminate many issues that needed to be resolved for a fully generalized formulation. Finally, the chapter concludes with a study of the effect of the inadequacy operator model on a prediction quantity of interest: the flamespeed of a hydrogen laminar flame. This shows the importance of including an inadequacy representation to make better predictions.

5.1 Hydrogen combustion

For the first example, the proposed inadequacy operator for a chemical mechanism model of hydrogen combustion is developed. Both the detailed model and its reduced version are described in [62]. In the detailed model, there are two types of atoms: hydrogen and oxygen; eight distinct species: H_2, O_2, H, O, OH, HO_2, H_2O, H_2O_2; and twenty-one elementary reactions. The reduced model includes five of the

given twenty-one reactions, and there are seven species tracked instead of eight. The resulting differential equations are much simpler than those given by the full model. Both the twenty-one- and five-step reaction mechanisms and corresponding forward reaction rates are listed in appendix A.

5.1.1 Calibration and validation of the reduced model

The first step is to calibrate the coefficients that make up the five reaction rates $\boldsymbol{k}$ using data generated by the detailed model. The observations are taken of each of the seven species tracked by the reduced model plus temperature, at five instances in time, and for one initial condition:

$$\boldsymbol{d} = \{d_{ijl}\}, \text{ where } d_{ijl} = x_i^D(t_j, IC_l), \quad i = 1, \ldots, 7; \quad j = 1, \ldots, 5; \quad l = 1, \quad (5.1)$$

and

$$d_{ijl} = T_i^D(t_j, IC_l), \quad i = 8; \quad j = 1, \ldots, 5; \quad l = 1. \quad (5.2)$$

Reindexing,

$$\boldsymbol{d} = \{d_i\}_{i=1}^{n_d}, \quad (5.3)$$

where $n_d = 8 \times 5 \times 1 = 40$. The set of time points is $\{20, 40, 60, 80, 100\}$µs. The initial condition is $\phi = 1.0$, $T_0 = 1500\,\mathrm{K}$. As usual, it is assumed that each observed value, d_i, is equal to the model output $\mathcal{M}_i^R(\boldsymbol{k})$ plus some measurement error, $\epsilon_i \sim \mathcal{N}(0, \sigma_{\epsilon_i}^2)$. Thus, the data model is:

$$d_i = \mathcal{M}_i^R(\boldsymbol{k}) + \epsilon_i. \quad (5.4)$$

As explained in § 4.3, the prior is $p(\boldsymbol{k}) = p(\boldsymbol{A})p(\boldsymbol{b})p(\boldsymbol{E})$, where

$$A_i \sim \log \mathcal{N}(\mu_i^A, \eta_i^A) \tag{5.5}$$

$$b_i \sim \mathcal{N}(\mu_i^b, \eta_i^b) \tag{5.6}$$

$$E_i \sim \mathcal{N}(\mu_i^E, \eta_i^E), \tag{5.7}$$

and $i = 1, \ldots, 5$. The values of μ^A, μ^b, and μ^E are the nominal values given in [62] (listed in appendix A). Given the data model above, the likelihood is:

$$p(\boldsymbol{d}|\boldsymbol{k}) = \frac{1}{(2\pi)^{40/2}|\Sigma|^{1/2}} \exp\left\{-\frac{1}{2}(\boldsymbol{d} - \mathcal{M}^R(\boldsymbol{k}))^T \Sigma^{-1} (\boldsymbol{d} - \mathcal{M}^R(\boldsymbol{k}))\right\}. \tag{5.8}$$

After calibrating the model parameters $\boldsymbol{k}$, the model output is compared to the observations. Figure 5.1 shows the observations, generated by the detailed model $\mathcal{D}$, compared to the reduced model $\mathcal{R}$ output. The distributions of the model account for parametric and measurement uncertainty. It is clear that some of the observations are not a plausible outcome of the reduced model, even with the calibrated parameters. There is also a severe difference between temperatures, shown in figure 5.2. Note that in each figure, the model output is shown with the mean and error bars corresponding to one and two standard deviations. The probability that many of the observations came from a system described by the reduced model is extremely low, especially those of H_2, H, H_2O, and temperature. By inspection of figures 5.1-5.2, it is obvious that several γ-values are essentially zero: the reduced model is thus deemed invalid and inadequate.

To account for the model inadequacy demonstrated above, the inadequacy operator $\mathcal{S}$ will now be constructed. In § 5.1.3, the full and proper derivation of $\mathcal{S}$ for this

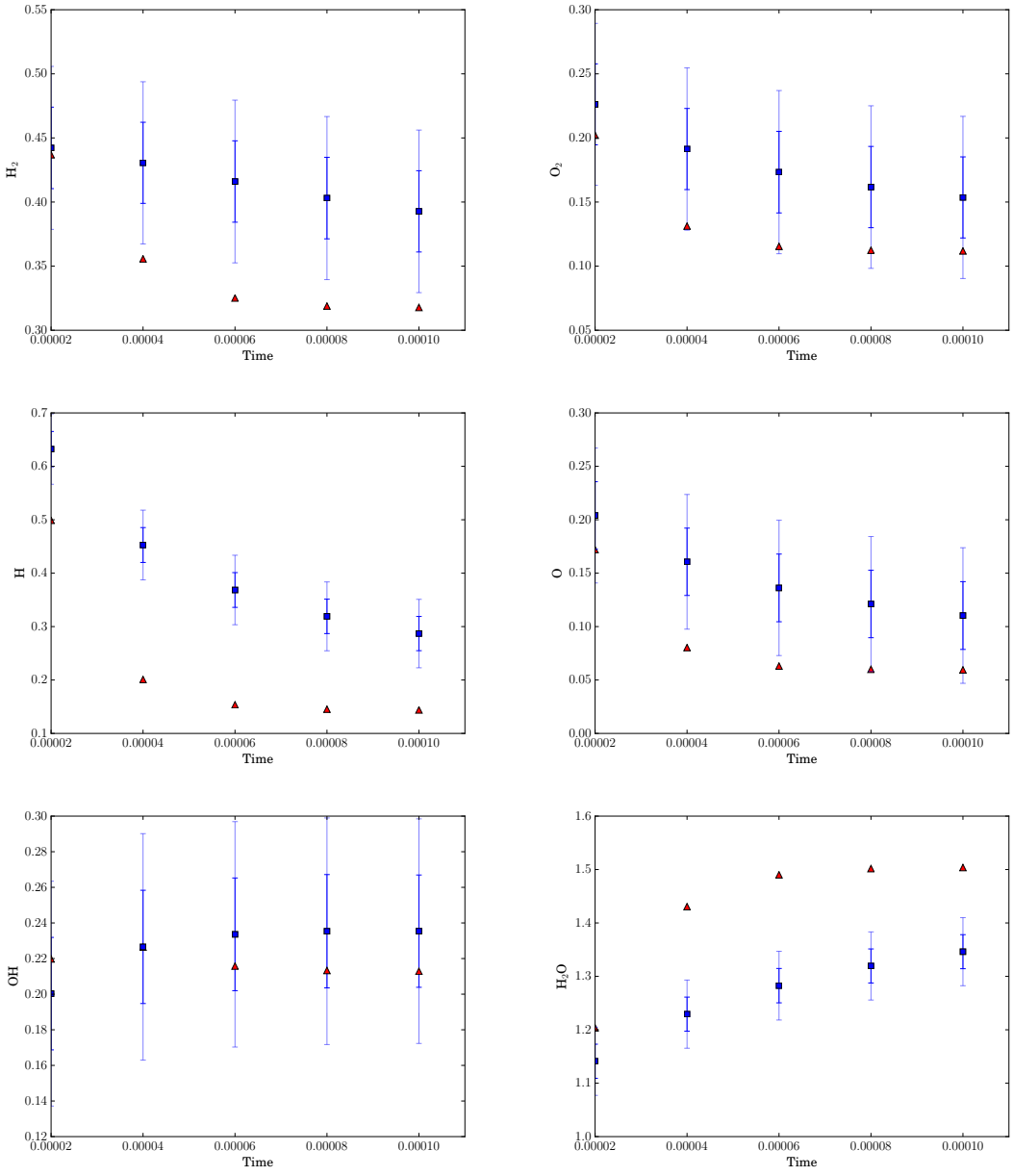

Figure 5.1: Concentrations [mol/m^3] versus time [s] for H_2/O_2 reaction, $\phi = 1.0$, $T_0 = 1500\,\mathrm{K}$. Observations (red), reduced model $\mathcal{R}$ (blue).

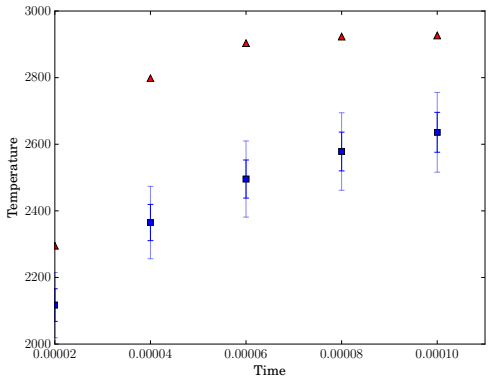

Figure 5.2: Temperature [K] versus time [s] for H_2/O_2 reaction, $\phi = 1.0$, $T_0 = 1500\,\mathrm{K}$. Observations (red), reduced model $\mathcal{R}$ (blue).

example problem will be presented. However, first a simplified version is presented. This simplified version only includes the linear parts S and W; there are no catchall species. This is possible since we know that the only omitted species in the reduced model is H_2O_2. Thus, the state vector is augmented by its concentration, as opposed to concentrations of each atom type (hydrogen and oxygen). This formulation was in fact the first approach taken towards formulating the operator. When reduced models with more than one omitted species were considered, it became clear that a more general formulation was needed, and so the catchall species and nonlinear reactions in $\mathcal{A}$ were included.

5.1.2 Case 1: The linear stochastic operator

As mentioned above, the state vector is augmented by the concentration of H_2O_2:

$$\boldsymbol{x}^S = [x_1, x_2, \ldots, x_8]^T, \tag{5.9}$$

with the concentrations given in the order of H_2, O_2, H, O, OH, HO_2, H_2O, H_2O_2. Note that in this example, $m_R = 5$ (number of reactions in $\mathcal{R}$), $n_R = 7$ (number of species in $\mathcal{R}$), $n_S = 8$ (number of species in $\mathcal{S}$), and $n_\alpha = 2$ (number of atom types).

To begin, theorem 3.3.1 showns that the matrix has the following structure:

$$S = \begin{pmatrix} s_{1,1} & 0 & s_{1,3} & 0 & s_{1,5} & s_{1,6} & s_{1,7} & s_{1,8} \\ 0 & s_{2,2} & 0 & s_{2,4} & s_{2,5} & s_{2,6} & s_{2,7} & s_{2,8} \\ s_{3,1} & 0 & s_{3,3} & 0 & s_{3,5} & s_{3,6} & s_{3,7} & s_{3,8} \\ 0 & s_{4,2} & 0 & s_{4,4} & s_{4,5} & s_{4,6} & s_{4,7} & s_{4,8} \\ 0 & 0 & 0 & 0 & s_{5,5} & s_{5,6} & s_{5,7} & s_{5,8} \\ 0 & 0 & 0 & 0 & s_{6,5} & s_{6,6} & s_{6,7} & s_{6,8} \\ 0 & 0 & 0 & 0 & s_{7,5} & s_{7,6} & s_{7,7} & s_{7,8} \\ 0 & 0 & 0 & 0 & s_{8,5} & s_{8,6} & s_{8,7} & s_{8,8} \end{pmatrix}. \tag{5.10}$$

Of the 64 entries of S, 24 are identically zero.

5.1.2.1 Constraints on the matrix S

Constraint (I) is that atoms be conserved. This is guaranteed by enforcing $ES = 0$, where E is the $n_\alpha \times n_S$ matrix:

$$E = \begin{pmatrix} 1 & 0 & 1 & 0 & 1/2 & 1/3 & 2/3 & 1/2 \\ 0 & 1 & 0 & 1 & 1/2 & 2/3 & 1/3 & 1/2 \end{pmatrix}. \tag{5.11}$$

The first row of E corresponds to hydrogen atoms and the second to oxygen. Entry e_{ij} denotes the fraction of atoms of type i in species j. Constraint (II) is that the concentrations cannot be negative. This is guaranteed by setting all off-diagonal elements of S to be non-negative.

5.1.2.2 Construction of the matrix S

The next step is to construct the matrix S, while simultaneously satisfying both constraints above. To do this, note that S lives in the nullspace of E, denoted null(E). Let C be the following 8×6 matrix whose columns span null(E):

$$C = \begin{pmatrix} -1 & 0 & -1/2 & -1/3 & -2/3 & -1/2 \\ 0 & -1 & -1/2 & -2/3 & -1/3 & -1/2 \\ 1 & 0 & 0 & 0 & 0 & 0 \\ 0 & 1 & 0 & 0 & 0 & 0 \\ 0 & 0 & 1 & 0 & 0 & 0 \\ 0 & 0 & 0 & 1 & 0 & 0 \\ 0 & 0 & 0 & 0 & 1 & 0 \\ 0 & 0 & 0 & 0 & 0 & 1 \end{pmatrix}. \tag{5.12}$$

The column vectors of C have been carefully chosen such that the lower 6×6 block is the identity matrix, and all entries in the first two rows are negative or zero. Now let P be a 6×8 matrix, where $S = CP$:

$$P = \begin{pmatrix} q_{1,1} & 0 & q_{1,3} & 0 & q_{1,5} & q_{1,6} & q_{1,7} & q_{1,8} \\ 0 & q_{2,2} & 0 & q_{2,4} & q_{2,5} & q_{2,6} & q_{2,7} & q_{2,8} \\ 0 & 0 & 0 & 0 & q_{3,5} & q_{3,6} & q_{3,7} & q_{3,8} \\ 0 & 0 & 0 & 0 & q_{4,5} & q_{4,6} & q_{4,7} & q_{4,8} \\ 0 & 0 & 0 & 0 & q_{5,5} & q_{5,6} & q_{5,7} & q_{5,8} \\ 0 & 0 & 0 & 0 & q_{6,5} & q_{6,6} & q_{6,7} & q_{6,8} \end{pmatrix}. \tag{5.13}$$

Clearly the matrix C is deterministic, but the entries of P are random. Moreover, constraints on S imply constraints on the distributions of each entry $p_{i,j}$. Through this decomposition, C is used to enforce conservation of atoms, and P serves to guarantee positivity of concentrations. In § 3.4, a more concise but generalized explanation of the inequality constraints placed on the entries of P is given. The following is a more verbose description to show the full process. To begin, the following is necessary to

ensure a negative diagonal in S:

$$s_{1,1} \leq 0 \quad \rightarrow \quad p_{1,1} \geq 0 \tag{5.14}$$

$$s_{2,2} \leq 0 \quad \rightarrow \quad p_{2,2} \geq 0 \tag{5.15}$$

$$s_{3,3} \leq 0 \quad \rightarrow \quad p_{1,3} \leq 0 \tag{5.16}$$

$$s_{4,4} \leq 0 \quad \rightarrow \quad p_{2,4} \leq 0 \tag{5.17}$$

$$s_{5,5} \leq 0 \quad \rightarrow \quad p_{3,5} \leq 0 \tag{5.18}$$

$$s_{6,6} \leq 0 \quad \rightarrow \quad p_{4,6} \leq 0 \tag{5.19}$$

$$s_{7,7} \leq 0 \quad \rightarrow \quad p_{5,7} \leq 0 \tag{5.20}$$

$$s_{8,8} \leq 0 \quad \rightarrow \quad p_{6,8} \leq 0. \tag{5.21}$$

To have a non-negative off-diagonal in S, all other nonzero entries of P must be non-negative:

$$s_{i,j} \geq 0, \quad \rightarrow \quad p_{k,l} \geq 0, \tag{5.22}$$

where

$$\begin{aligned}(ij) \in \{&(35),(36),(37),(38),(45),(46),(47),(48),(56),(57)\\ &(58),(65),(67),(68),(75),(76),(78),(85),(86),(87)\}\end{aligned} \tag{5.23}$$

with the corresponding (kl):

$$\begin{aligned}(kl) \in \{&(15),(16),(17),(18),(25),(26),(27),(28),(36),(37),\\ &(38),(45),(47),(48),(55),(56),(58),(65),(66),(67)\}.\end{aligned} \tag{5.24}$$

Next, the negative entries must have sufficiently large magnitudes to ensure that the elements in the top two rows of S are positive:

$$s_{1,5} \geq 0 \quad \rightarrow \quad p_{3,5} \leq -2\left(-p_{1,5} - \frac{1}{3}p_{4,5} - \frac{2}{3}p_{5,5} - \frac{1}{2}p_{6,5}\right) \tag{5.25}$$

$$s_{2,5} \geq 0 \quad \rightarrow \quad p_{3,5} \leq -2\left(-p_{2,5} - \frac{2}{3}p_{4,5} - \frac{1}{3}p_{5,5} - \frac{1}{2}p_{6,5}\right) \tag{5.26}$$

$$s_{1,6} \geq 0 \quad \rightarrow \quad p_{4,6} \leq -3\left(-p_{1,6} - \frac{1}{2}p_{3,6} - \frac{2}{3}p_{5,6} - \frac{1}{2}p_{6,6}\right) \tag{5.27}$$

$$s_{2,6} \geq 0 \quad \rightarrow \quad p_{4,6} \leq -2\left(-p_{2,6} - \frac{1}{2}p_{3,6} - \frac{1}{3}p_{5,6} - \frac{2}{3}p_{6,6}\right) \tag{5.28}$$

$$s_{1,7} \geq 0 \quad \rightarrow \quad p_{6,8} \leq -\frac{3}{2}\left(-p_{1,7} - \frac{1}{2}p_{3,7} - \frac{1}{3}p_{4,7} - \frac{1}{2}p_{6,7}\right) \tag{5.29}$$

$$s_{2,7} \geq 0 \quad \rightarrow \quad p_{6,8} \leq -3\left(-p_{2,7} - \frac{1}{2}p_{3,7} - \frac{2}{3}p_{4,7} - \frac{1}{2}p_{6,7}\right) \tag{5.30}$$

$$s_{1,8} \geq 0 \quad \rightarrow \quad p_{6,8} \leq -2\left(-p_{1,8} - \frac{1}{2}p_{3,8} - \frac{1}{3}p_{4,8} - \frac{2}{3}p_{5,8}\right) \tag{5.31}$$

$$s_{2,8} \geq 0 \quad \rightarrow \quad p_{6,8} \leq -2\left(-p_{2,8} - \frac{1}{2}p_{3,8} - \frac{2}{3}p_{4,8} - \frac{1}{3}p_{5,8}\right). \tag{5.32}$$

These are more constraining than some listed in lines (5.14) - (5.21). Also, for each entry of P above, two inequalities are given. These can be condensed into a single inequality which satisfies both inequalities above:

$$p_{3,5} \leq -2\left(-p_{1,5} - p_{2,5} - \frac{2}{3}p_{4,5} - \frac{2}{3}p_{5,5} - \frac{1}{2}p_{6,5}\right) \tag{5.33}$$

$$p_{4,6} \leq -3\left(-p_{1,6} - p_{2,6} - \frac{1}{2}p_{3,6} - \frac{2}{3}p_{5,6} - \frac{1}{2}p_{6,6}\right) \tag{5.34}$$

$$p_{6,8} \leq -3\left(-p_{1,7} - p_{2,7} - \frac{1}{2}p_{3,7} - \frac{2}{3}p_{4,7} - \frac{1}{2}p_{6,7}\right) \tag{5.35}$$

$$p_{6,8} \leq -2\left(-p_{1,8} - p_{2,8} - \frac{1}{2}p_{3,8} - \frac{2}{3}p_{4,8} - \frac{2}{3}q_{5,8}\right). \tag{5.36}$$

The final four inequalities correspond to equation 3.37 in the general operator formulation.

To account for these inequalities, the nonzero entries of P are transformed to a new set ξ_i, $i = 1, \ldots, 28$. The transform is given in table 5.1. This new set makes use of translation and reflection so that the constraints take the simple form

$$\xi_i \geq 0, \quad i = 1, \ldots, 28. \tag{5.37}$$

5.1.2.3 The catchall reactions $\mathcal{A}$

Since $\mathcal{A}$ only includes reactions whose reactants are catchall species, there is no operator $\mathcal{A}$ in this case.

5.1.2.4 The energy operator W

Recall that the energy equation was removed from $\mathcal{R}$ and placed in W. In this case, there are no catchall species but instead the set of species is augmented by H_2O_2. But internal energy and specific heats for hydrogen peroxide are of course known (at least as well as the other chemical species), so there are no new random variables introduced with this component of the operator. Therefore, the only inadequacy parameters are $\boldsymbol{\xi}$.

5.1.2.5 The probabilistic structure of the random matrix

The final step in construction of the stochastic operator is to describe the probabilistic structure. At this point, each $\xi_i \geq 0$; let

$$\xi_i \sim \log \mathcal{N}(\mu_i^{\xi}, \eta_i^{\xi}), \quad i = 1, \ldots, 28. \tag{5.38}$$

ξ_i	$=$	$p_{j,k}$
ξ_1	$=$	$p_{1,1}$
ξ_2	$=$	$-p_{1,3}$
ξ_3	$=$	$p_{1,5}$
ξ_4	$=$	$p_{1,6}$
ξ_5	$=$	$p_{1,7}$
ξ_6	$=$	$p_{1,8}$
ξ_7	$=$	$p_{2,2}$
ξ_8	$=$	$-p_{2,4}$
ξ_9	$=$	$p_{2,5}$
ξ_{10}	$=$	$p_{2,6}$
ξ_{11}	$=$	$p_{2,7}$
ξ_{12}	$=$	$p_{2,8}$
ξ_{13}	$=$	$-\left[p_{3,5} - 2(p_{1,5} + p_{2,5} + (2/3)p_{4,5} + (2/3)p_{5,5} + (1/2)p_{65})\right]$
ξ_{14}	$=$	$p_{3,6}$
ξ_{15}	$=$	$p_{3,7}$
ξ_{16}	$=$	$p_{3,8}$
ξ_{17}	$=$	$p_{4,5}$
ξ_{18}	$=$	$-\left[p_{4,6} - 3(p_{1,6} + p_{2,6} + (1/2)p_{3,6} + (2/3)p_{5,6} + (1/2)p_{66})\right]$
ξ_{19}	$=$	$p_{4,7}$
ξ_{20}	$=$	$p_{4,8}$
ξ_{21}	$=$	$p_{5,5}$
ξ_{22}	$=$	$p_{5,6}$
ξ_{23}	$=$	$-\left[p_{5,7} - 3(p_{1,7} + p_{2,7} + (1/2)p_{3,7} + (2/3)p_{4,7} + (1/2)p_{6,7})\right]$
ξ_{24}	$=$	$p_{5,8}$
ξ_{25}	$=$	$p_{6,5}$
ξ_{26}	$=$	$p_{6,6}$
ξ_{27}	$=$	$p_{6,7}$
ξ_{28}	$=$	$-\left[p_{6,8} - 2(p_{1,8} + p_{2,8} + (1/2)p_{3,8} + (2/3)p_{4,8} + (2/3)p_{5,8})\right]$

Table 5.1: The transformed variables $\boldsymbol{\xi}$ for the case 1 H_2/O_2 operator.

This completes the description of the operator, that is, the form of the operator is set but has not been calibrated. The next subsection describes the calibration of the inadequacy parameters $\boldsymbol{\xi}$ and their hyperparameters $\boldsymbol{\mu}^{\xi}$ and $\boldsymbol{\eta}^{\xi}$.

5.1.2.6 Calibration of the case 1 operator

The complete set of observations used in this calibration is

$$\boldsymbol{d} = \{d_{ijk}\}, \quad i = 1, \ldots, 8; \quad j = 1, \ldots, 5; \quad l = 1, \ldots, 3, \tag{5.39}$$

where i corresponds to species type or temperature, j to time of measurement, and l to initial condition. The initial condition is $IC = \{\phi, T_0\}$. Here this includes three different ϕ (0.9, 1.0, 1.1) at a single initial temperature $T_0 = 1500\,\mathrm{K}$. (In the more general operator with catchall species, the intial conditions will also include a range of temperatures.) The set can be rewritten as

$$\boldsymbol{d} = \{d_i\}_{i=1}^{n_d}, \tag{5.40}$$

where $n_d = 8 \times 5 \times 3 = 120$.

The prior distribution is:

$$p(\boldsymbol{\xi}, \boldsymbol{\mu}^{\xi}, \boldsymbol{\eta}^{\xi}, \boldsymbol{k}) = p(\boldsymbol{\xi}|\boldsymbol{\mu}^{\xi}, \boldsymbol{\eta}^{\xi}) p(\boldsymbol{\mu}^{\xi}) p(\boldsymbol{\eta}^{\xi}) p(\boldsymbol{A}) p(\boldsymbol{b}) p(\boldsymbol{E}), \tag{5.41}$$

where

$$\xi_i \sim \log \mathcal{N}(\mu_i^{\xi}, \eta_i^{\xi}) \tag{5.42}$$

$$\mu_i^{\xi} \sim \mathcal{N}(\mu_i^{\mu^{\xi}}, \eta_i^{\mu^{\xi}}) \tag{5.43}$$

$$\eta_i^{\xi} \sim \mathcal{J}(0, \infty), \tag{5.44}$$

for $i = 1, \ldots, 28$. The prior distribution for the reaction rate constants is the same as for the reduced model.

The likelihood is given by

$$p(\boldsymbol{d}|\boldsymbol{\xi}, \boldsymbol{\mu}^{\xi}, \boldsymbol{\eta}^{\xi}, \boldsymbol{k}) = p(\boldsymbol{d}|\boldsymbol{\xi}, \boldsymbol{k}) \tag{5.45}$$

$$= \frac{1}{(2\pi)^{120/2}|\Sigma|^{1/2}} \exp\left\{-\frac{1}{2}(\boldsymbol{d} - \mathcal{M}^S(\boldsymbol{\xi}, \boldsymbol{k}))^T \Sigma^{-1} (\boldsymbol{d} - \mathcal{M}^S(\boldsymbol{\xi}, \boldsymbol{k}))\right\}. \tag{5.46}$$

Finally, the posterior is proportional to the product of the likelihood and the prior, which yields

$$p(\boldsymbol{\xi}, \boldsymbol{\mu}^{\xi}, \boldsymbol{\eta}^{\xi}, \boldsymbol{k}|\boldsymbol{d}) \propto p(\boldsymbol{d}|\boldsymbol{\xi}, \boldsymbol{\mu}^{\xi}, \boldsymbol{\eta}^{\xi}, \boldsymbol{k}) p(\boldsymbol{\xi}, \boldsymbol{\mu}^{\xi}, \boldsymbol{\eta}^{\xi}, \boldsymbol{k}) \tag{5.47}$$

$$= \left[p(\boldsymbol{d}|\boldsymbol{\xi}, \boldsymbol{k})\right] \left[p(\boldsymbol{\xi}|\boldsymbol{\mu}^{\xi}, \boldsymbol{\eta}^{\xi}) p(\boldsymbol{\mu}^{\xi}) p(\boldsymbol{\eta}^{\xi}) p(\boldsymbol{k})\right], \tag{5.48}$$

with the two bracketed terms given by (5.46) and (5.41), respectively.

As described previously, the posterior distribution $p(\boldsymbol{\xi}, \boldsymbol{\mu}^{\xi}, \boldsymbol{\eta}^{\xi}, \boldsymbol{k}|\boldsymbol{d})$ (of dimension 99) is sampled using Delayed Rejection Adaptive Metroplis (DRAM) [29], implemented with the software QUESO [14, 48].

5.1.2.7 Validation of the case 1 operator

In this subsection selected results from the operator are presented. Overall, the calibrated operator works very well and is able to account for the discrepancy between the reduced model $\mathcal{R}$ and the data. For example, figure 5.4 shows the same data points as in figure 5.1, where it was shown that the reduced model was unable to predict H_2, H, and H_2O concentrations. With the inadequacy operator, the data

is clearly consistent with the model. The other two initial conditions are shown in figures 5.3 and 5.5. Finally, the operator output matches the temperature for most of the points, although there are some, especially for the second time point, that is missed by model $\mathcal{O}$ output. In the next subsection, with the more complete operator formulation and broader set of initial conditions, this will be improved. Figure 5.6 displays the temperature time-series for the three cases of ϕ.

5.1.3 Case 2: Catchall species

While it was helpful (and easier) to know that the only missing species was hydrogen peroxide, in general there may be close to fifty or so unrepresented species. If so, the catchall formulation is necessary; this is now developed for the same hydrogen-oxygen reaction. That is, the general formulation of $\mathcal{S}$ as described in chapter 3 follows.

First,

$$\boldsymbol{x}^S = [x_1, x_2, \ldots, x_9]^T, \tag{5.49}$$

with the concentrations given in the order of H′, O′, H_2, O_2, H, O, OH, HO_2, H_2O. Note $m_R = 5$, $n_R = 7$, $n_\alpha = 2$, $n_S = 9$.

5.1.3.1 The random matrix S

The explanation of the matrices S, E, C, and P and of the random variables $\boldsymbol{\xi}$ is completely analogous to the previous case. Therefore, these are given with minimal motivation. Later, we focus on the additional pieces of the operator, $\mathcal{A}$ and W.

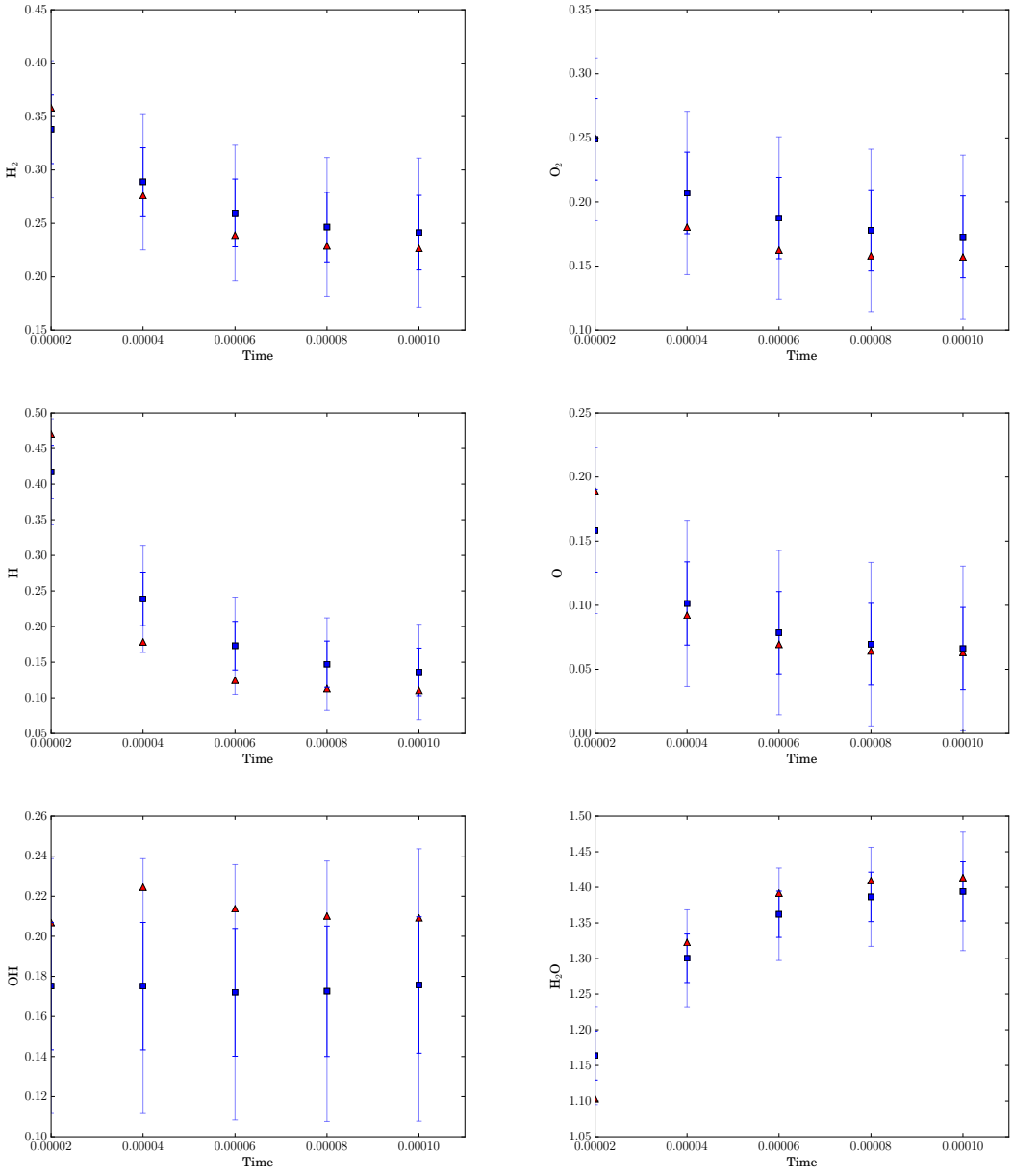

Figure 5.3: Concentrations [mol/m^3] versus time [s] for H_2/O_2 reaction, $\phi = 0.9$, $T_0 = 1500\,\mathrm{K}$. Observations (red), case 1 operator model $\mathcal{O}$ (blue).

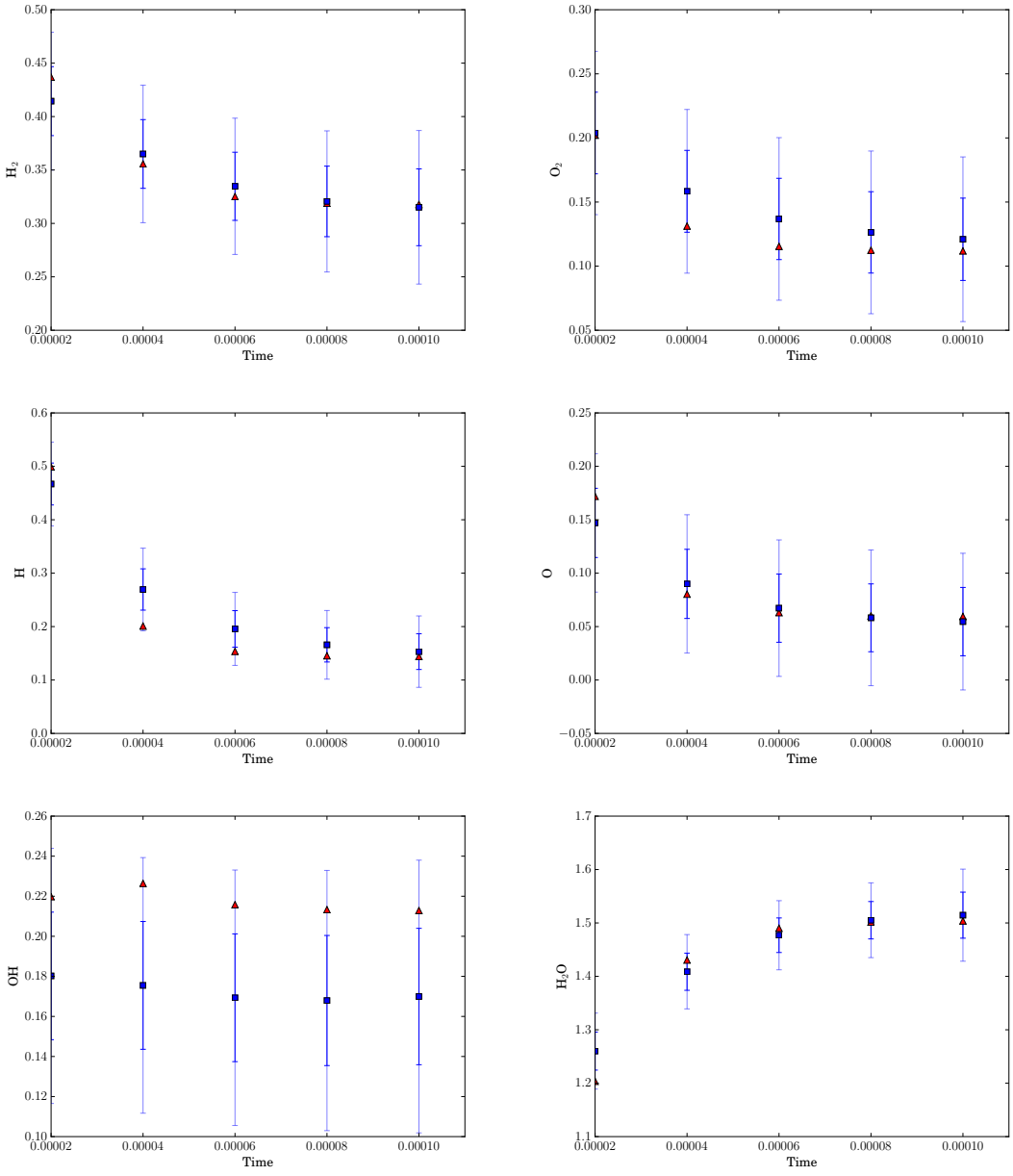

Figure 5.4: Concentrations [mol/m^3] versus time [s] for H_2/O_2 reaction, $\phi = 1.0$, $T_0 = 1500\,\mathrm{K}$. Observations (red), case 1 operator model $\mathcal{O}$ (blue).

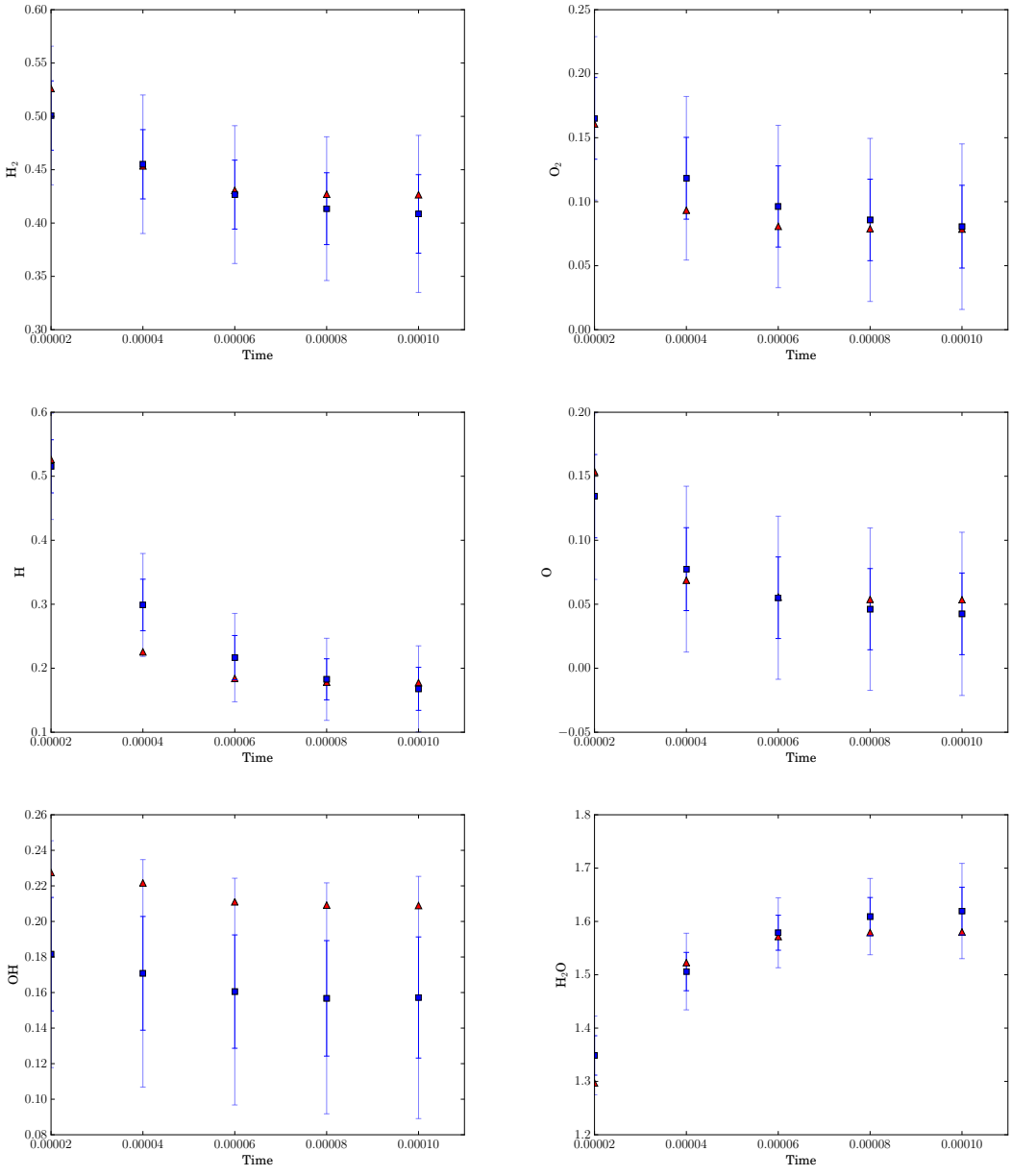

Figure 5.5: Concentrations [mol/m^3] versus time [s] for H_2/O_2 reaction, $\phi = 1.1$, $T_0 = 1500\,\mathrm{K}$. Observations (red), case 1 operator model $\mathcal{O}$ (blue).

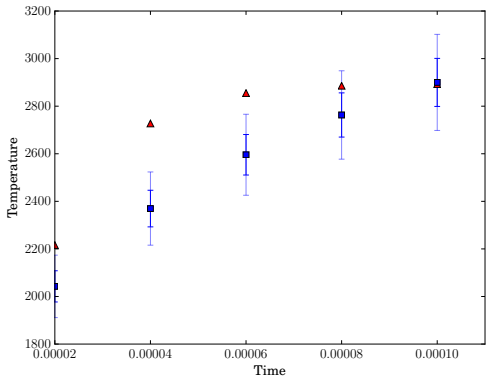

(a) $\phi = 0.9$

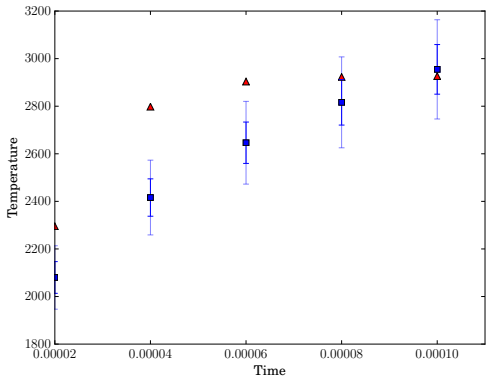

(b) $\phi = 1.0$

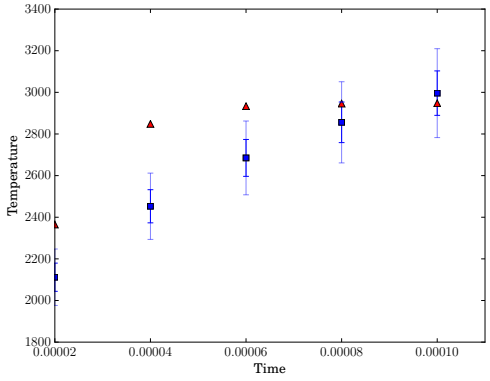

(c) $\phi = 1.1$

Figure 5.6: Temperature [K] versus time [s] for H_2/O_2 reaction, $\phi = \{0.9, 1.0, 1.1\}$, $T_0 = 1500\,\mathrm{K}$. Observations (red), case 1 operator model $\mathcal{O}$ (blue).

From theorem 3.3.1, we know that the matrix has the following structure:

$$S = \begin{pmatrix} s_{1,1} & 0 & s_{1,3} & 0 & s_{1,5} & 0 & s_{1,7} & s_{1,8} & s_{1,9} \\ 0 & s_{2,2} & 0 & s_{2,4} & 0 & s_{2,6} & s_{2,7} & s_{2,8} & s_{2,9} \\ s_{3,1} & 0 & s_{3,3} & 0 & s_{3,5} & 0 & s_{3,7} & s_{3,8} & s_{3,9} \\ 0 & s_{4,2} & 0 & s_{4,4} & 0 & s_{4,6} & s_{4,7} & s_{4,8} & s_{4,9} \\ s_{5,1} & 0 & s_{5,3} & 0 & s_{5,5} & 0 & s_{5,7} & s_{5,8} & s_{5,9} \\ 0 & s_{6,2} & 0 & s_{6,4} & 0 & s_{6,6} & s_{6,7} & s_{6,8} & s_{6,9} \\ 0 & 0 & 0 & 0 & 0 & 0 & s_{7,7} & s_{7,8} & s_{7,9} \\ 0 & 0 & 0 & 0 & 0 & 0 & s_{8,7} & s_{8,8} & s_{8,9} \\ 0 & 0 & 0 & 0 & 0 & 0 & s_{9,7} & s_{9,8} & s_{9,9} \end{pmatrix}. \tag{5.50}$$

Here, of the 81 entries of S, 42 are identically zero. E is the $n_\alpha \times n_S$ matrix:

$$E = \begin{pmatrix} 1 & 0 & 1 & 0 & 1 & 0 & 1/2 & 1/3 & 2/3 \\ 0 & 1 & 0 & 1 & 0 & 1 & 1/2 & 2/3 & 1/3 \end{pmatrix}. \tag{5.51}$$

Again, the first row of E corresponds to hydrogen atoms and the second to oxygen. C is the following $n_S \times n_R$ matrix whose columns span null(E):

$$C = \begin{pmatrix} -1 & 0 & -1 & 0 & -1/2 & -1/3 & -2/3 \\ 0 & -1 & 0 & -1 & -1/2 & -2/3 & -1/3 \\ 1 & 0 & 0 & 0 & 0 & 0 & 0 \\ 0 & 1 & 0 & 0 & 0 & 0 & 0 \\ 0 & 0 & 1 & 0 & 0 & 0 & 0 \\ 0 & 0 & 0 & 1 & 0 & 0 & 0 \\ 0 & 0 & 0 & 0 & 1 & 0 & 0 \\ 0 & 0 & 0 & 0 & 0 & 1 & 0 \\ 0 & 0 & 0 & 0 & 0 & 0 & 1 \end{pmatrix}. \tag{5.52}$$

P is an $n_R \times n_S$ matrix, where $S = CP$:

$$P = \begin{pmatrix} p_{1,1} & 0 & p_{1,3} & 0 & p_{1,5} & 0 & p_{1,7} & p_{1,8} & p_{1,9} \\ 0 & p_{2,2} & 0 & p_{2,4} & 0 & p_{2,6} & p_{2,7} & p_{2,8} & p_{2,9} \\ p_{3,1} & 0 & p_{3,3} & 0 & p_{3,5} & 0 & p_{3,7} & p_{3,8} & p_{3,9} \\ 0 & p_{4,2} & 0 & p_{4,4} & 0 & p_{4,6} & p_{4,7} & p_{4,8} & p_{4,9} \\ 0 & 0 & 0 & 0 & 0 & 0 & p_{5,7} & p_{5,8} & p_{5,9} \\ 0 & 0 & 0 & 0 & 0 & 0 & p_{6,7} & p_{6,8} & p_{6,9} \\ 0 & 0 & 0 & 0 & 0 & 0 & p_{7,7} & p_{7,8} & p_{7,9} \end{pmatrix}. \tag{5.53}$$

The transform is given in table 5.2, and the constraints are now

$$\xi_i \geq 0, \quad i = 1, \ldots, 33. \tag{5.54}$$

Finally, to complete the formulation of S,

$$\xi_i \sim \log \mathcal{N}(\mu_i^{\xi}, \eta_i^{\xi}), \quad i = 1, \ldots, 33. \tag{5.55}$$

5.1.3.2 The catchall reactions $\mathcal{A}$

The catchall reactions allow the catchall species to directly form any species made up of more than one type of atom. Otherwise, that reaction is already allowed via S ($\mathrm{H}' \longrightarrow \mathrm{H}$ is allowed by S for example). Thus, there are three catchall reactions:

$$\mathrm{H}' + \mathrm{O}' \xrightarrow{\kappa_1} \mathrm{OH} \tag{5.56}$$

$$\mathrm{H}' + 2\,\mathrm{O}' \xrightarrow{\kappa_2} \mathrm{HO_2} \tag{5.57}$$

$$2\,\mathrm{H}' + \mathrm{O}' \xrightarrow{\kappa_3} \mathrm{H_2O}. \tag{5.58}$$

The reaction rate coefficients are denoted κ, and these are included in the set of inadequacy parameters. Like the variables $\boldsymbol{\xi}$, each κ will be modeled with a lognormal distribution whose hyperparameters are also calibrated. From the reactions above, the associated rates of each is:

$$r_1' = \kappa_1 x_1 x_2 \tag{5.59}$$

$$r_2' = \kappa_2 x_1 x_2 \tag{5.60}$$

$$r_3' = \kappa_3 x_1 x_2, \tag{5.61}$$

ξ_i	=	$p_{j,k}$
ξ_1	=	$p_{1,1}$
ξ_2	=	$-(p_{1,3}+p_{3,3})$
ξ_3	=	$p_{1,5}$
ξ_4	=	$p_{1,7}$
ξ_5	=	$p_{1,8}$
ξ_6	=	$p_{1,9}$
ξ_7	=	$p_{2,2}$
ξ_8	=	$-(p_{2,4}+p_{4,4})$
ξ_9	=	$p_{2,6}$
ξ_{10}	=	$p_{2,7}$
ξ_{11}	=	$p_{2,8}$
ξ_{12}	=	$p_{2,9}$
ξ_{13}	=	$p_{3,1}$
ξ_{14}	=	$p_{3,3}$
ξ_{15}	=	$-(p_{3,5}+p_{1,5})$
ξ_{16}	=	$p_{3,7}$
ξ_{17}	=	$p_{3,8}$
ξ_{18}	=	$p_{3,9}$
ξ_{19}	=	$p_{4,2}$
ξ_{20}	=	$p_{4,4}$
ξ_{21}	=	$-(p_{4,6}+p_{2,6})$
ξ_{22}	=	$p_{4,7}$
ξ_{23}	=	$p_{4,8}$
ξ_{24}	=	$p_{4,9}$
ξ_{25}	=	$-p_{5,7}-2(p_{1,7}+p_{2,7}+p_{3,7}+p_{4,7}+(2/3)p_{6,7}+(2/3)p_{7,7})$
ξ_{26}	=	$p_{5,8}$
ξ_{27}	=	$p_{5,9}$
ξ_{28}	=	$p_{6,7}$
ξ_{29}	=	$-p_{6,8}-3(p_{1,8}+p_{2,8}+p_{3,8}+p_{4,8}+(1/2)p_{5,8}+(2/3)p_{7,8})$
ξ_{30}	=	$p_{6,9}$
ξ_{31}	=	$p_{7,7}$
ξ_{32}	=	$p_{7,8}$
ξ_{33}	=	$-p_{7,9}-3(p_{1,9}+p_{2,9}+p_{3,9}+p_{4,9}+(1/2)p_{5,9}+(2/3)p_{6,9})$

Table 5.2: The transformed variables $\boldsymbol{\xi}$ for the case 2 H_2/O_2 operator.

and the resulting additions to the differential equations for H′, O′, OH, HO_2, and H_2O are

$$\text{H}': \quad -r_1' - r_2' - 2r_3' \tag{5.62}$$

$$\text{O}': \quad -r_1' - 2r_2' - r_3' \tag{5.63}$$

$$\text{OH}: \quad +r_1' \tag{5.64}$$

$$\text{HO}_2: \quad +r_2' \tag{5.65}$$

$$\text{H}_2\text{O}: \quad +r_3'. \tag{5.66}$$

The terms above (5.62) - (5.66) are written as $\mathcal{A}(\boldsymbol{x})$.

5.1.3.3 The energy operator W

The third and final piece of the operator $\mathcal{S}$ is the energy operator W. Recall

$$\frac{dT}{dt} = W(\boldsymbol{x}, \dot{\boldsymbol{x}}, T) = -\left(\frac{1}{\sum_i^{n_S} c_{v_i}(T) x_i}\right)\left(\sum_i^{n_S} u_i(T)\dot{x}_i\right) \tag{5.67}$$

and so a description of $u(T)$ and $c_v(T)$ for each catchall species is necessary. To do so, the new parameters α_0, α_1, and α_2 are introduced. That is,

$$u_i(T) = \alpha_{0_i} + \alpha_{1_i} T + \alpha_{2_i} T^2 \tag{5.68}$$

$$c_{v_i}(T) = \alpha_{1_i} + 2\alpha_{2_i} T, \tag{5.69}$$

where $i = 1$ corresponds to H′ and $i = 2$ to O′.

5.1.3.4 Calibration and validation of the case 2 operator

In case 1, data was generated for three initial conditions corresponding to three different values of ϕ. In case 2 there are nine initial conditions given by the

combinations of $\phi = \{.9, 1.0, 1.1\}$ and initial temperature $T_0 = \{1450, 1500, 1550\}$K. The set of time points is again $\{20, 40, 60, 80, 100\}$µs. The prior, likelihood, and posterior distributions exactly follow from the general form in § 4.5. After calibration, and similar to the first case, the stochastic operator with catchall species displays excellent agreement with the data. Figures 5.7- 5.15 shows the model output for the nine different initial conditions. Finally, the temperature output also shows good agreement with the data, shown in figure 5.17.

This concludes the section on the H_2/O_2 reaction. In the final section of this chapter, the calibrated case 1 inadequacy operator found here is used to predict the flamespeed of a 1D hydrogen laminar flame. First, however, another example reaction is presented: methane-air combustion.

5.2 Methane combustion

The second main example problem investigated is methane-air combustion. Methane combustion is an incredibly complex process: detailed mechanisms include over 300 elementary reactions and fifty or more species. At the same time, methane is the simplest hydrocarbon— combustion models with ethane (C_2H_4) or propane (C_3H_8) are even less well understood but might involve close to 500 reactions [26]. In any case, solving for these reactions is very time-consuming. Moreover, in a larger fluids problem, this model may be incorporated to provide source terms at every point in space and time. The resulting computational complexity is the true motivation for the use of reduced models, and in turn, characterizing the inadequacy of such reduced models without scaling back up in complexity to the detailed model.

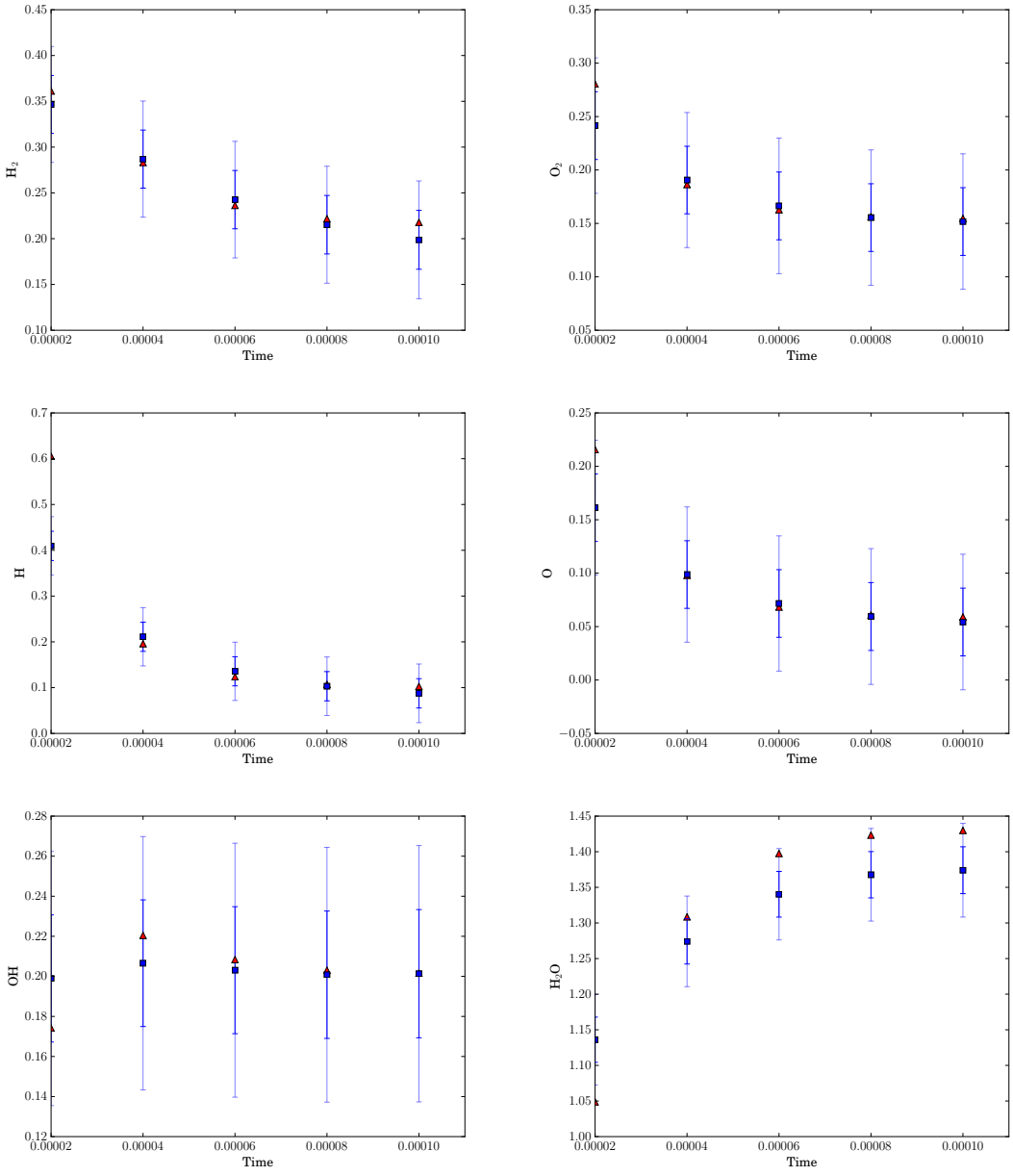

Figure 5.7: Concentrations [mol/m^3] versus time [s] for H_2/O_2 reaction, $\phi = 0.9$, $T_0 = 1450\,\mathrm{K}$. Observations (red), case 2 operator model $\mathcal{O}$ (blue).

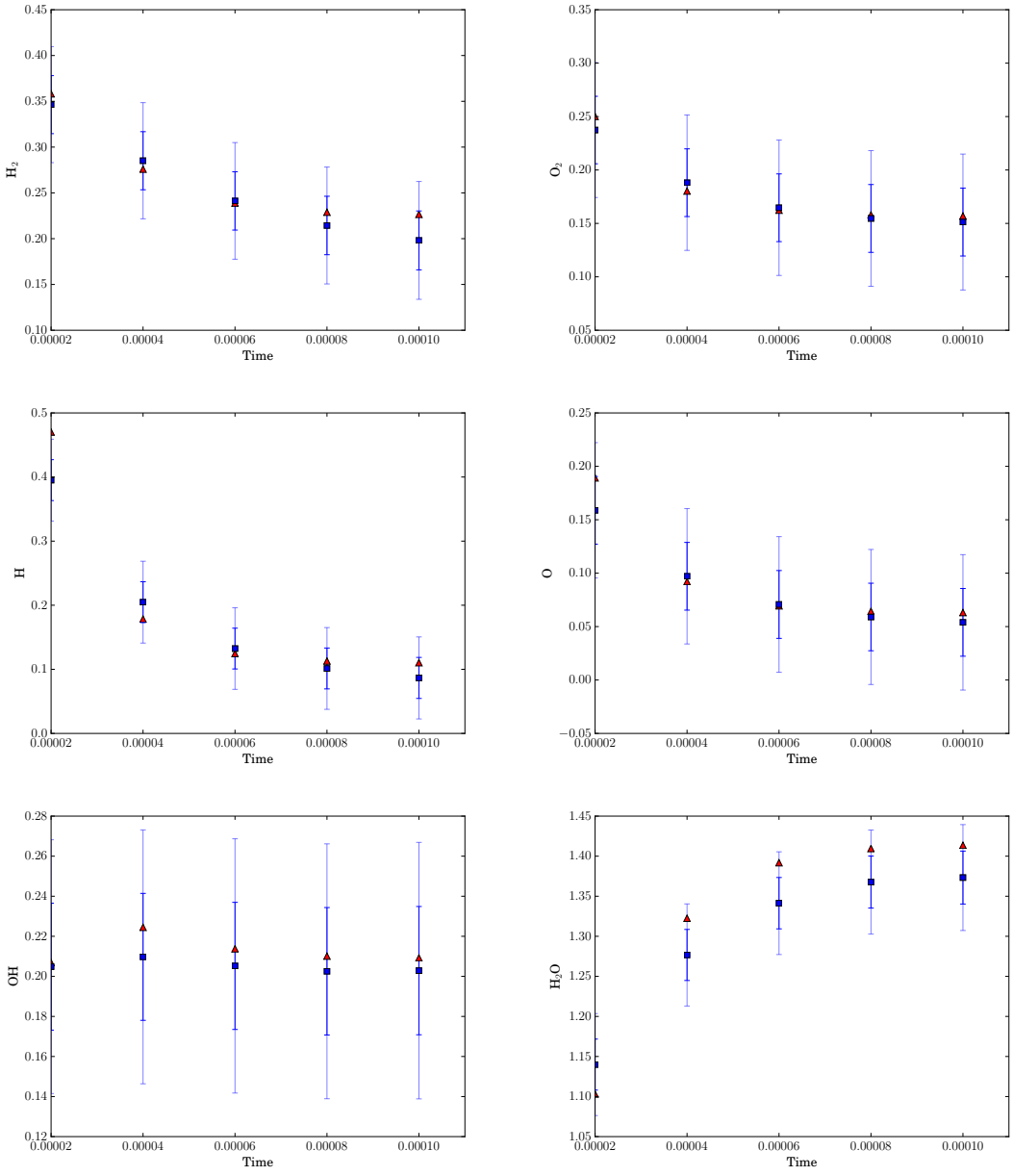

Figure 5.8: Concentrations [mol/m^3] versus time [s] for $\phi = 0.9$, $T_0 = 1500\,\mathrm{K}$. Observations (red), case 2 operator model $\mathcal{O}$ (blue).

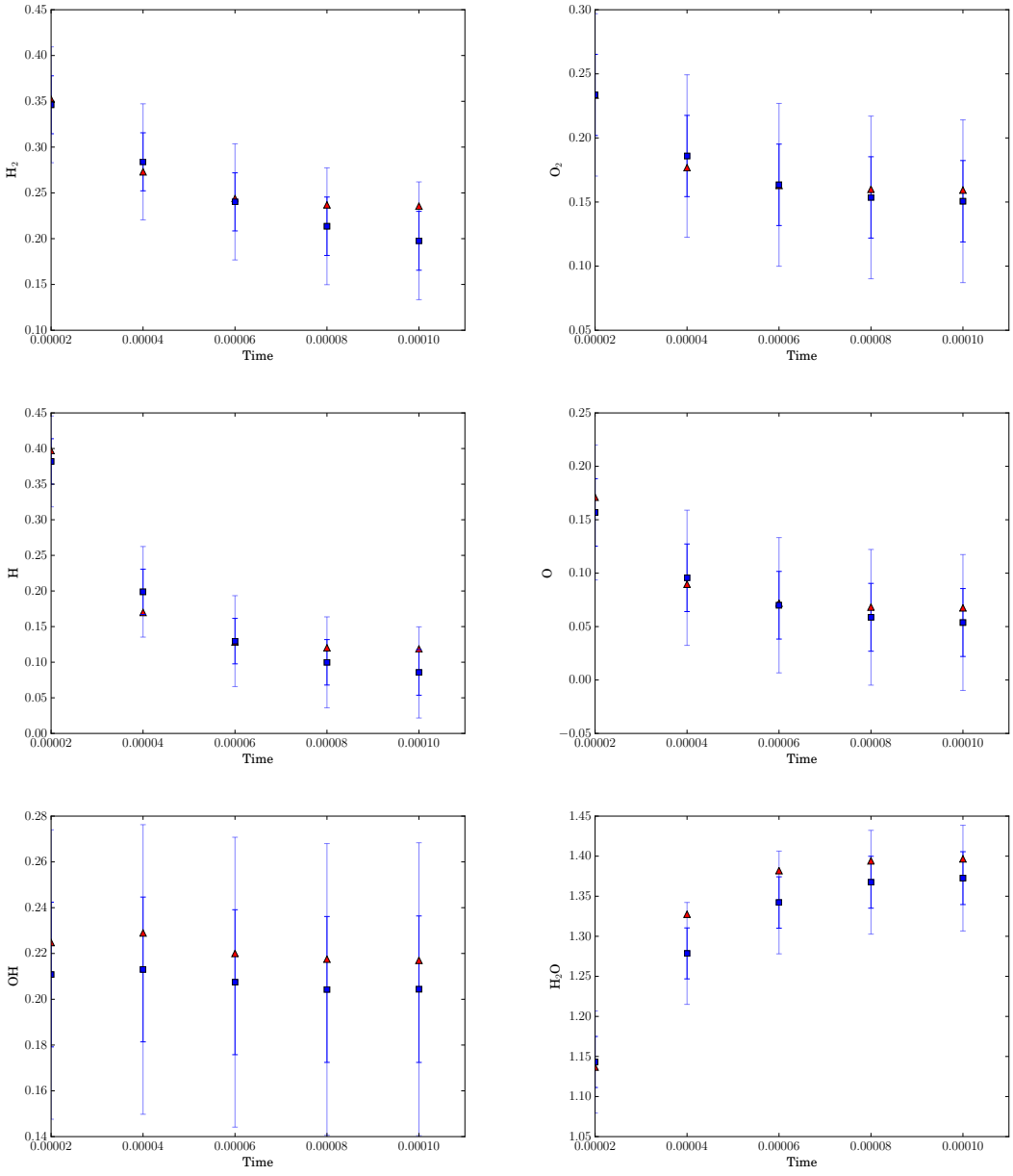

Figure 5.9: Concentrations [mol/m^3] versus time [s] for $\phi = 0.9$, $T_0 = 1550\,\mathrm{K}$. Observations (red), case 2 operator model $\mathcal{O}$ (blue).

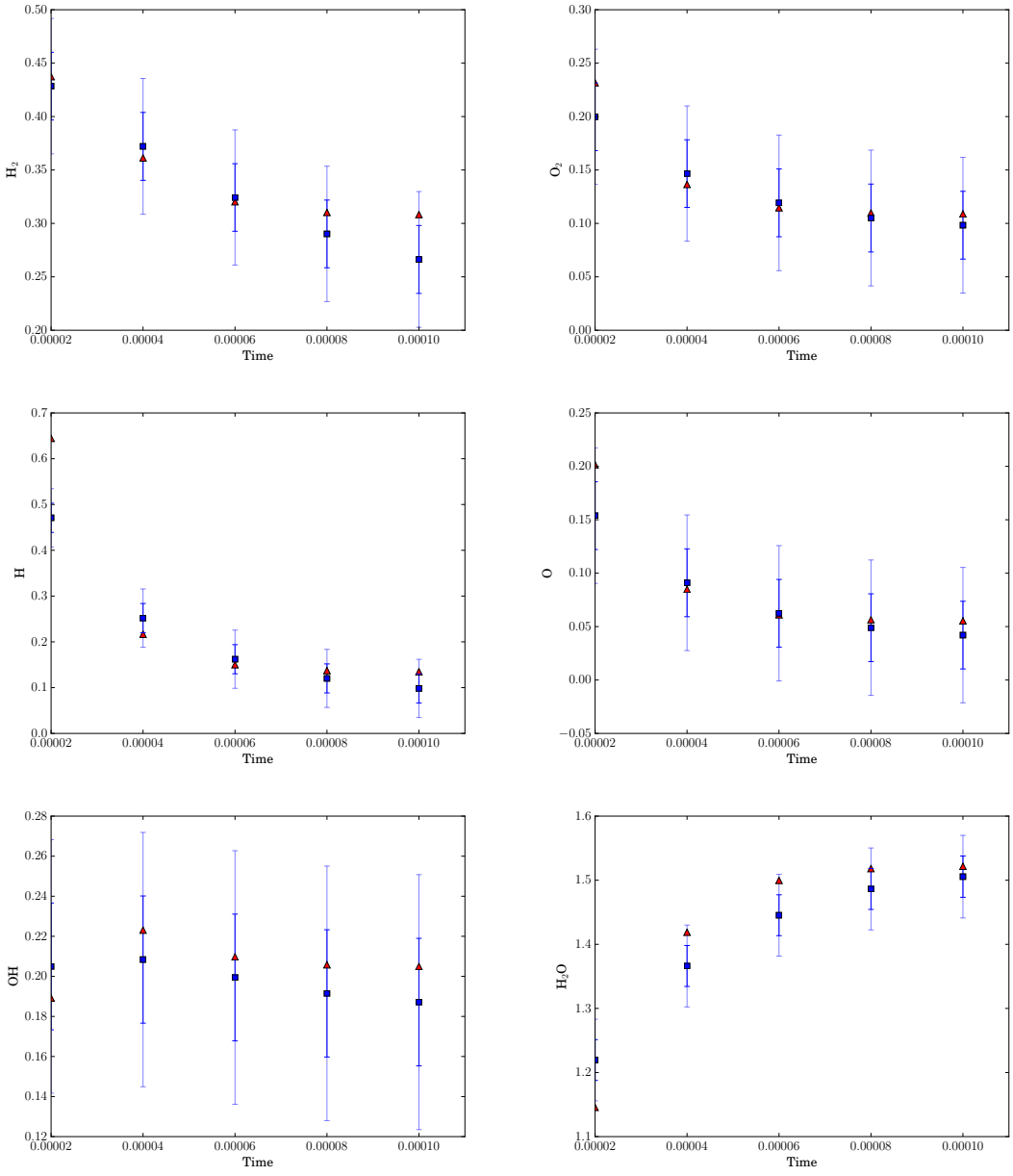

Figure 5.10: Concentrations [mol/m^3] versus time [s] for $\phi = 1.0$, $T_0 = 1450\,\mathrm{K}$. Observations (red), case 2 operator model $\mathcal{O}$ (blue).

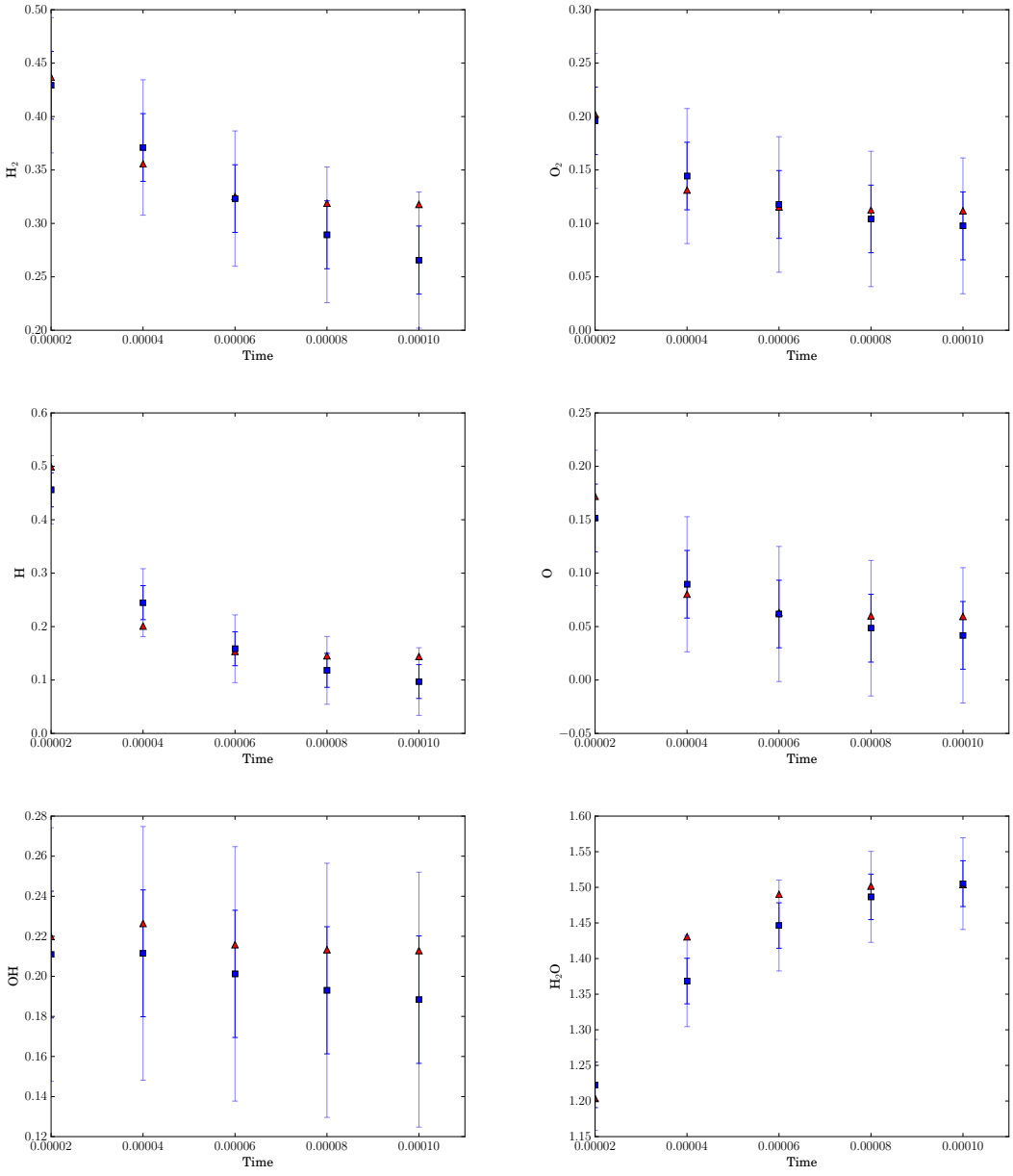

Figure 5.11: Concentrations [mol/m^3] versus time [s] for $\phi = 1.0$, $T_0 = 1500\,\mathrm{K}$. Observations (red), case 2 operator model $\mathcal{O}$ (blue).

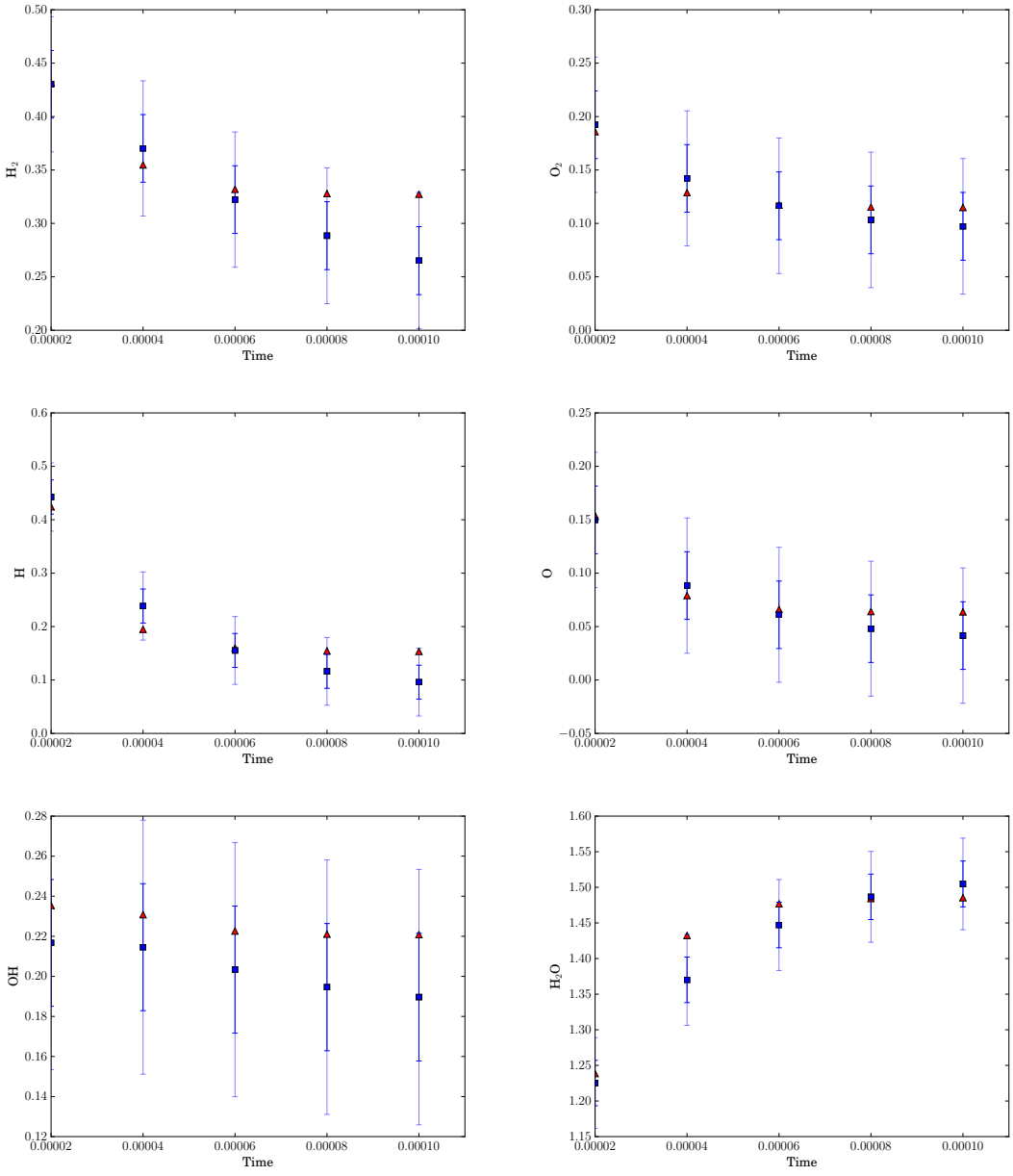

Figure 5.12: Concentrations [mol/m^3] versus time [s] for $\phi = 1.0$, $T_0 = 1550\,\mathrm{K}$. Observations (red), case 2 operator model $\mathcal{O}$ (blue).

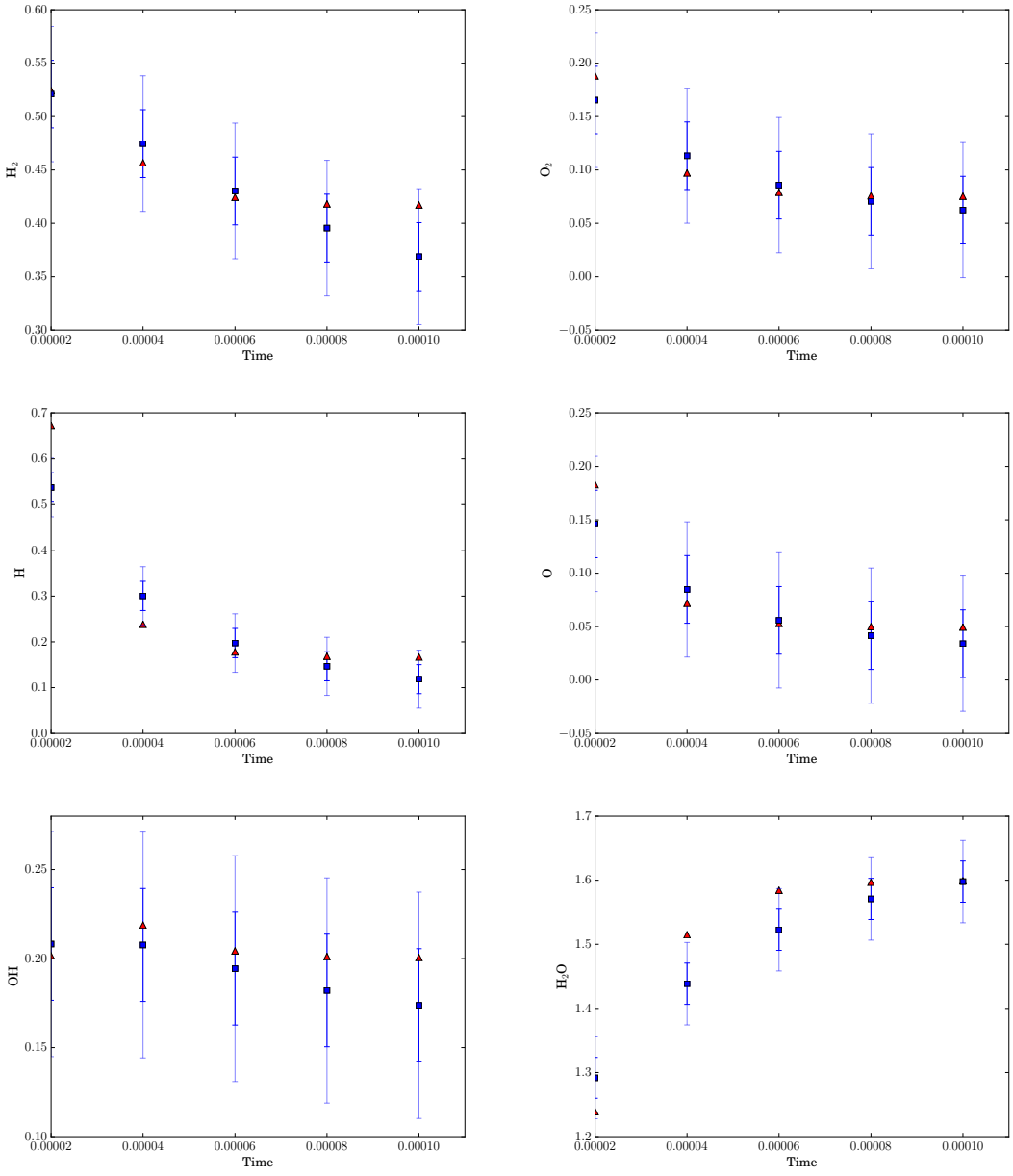

Figure 5.13: Concentrations [mol/m^3] versus time [s] for $\phi = 1.1$, $T_0 = 1450\,\mathrm{K}$. Observations (red), case 2 operator model $\mathcal{O}$ (blue).

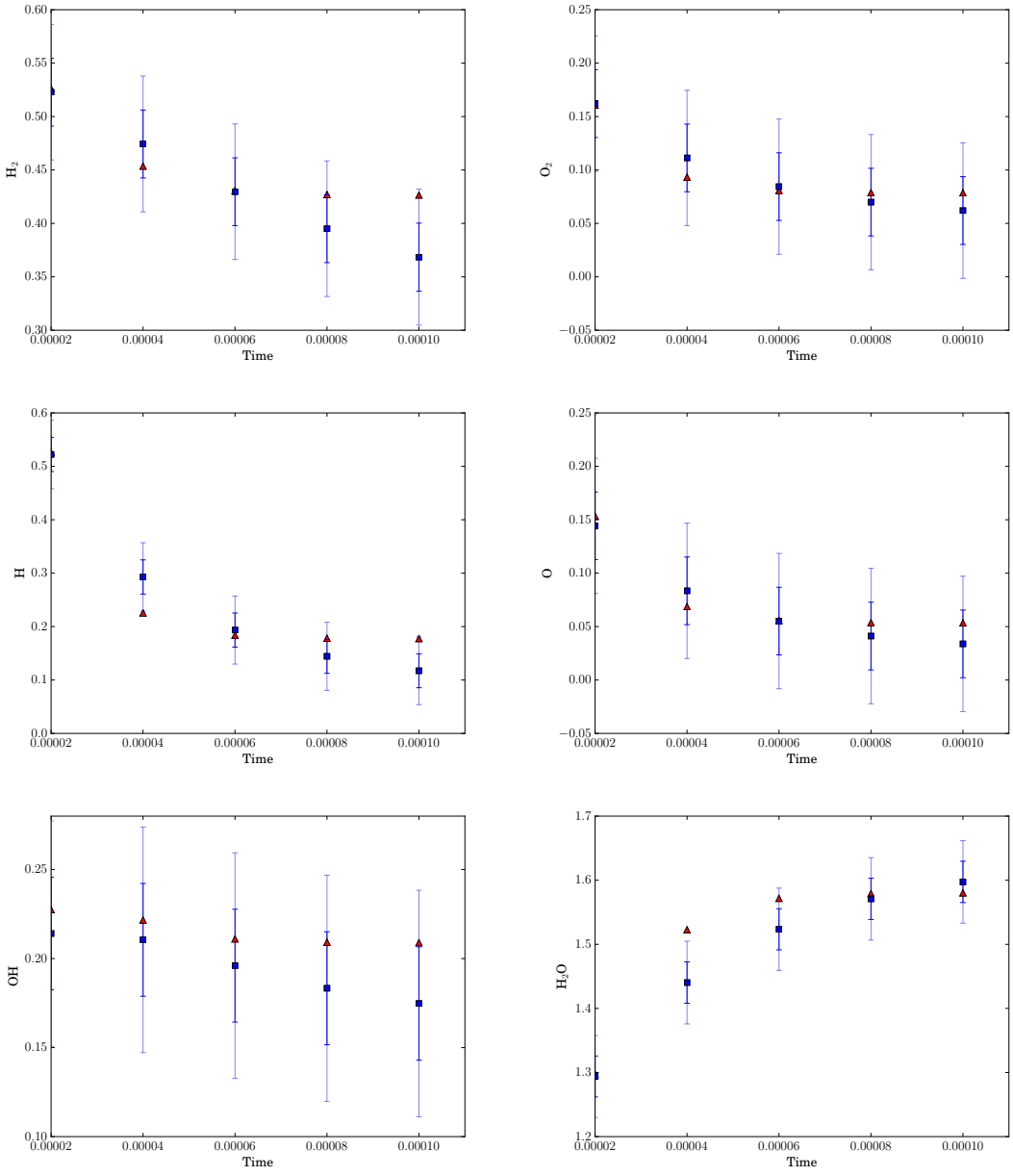

Figure 5.14: Concentrations [mol/m^3] versus time [s] for $\phi = 1.1$, $T_0 = 1500\,\mathrm{K}$. Observations (red), case 2 operator model $\mathcal{O}$ (blue).

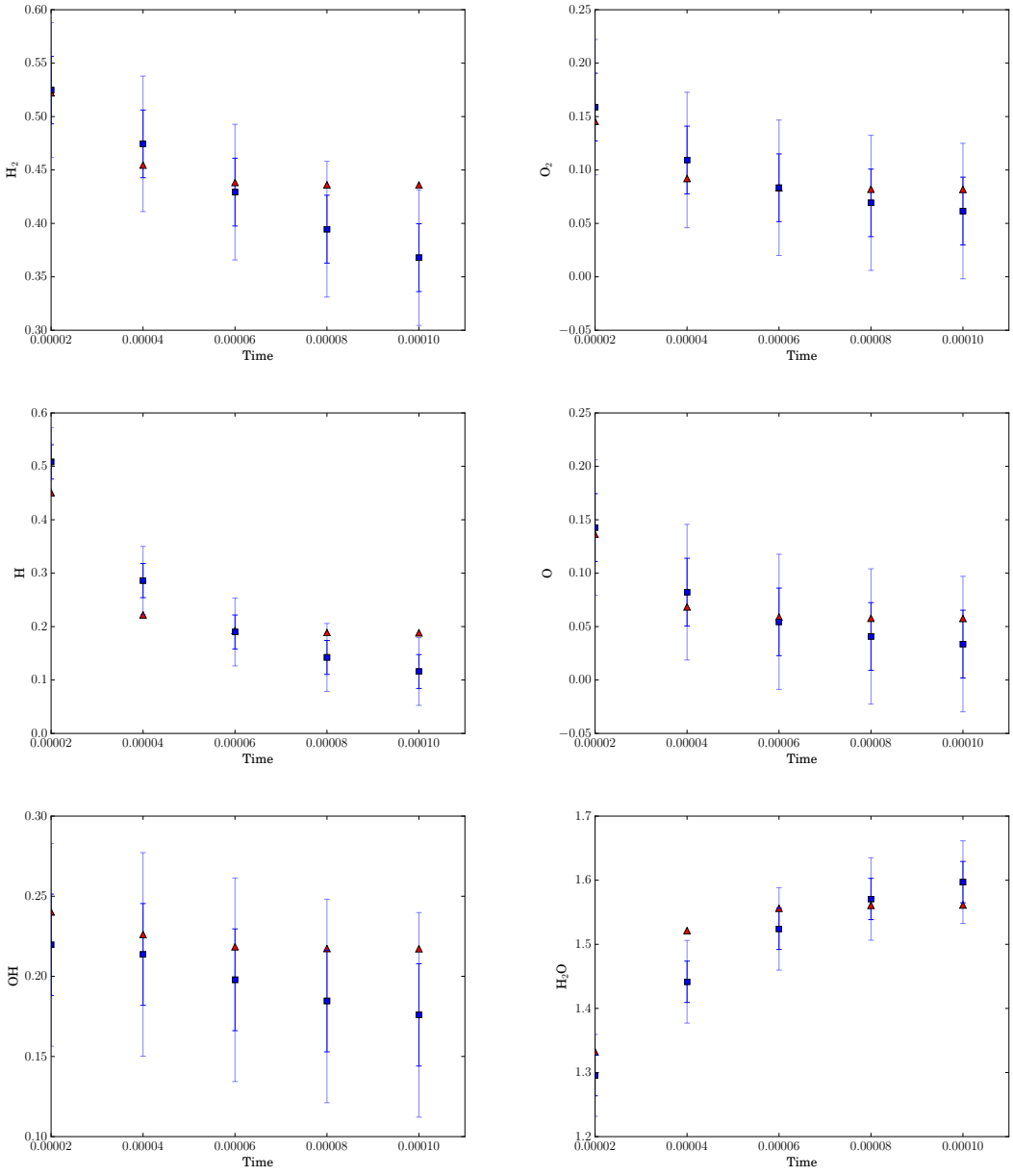

Figure 5.15: Concentrations [mol/m^3] versus time [s] for $\phi = 1.1$, $T_0 = 1550\,\mathrm{K}$. Observations (red), case 2 operator model $\mathcal{O}$ (blue).

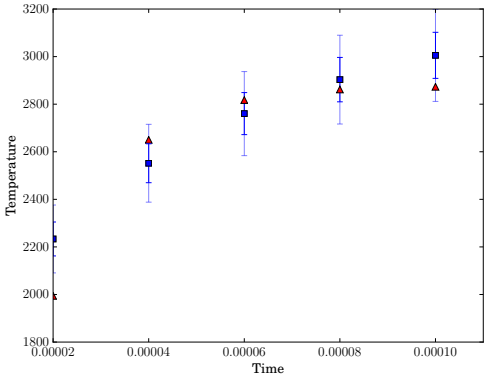

(a) $\phi = 0.9$, $T_0 = 1450\,\mathrm{K}$

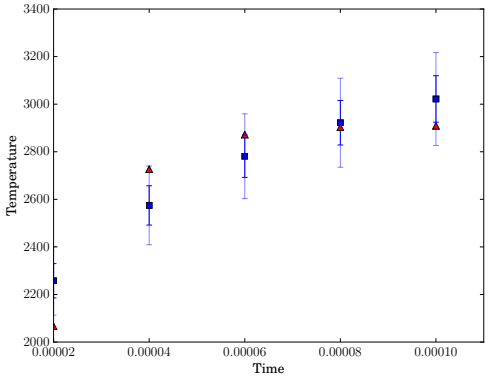

(b) $\phi = 1.0$, $T_0 = 1450\,\mathrm{K}$

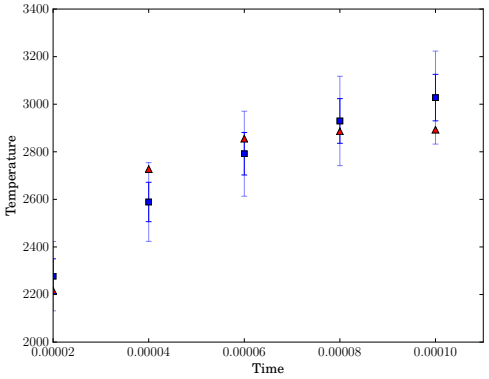

(c) $\phi = 0.9$, $T_0 = 1500\,\mathrm{K}$

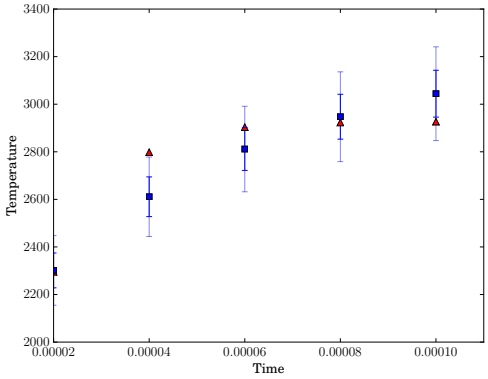

(d) $\phi = 1.0$, $T_0 = 1500\,\mathrm{K}$

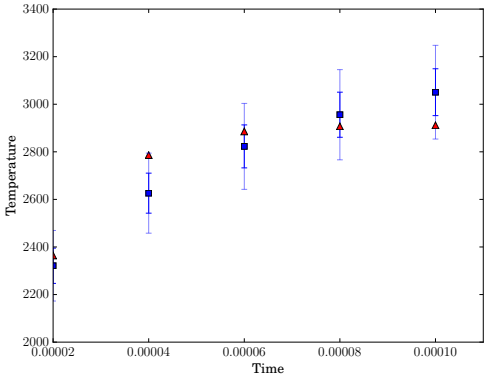

(e) $\phi = 0.9$, $T_0 = 1550\,\mathrm{K}$

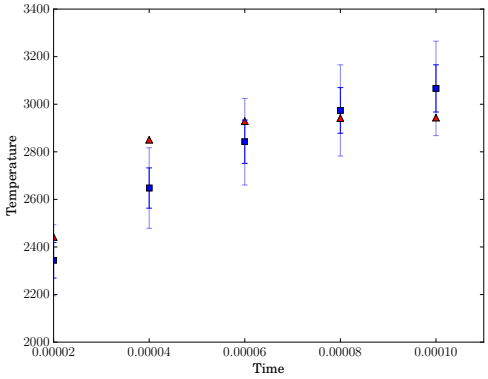

(f) $\phi = 1.0$, $T_0 = 1550\,\mathrm{K}$

Figure 5.16: Temperature [K] versus time [s] for H_2/O_2 reaction, $\phi = \{0.9, 1.0\}$, $T_0 = \{1450, 1500, 1550\}$K. Observations (red), case 2 operator model $\mathcal{O}$ (blue).

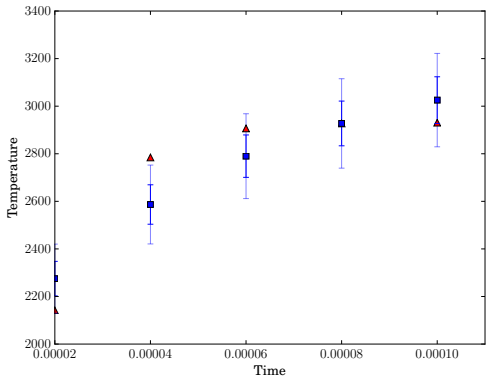

(a) $\phi = 1.1$, $T_0 = 1450\,\mathrm{K}$

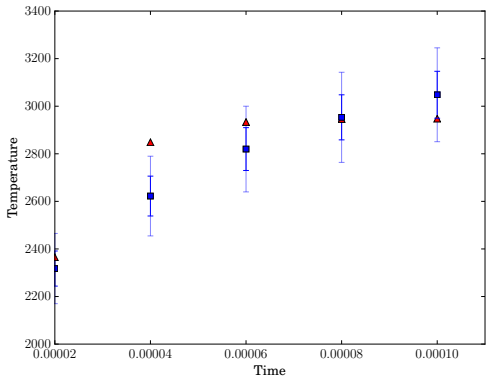

(b) $\phi = 1.1$, $T_0 = 1500\,\mathrm{K}$

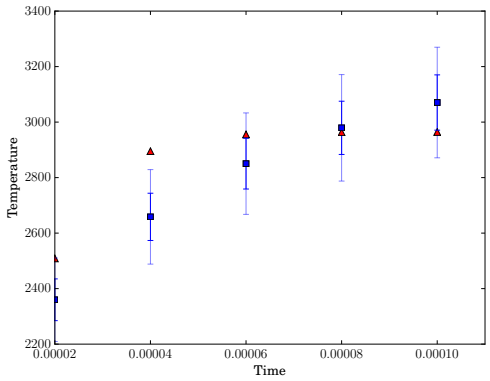

(c) $\phi = 1.1$, $T_0 = 1550\,\mathrm{K}$

Figure 5.17: Temperature [K] versus time [s] for H_2/O_2 reaction, $\phi = 1.1$, $T_0 = \{1450, 1500, 1550\}$K. Observations (red), case 2 operator model $\mathcal{O}$ (blue).

Reaction	Rate coefficient	A	b	E
1	k_1^f	$7.82e10$	0	125604
2	k_2^f	$3.0e5$	0	125604
3	k_3^f	$3.82e12$	-1	167472
4	k_4^f	$2.75e6$	0	83736

Units: J, mol, m^3, s.

Table 5.3: Forward rate constants of the JL mechanism.

The detailed model considered here is given in [52]. It includes 325 reactions and 53 species made up from elements H, O, C, and N. The reduced model used is the Jones-Linstedt (JL) model [34]. After a drastic reduction, the model includes four global reactions, six species, and three elements, H, O, and C (N_2 is treated as a bath species which does not react). The species included are H_2, O_2, H_2O, CH_4, CO, and CO_2, and the four reactions are

$$(1) \quad 2\,CH_4 + O_2 \longrightarrow 2\,CO + 4\,H_2 \tag{5.70}$$

$$(2) \quad CH_4 + H_2O \longrightarrow CO + 3\,H_2 \tag{5.71}$$

$$(3) \quad 2\,H_2 + O_2 \rightleftharpoons H_2O \tag{5.72}$$

$$(4) \quad CO + H_2O \rightleftharpoons CO_2 + H_2, \tag{5.73}$$

with the reaction rates given in table 5.3. Because the four reactions are global, many

of the orders are non-unity. The corresponding rate expressions are given below:

$$(1) \quad r_1^f = k_1^f x_2^{5/4} x_4^{1/2} \tag{5.74}$$

$$(2) \quad r_2^f = k_2^f x_3 x_4 \tag{5.75}$$

$$(3) \quad r_3^f = k_3^f x_1^{1/4} x_2^{3/2} \tag{5.76}$$

$$(4) \quad r_4^f = k_4^f x_3 x_5. \tag{5.77}$$

Despite the severe reduction, this reaction has been cited extensively in the combustion literature and used commonly in practice [2, 19, 39, 57]. It appeared to be an ideal candidate for this study: a widely used reduced model that was probably inadequate in some respects. However, further investigation revealed that the large difference between this model and the detailed one became a particular challenge for the stochastic operator. This discussion is continued later in this chapter, but first the calibration and validation of the reduced model is presented.

5.2.1 Calibration and validation of the reduced model

The reduced model was calibrated using data generated by the detailed model of the six species at equilibrium. There was one initial condition: $\phi = 1.0$ and $T_0 = 1500\,\mathrm{K}$. As expected, it was not difficult to show that this model was inadequate. After calibrating the coefficients A, b, and E, the equilibrium concentrations of five of the six species are shown in figure 5.18. The final concentration of methane is not shown here because, in both the data and reduced model, it is essentially zero. As is apparent in this figure, the γ-values of O_2 and H_2O are numerically zero: there are no values of the model output less probable than the observation. This alone would

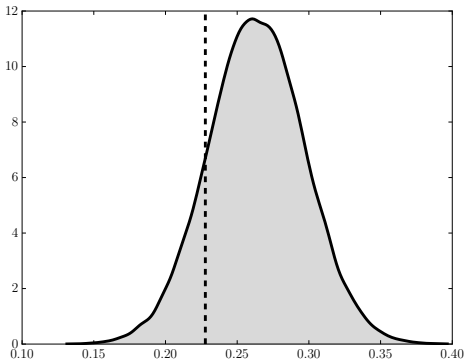

(a) H_2

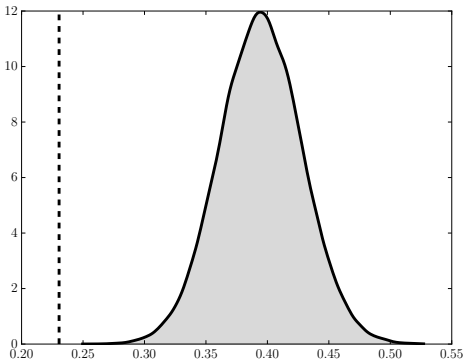

(b) O_2

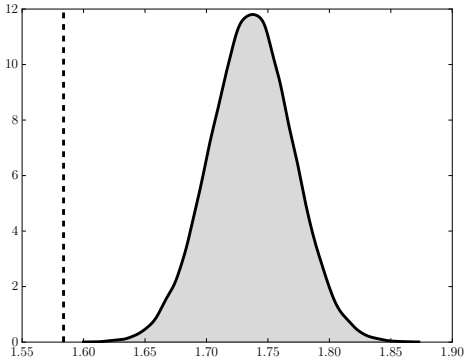

(c) H_2O

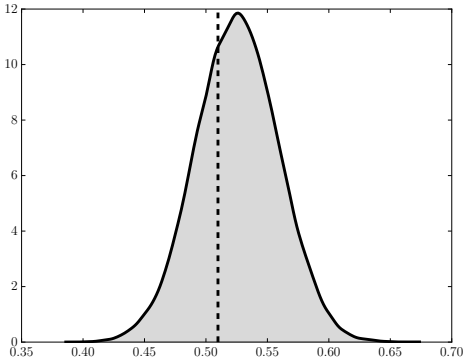

(d) CO

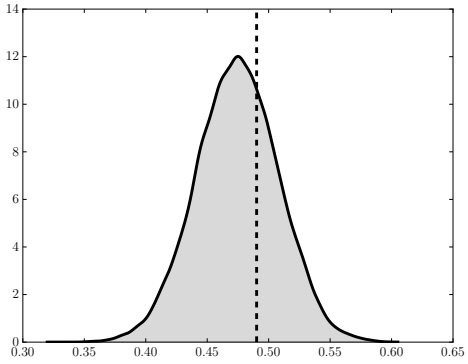

(e) CO_2

Figure 5.18: Observations (dotted) compared to reduced model $\mathcal{R}$ (solid) for CH_4/air reaction, $\phi = 1.0$, $T_0 = 1500$K, at equilibrium.

be enough to invalidate this model. However, an even bigger issue is the significant difference in the ignition time between the detailed and reduced models. In fact, they differ by orders of magnitude: the detailed model takes about 0.003 s to ignite, while the reduced model completes the reaction in only 1e−5 s.

Clearly, there is a substantial difference between the resulting behavior of the two models. Many others have reported similar problems, especially with respect to the ignition delay [4, 21, 37, 50, 58]. As explained in [21], one major cause for the discrepancy is that the reduced model does not include radicals which consume much heat in the beginning of the reaction and thus delay the ignition time (release of heat). The authors develop a modification to the JL mechanism by including dissociation reactions and radical species. Their modified mechanism is shown below:

$$(1) \quad 2\,CH_4 + O_2 \longrightarrow 2\,CO + 4\,H_2 \tag{5.78}$$

$$(2) \quad CH_4 + H_2O \longrightarrow CO + 3\,H_2 \tag{5.79}$$

$$(3) \quad 2\,H_2 + O_2 \rightleftharpoons H_2O \tag{5.80}$$

$$(4) \quad CO + H_2O \rightleftharpoons CO_2 + H_2 \tag{5.81}$$

$$(5) \quad O_2 \rightleftharpoons 2O \tag{5.82}$$

$$(6) \quad H_2O \rightleftharpoons H + OH, \tag{5.83}$$

with the reaction rate constants given in table 5.4. The two new rate expressions are $r_5^f = k_5^f x_2$ and $r_6^f = k_6^f x_3$.

At first, it appeared that these modifications could be accounted for directly with the operator— H′ and O′ in particular could assume the role of the radicals. This

Reaction	Rate coefficient	A	b	E
1	k_1^f	$7.82e10$	0	125604
2	k_2^f	$3.0e5$	0	125604
3	k_3^f	$3.82e12$	-1	167472
4	k_4^f	$2.75e6$	0	83736
5	k_5^f	$1.5e9$	0	473108
6	k_6^f	$2.3e22$	-3	502416

Units: J, mol, m^3, s.

Table 5.4: Forward rate constants of the modified JL mechanism.

modified JL mechanism would then provide another missing piece of information: new physical information about the rates of the dissociation reactions. With a more informed prior for the rates and thermodynamic variables in the operator, it might be able to capture the slower ignition time of the detailed model.

Unfortunately, there was another problem: the rates of the dissociation reactions of the modified JL mechanism are highly temperature-dependent. This is beyond the scope of the operator as currently formulated (there is no temperature-dependence included in the rate parameters $\boldsymbol{\xi}$ or $\boldsymbol{\kappa}$). In the end, we found that the operator was able to improve the equilibrium concentrations, but not able to account for the difference in ignition time. The formulation of the stochastic operator and its performance are the topics of the next subsections.

5.2.2 The random matrix S

This subsection gives a brief review of the matrices S, E, C, and P. The species are given in the order of H′, O′, C′, H_2, O_2, H_2O, CH_4, CO, and CO_2. First,

S is of the following form, with negative diagonal elements:

$$S = \begin{pmatrix} s_{1,1} & 0 & 0 & s_{1,4} & 0 & s_{1,6} & s_{1,7} & 0 & 0 \\ 0 & s_{2,2} & 0 & 0 & s_{2,5} & s_{2,6} & 0 & s_{2,8} & s_{2,9} \\ 0 & 0 & s_{3,3} & 0 & 0 & 0 & s_{3,7} & s_{3,8} & s_{3,9} \\ s_{4,1} & 0 & 0 & s_{4,4} & 0 & s_{4,6} & s_{4,7} & 0 & 0 \\ 0 & s_{5,2} & 0 & 0 & s_{5,5} & s_{5,6} & 0 & s_{5,8} & s_{5,9} \\ 0 & 0 & 0 & 0 & 0 & s_{6,6} & 0 & 0 & 0 \\ 0 & 0 & 0 & 0 & 0 & 0 & s_{7,7} & 0 & 0 \\ 0 & 0 & 0 & 0 & 0 & 0 & 0 & s_{8,8} & s_{8,9} \\ 0 & 0 & 0 & 0 & 0 & 0 & 0 & s_{9,8} & s_{9,9} \end{pmatrix}. \tag{5.84}$$

Conservation of atoms is shown through E, where $ES = 0$:

$$E = \begin{pmatrix} 1 & 0 & 0 & 1 & 0 & 2/3 & 4/5 & 0 & 0 \\ 0 & 1 & 0 & 0 & 1 & 1/3 & 0 & 1/2 & 2/3 \\ 0 & 0 & 1 & 0 & 0 & 0 & 1/5 & 1/2 & 1/3 \end{pmatrix}. \tag{5.85}$$

The three rows of E correspond to atom types H, O, and C, respectively. The conservation constraint is guaranteed using the matrix C, where C spans null(E):

$$C = \begin{pmatrix} -1 & 0 & -2/3 & -4/5 & 0 & 0 \\ 0 & -1 & -1/3 & 0 & -1/2 & -2/3 \\ 0 & 0 & 0 & -1/5 & -1/2 & -1/3 \\ 1 & 0 & 0 & 0 & 0 & 0 \\ 0 & 1 & 0 & 0 & 0 & 0 \\ 0 & 0 & 1 & 0 & 0 & 0 \\ 0 & 0 & 0 & 1 & 0 & 0 \\ 0 & 0 & 0 & 0 & 1 & 0 \\ 0 & 0 & 0 & 0 & 0 & 1 \end{pmatrix}. \tag{5.86}$$

Finally, the non-negativity constraints on the concentrations are enforced via P, where

$$P = \begin{pmatrix} p_{1,1} & 0 & 0 & p_{1,4} & 0 & p_{1,6} & p_{1,7} & 0 & 0 \\ 0 & p_{2,2} & 0 & 0 & p_{2,5} & p_{2,6} & 0 & p_{2,8} & p_{2,9} \\ 0 & 0 & 0 & 0 & 0 & p_{3,6} & 0 & 0 & 0 \\ 0 & 0 & 0 & 0 & 0 & 0 & p_{4,7} & 0 & 0 \\ 0 & 0 & 0 & 0 & 0 & 0 & 0 & p_{5,8} & p_{5,9} \\ 0 & 0 & 0 & 0 & 0 & 0 & 0 & p_{6,9} & p_{6,9} \end{pmatrix}. \tag{5.87}$$

ξ_i	=	$p_{j,k}$
ξ_1	=	$p_{1,1}$
ξ_2	=	$-p_{1,4}$
ξ_3	=	$p_{1,6}$
ξ_4	=	$p_{1,7}$
ξ_5	=	$p_{2,2}$
ξ_6	=	$-p_{2,5}$
ξ_7	=	$p_{2,6}$
ξ_8	=	$p_{2,8}$
ξ_9	=	$p_{2,9}$
ξ_{10}	=	$-p_{3,6} - 3(p_{1,6} + p_{2,6})$
ξ_{11}	=	$-p_{4,7} - \frac{5}{4}p_{1,7}$
ξ_{12}	=	$p_{2,9} - 2(p_{2,8} + \frac{2}{3}p_{6,8})$
ξ_{13}	=	$p_{5,9}$
ξ_{14}	=	$p_{6,8}$
ξ_{15}	=	$-p_{6,9} - 3(p_{2,9} + \frac{1}{2}p_{5,9})$

Table 5.5: The transformed variables $\boldsymbol{\xi}$ for the CH_4/air operator.

The transform from P to the random variables $\boldsymbol{\xi}$ is given in table 5.5.

5.2.3 The catchall reactions $\mathcal{A}$

In this example, it is critical that the nonlinear reactions in $\mathcal{A}$ are included. With S, hydrogen atoms held in H$'$ and oxygen atoms held in O$'$ can only move back to H_2 and O_2, respectively. This is more limited that the previous example (hydrogen atoms in H$'$ could move to both H_2 and H, and oxygen to O_2 and O), but at least there is some mechanism by which the catchall species H$'$ and O$'$ can react. However, with respect to the carbon atoms, there is no species in the reduced species set made up of only carbon atoms. Therefore, there is no linear term that can move atoms in C$'$ to anything else: once a carbon atom moves to the catchall

species, it can never return. This quality of the methane-air reduced mechanism was the motivation behind the addition of the nonlinear reactions in $\mathcal{A}$.

With that said, the reactions in $\mathcal{A}$ are:

$$2\,\mathrm{H}' + \mathrm{O}' \xrightarrow{\kappa_1} \mathrm{H_2O} \tag{5.88}$$

$$4\,\mathrm{H}' + \mathrm{C}' \xrightarrow{\kappa_2} \mathrm{CH_4} \tag{5.89}$$

$$\mathrm{O}' + \mathrm{C}' \xrightarrow{\kappa_3} \mathrm{CO} \tag{5.90}$$

$$2\,\mathrm{O}' + \mathrm{C}' \xrightarrow{\kappa_4} \mathrm{CO_2}. \tag{5.91}$$

5.2.4 The energy operator W

Finally, the energy and specific heat terms for the catchall species are incorporated:

$$u_i(T) = \alpha_{0_i} + \alpha_{1_i} T + \alpha_{2_i} T^2 \tag{5.92}$$

$$c_{v_i}(T) = \alpha_{1_i} + 2\alpha_{2_i} T, \tag{5.93}$$

where $i = 1$ corresponds to H′, $i = 2$ to O′, and $i = 3$ to C′.

5.2.5 Calibration and validation of the operator model

The operator model was also calibrated using data generated by the detailed model of the six species at equilibrium. For this case, there were again nine different initial conditions: $\phi = \{0.9, 1.0, 1.1\}$ with $T_0 = \{1450, 1500, 1550\}$K. After calibration, the operator model $\mathcal{O}$ was able to better capture the equilibrium concentrations; see figures 5.19-5.27. For example, the same observations shown in figure 5.18 for the reduced model are now covered by the stochastic operator model output in figure 5.23.

Finally, the temperature output covers the observations well, shown in figures 5.28 and 5.29.

Although the equlibrium concentrations have been improved by the operator model, it should be stressed that the range and reliability of the inadequacy representation is very limited. We know that the model output of $\mathcal{O}$ is still quite different in time scales than the detailed model $\mathcal{D}$. Unfortunately, we would be hard-pressed to use this model for anything besides equilibrium concentrations; that is, the model should not be used for extrapolative predictions.

5.2.6 Discussion

As mentioned above, the results of the methane operator were very limited and properly accounting for the inadequacy of the reduced model was out of scope. Of course, the dissociation reactions could be added explicitly to improve the reduced model. But, the value of an inadequacy model is that it should be rich enough to deal with a reduced physics model that is very poor, and at least indicate the severity of the model error. This would be reflected in the parameterized inadequacy representation by very large uncertainties. For this, apparently, a richer temperature-dependence in the inadequacy representation is needed. At the same time, much was learned from implementing this example. First, there were almost fifty untracked species, so the catchall species became necessary. Second, this example motivated the inclusion of nonlinear catchall reactions so that the atoms in H', O' and especially C' would be able to feed back into the original reduced species. Finally, the process made clear the importance of domain-specific information while formulating the

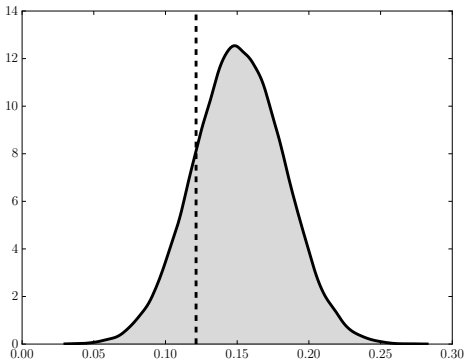

(a) H_2

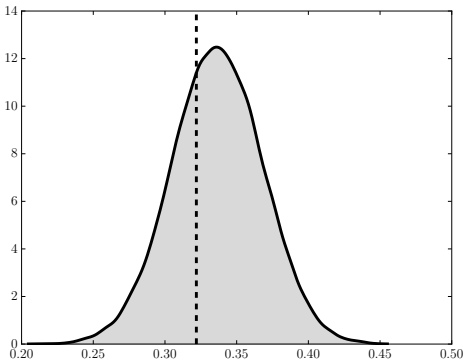

(b) O_2

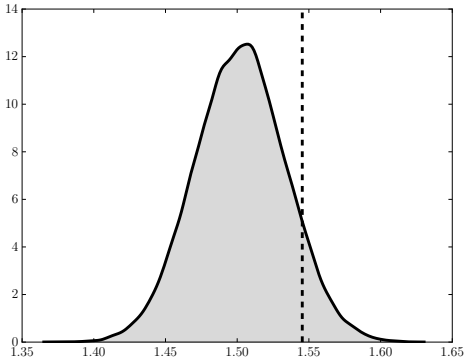

(c) H_2O

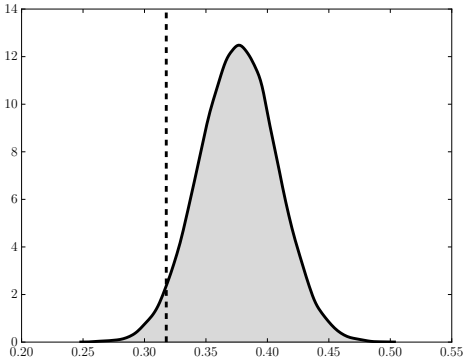

(d) CO

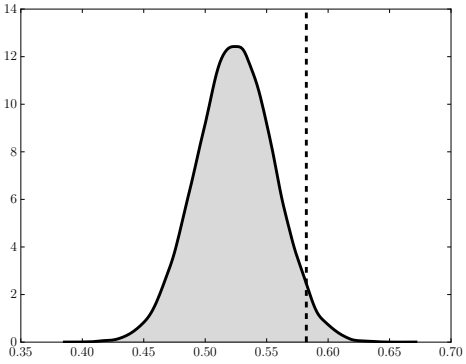

(e) CO_2

Figure 5.19: Observations (dotted) compared to operator model $\mathcal{O}$ (solid) for CH_4/air reaction, $\phi = 0.9$, $T_0 = 1450$K, at equilibrium.

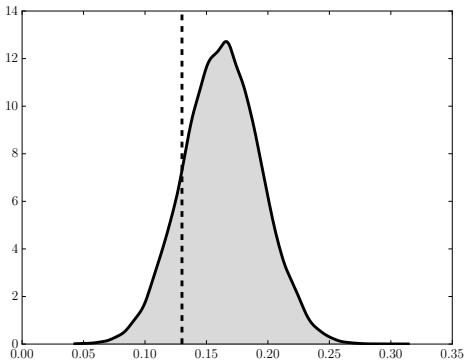

(a) H_2

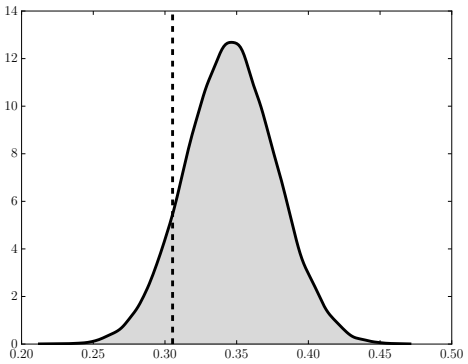

(b) O_2

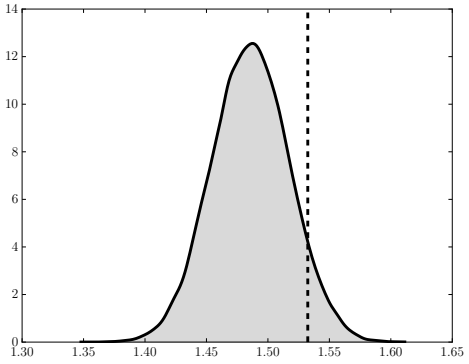

(c) H_2O

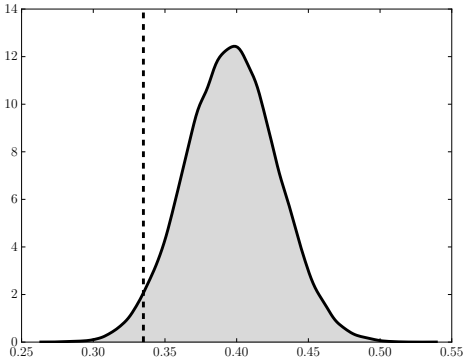

(d) CO

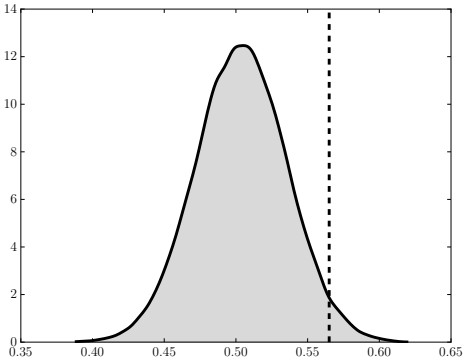

(e) CO_2

Figure 5.20: Observations (dotted) compared to operator model $\mathcal{O}$ (solid) for CH_4/air reaction, $\phi = 0.9$, $T_0 = 1500$K, at equilibrium.

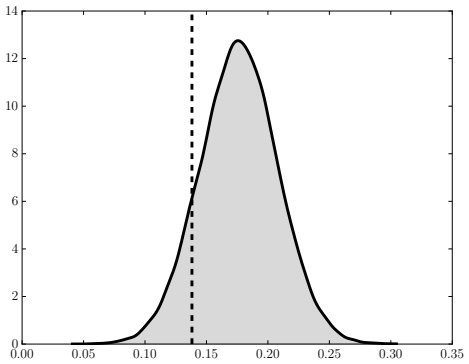

(a) H_2

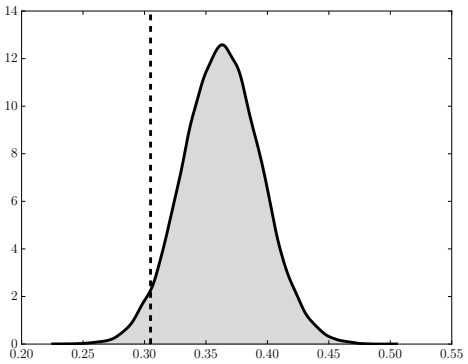

(b) O_2

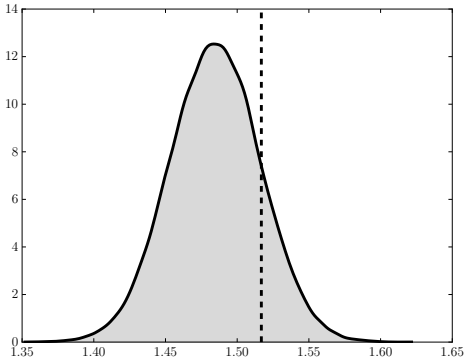

(c) H_2O

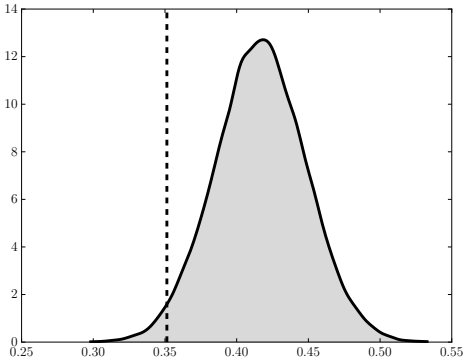

(d) CO

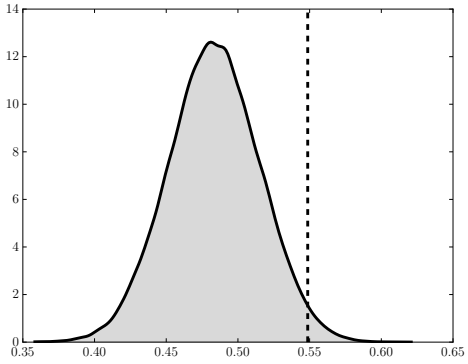

(e) CO_2

Figure 5.21: Observations (dotted) compared to operator model $\mathcal{O}$ (solid) for CH_4/air reaction, $\phi = 0.9$, $T_0 = 1550$K, at equilibrium.

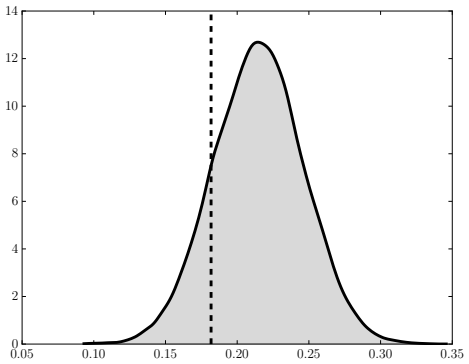

(a) H_2

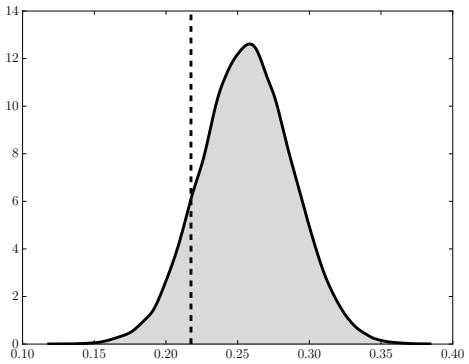

(b) O_2

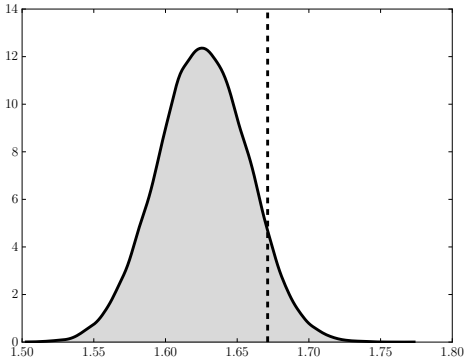

(c) H_2O

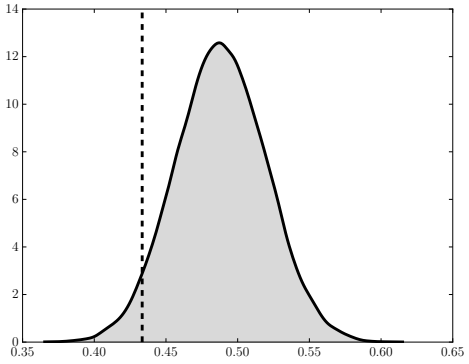

(d) CO

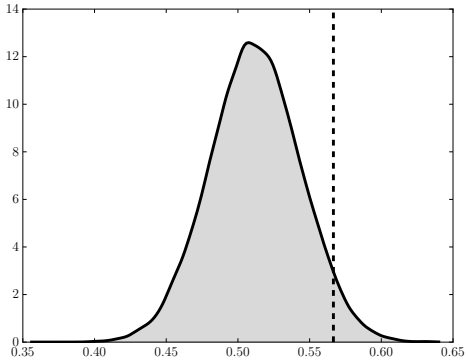

(e) CO_2

Figure 5.22: Observations (dotted) compared to operator model $\mathcal{O}$ (solid) for CH_4/air reaction, $\phi = 1.0$, $T_0 = 1450$K, at equilibrium.

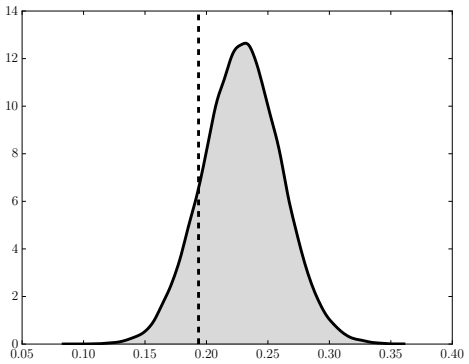

(a) H_2

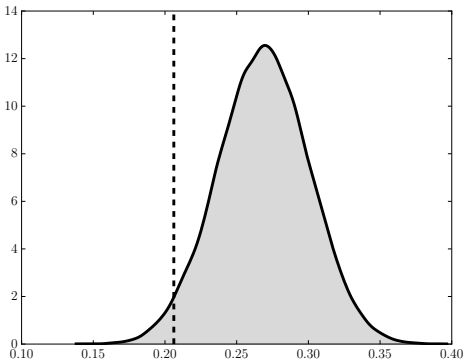

(b) O_2

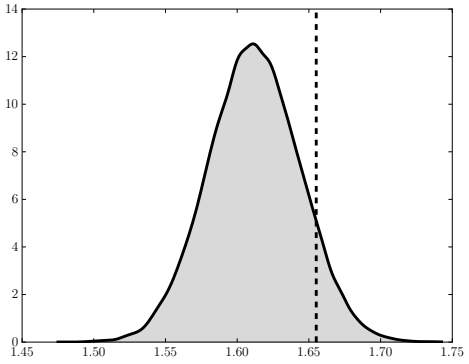

(c) H_2O

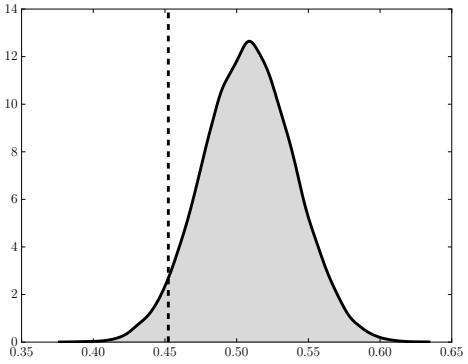

(d) CO

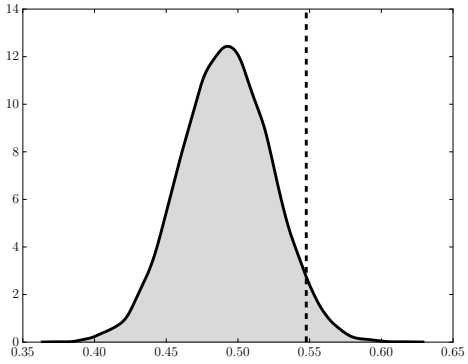

(e) CO_2

Figure 5.23: Observations (dotted) compared to operator model $\mathcal{O}$ (solid) for CH_4/air reaction, $\phi = 1.0$, $T_0 = 1500$K, at equilibrium.

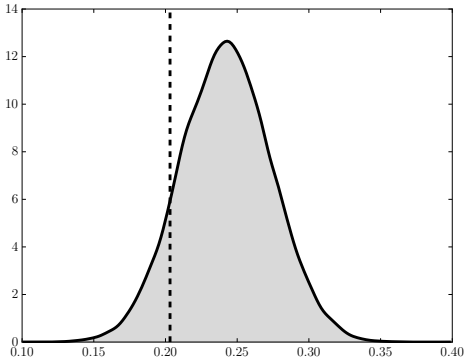

(a) H_2

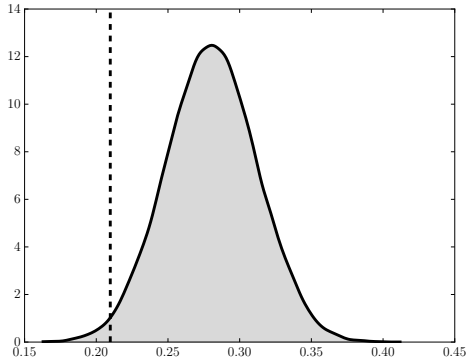

(b) O_2

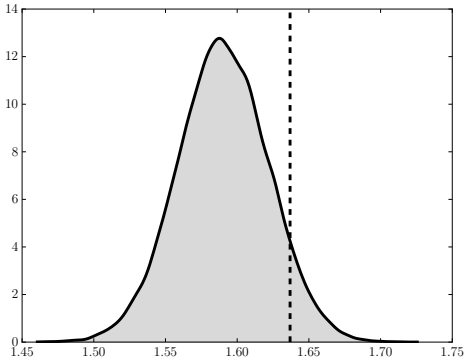

(c) H_2O

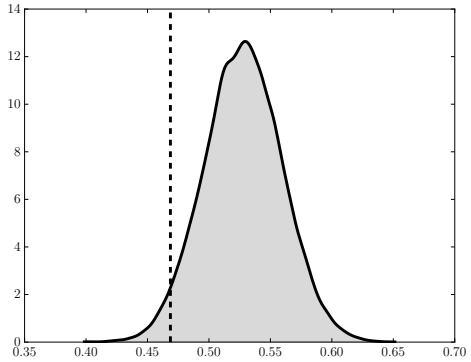

(d) CO

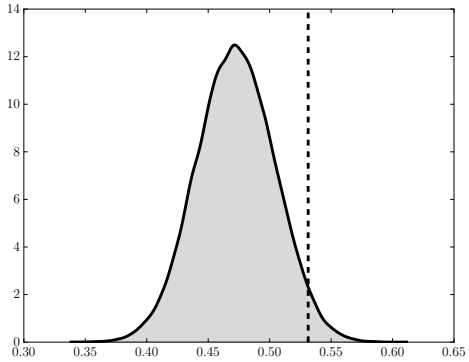

(e) CO_2

Figure 5.24: Observations (dotted) compared to operator model $\mathcal{O}$ (solid) for CH_4/air reaction, $\phi = 1.0$, $T_0 = 1550$K, at equilibrium.

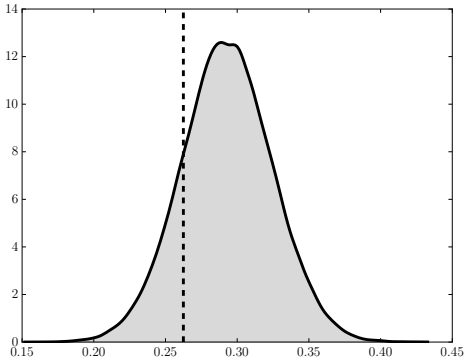

(a) H_2

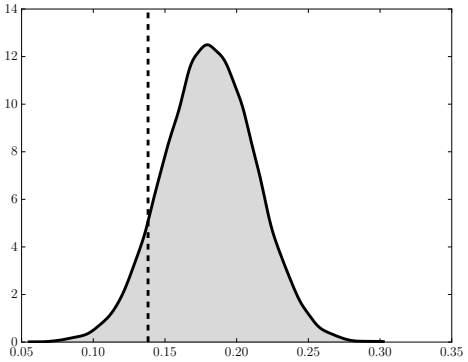

(b) O_2

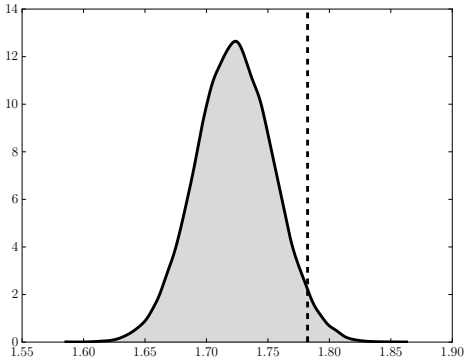

(c) H_2O

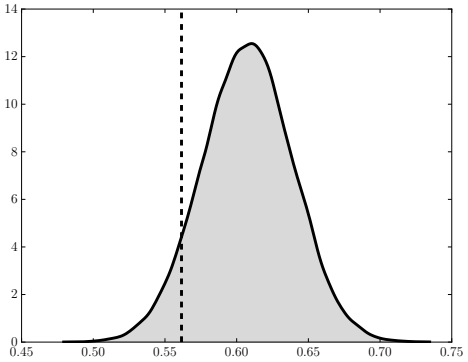

(d) CO

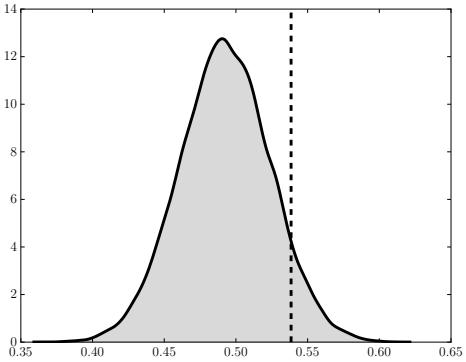

(e) CO_2

Figure 5.25: Observations (dotted) compared to operator model $\mathcal{O}$ (solid) for CH_4/air reaction, $\phi = 1.1$, $T_0 = 1450$K, at equilibrium.

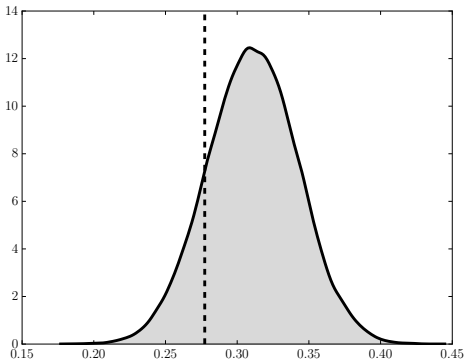

(a) H_2

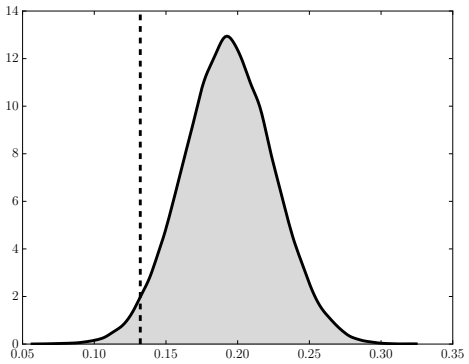

(b) O_2

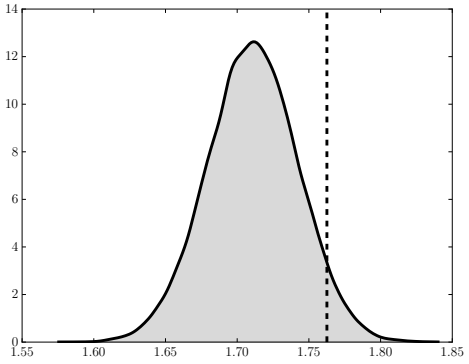

(c) H_2O

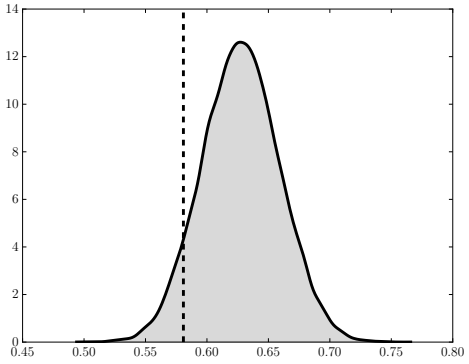

(d) CO

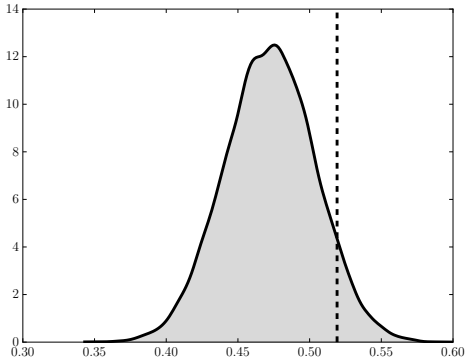

(e) CO_2

Figure 5.26: Observations (dotted) compared to operator model $\mathcal{O}$ (solid) for CH_4/air reaction, $\phi = 1.0$, $T_0 = 1500$K, at equilibrium.

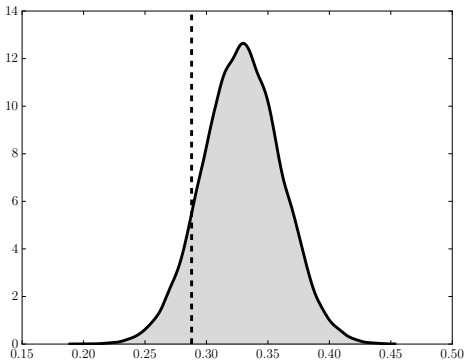

(a) H_2

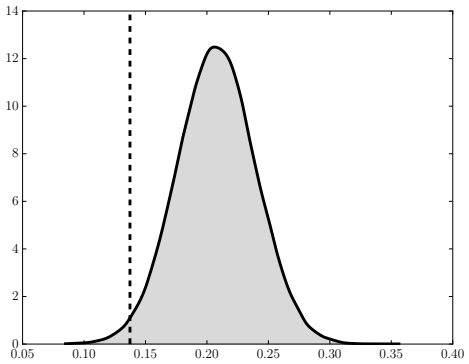

(b) O_2

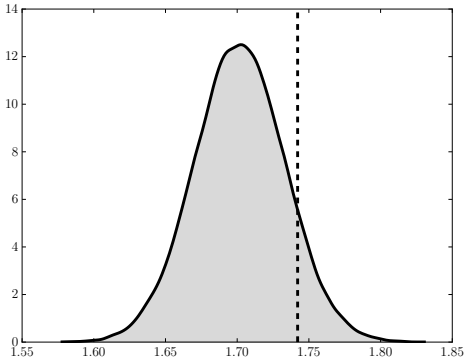

(c) H_2O

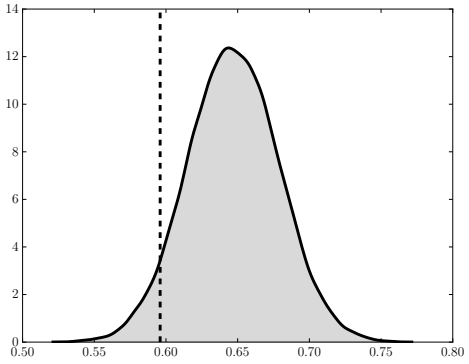

(d) CO

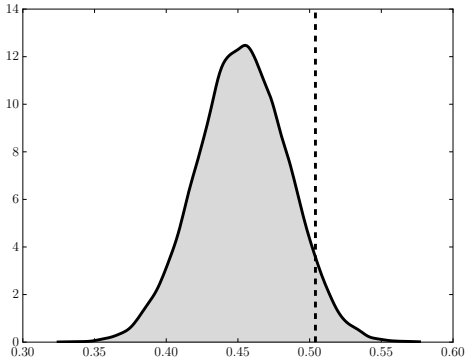

(e) CO_2

Figure 5.27: Observations (dotted) compared to operator model $\mathcal{O}$ (solid) for CH_4/air reaction, $\phi = 1.0$, $T_0 = 1550$K, at equilibrium.

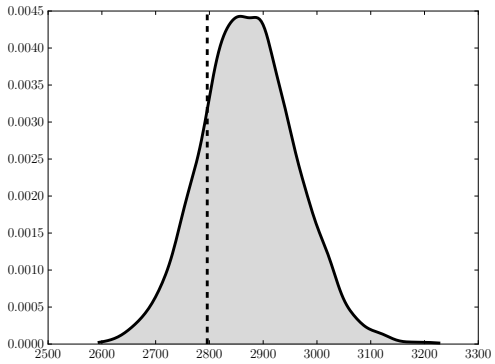

(a) $\phi = .9$, $T_0 = 1450\,\mathrm{K}$

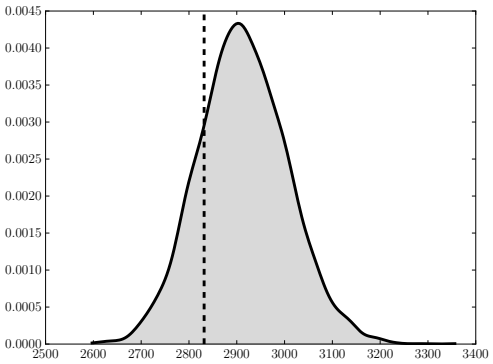

(b) $\phi = 1.0$, $T_0 = 1450\,\mathrm{K}$

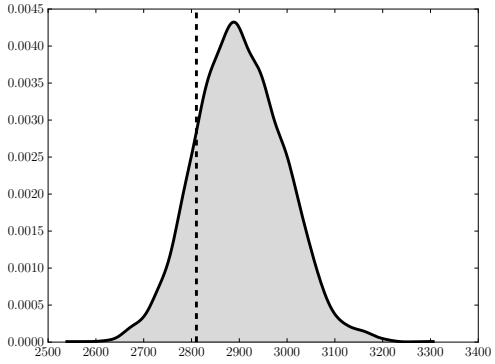

(c) $\phi = .9$, $T_0 = 1500\,\mathrm{K}$

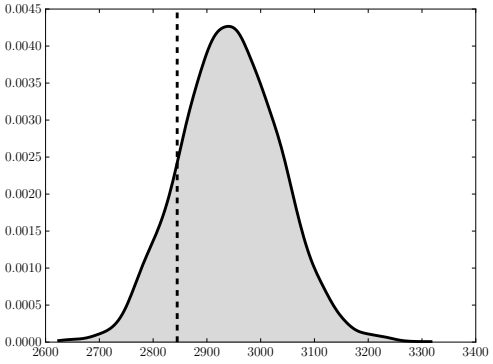

(d) $\phi = 1.0$, $T_0 = 1500\,\mathrm{K}$

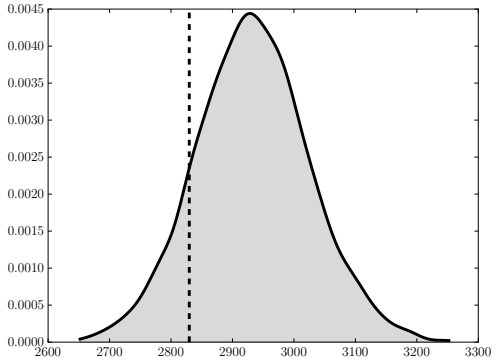

(e) $\phi = .9$, $T_0 = 1550\,\mathrm{K}$

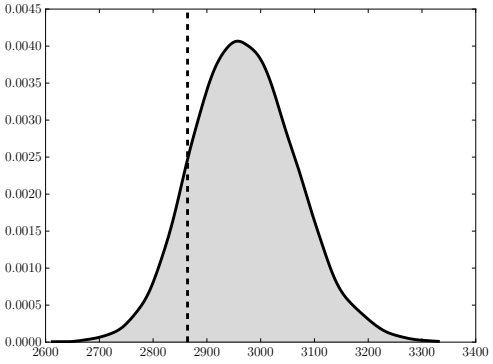

(f) $\phi = 1.0$, $T_0 = 1550\,\mathrm{K}$

Figure 5.28: Temperature observations (dotted) compared to operator model $\mathcal{O}$ (solid) for CH_4/air reaction, $\phi = \{0.9, 1.0\}$, $T_0 = \{1450, 1500, 1550\}$K, at equilibrium.

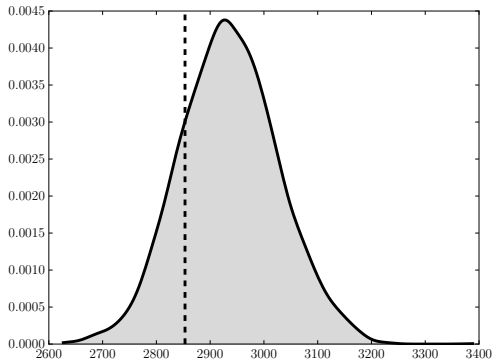

(a) $\phi = 1.1$, $T_0 = 1450\,\mathrm{K}$

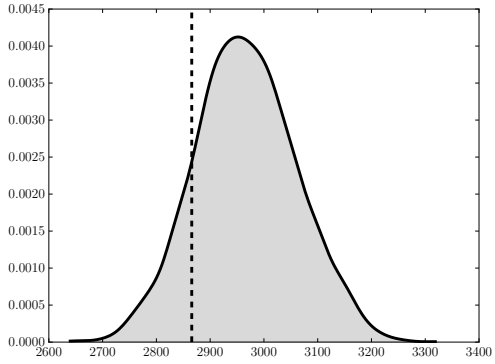

(b) $\phi = 1.1$, $T_0 = 1500\,\mathrm{K}$

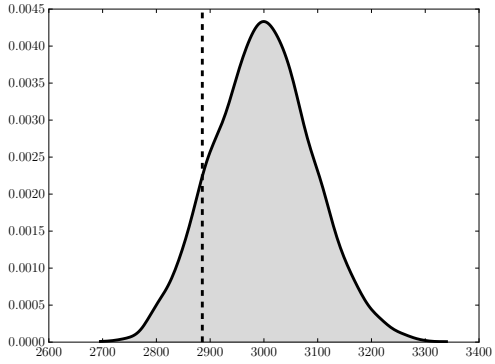

(c) $\phi = 1.1$, $T_0 = 1550\,\mathrm{K}$

Figure 5.29: Temperature observations (dotted) compared to operator model $\mathcal{O}$ (solid) for CH_4/air reaction, $\phi = 1.1$, $T_0 = \{1450, 1500, 1550\}$K, at equilibrium.

inadequacy model. That is, the inadequacy model may not necessarily represent the exact physical process (like an elementary reaction would) but it may need to be strongly informed by any available knowledge about the missing physics.

5.3 A flame problem

The final application of the stochastic operator is to a hydrogen flame. A 1D adiabatic, steady, premixed, laminar flame was modeled. The goal is to predict the flamespeed using the operator as calibrated by the 0D reaction data. Recall that to make this prediction, samples of the hyperparameters are used to generate values of the inadquacy parameters, and it is these that are propagated through the foward problem of the flame.

5.3.1 Governing equations

The governing equations for an adiabatic steady premixed laminar flame are as follows:

Mass continuity:

$$\dot{M} = \rho u = \text{constant} \tag{5.94}$$

Species continuity:

$$\dot{M}\frac{dY_s}{dz} = -\frac{d}{dz}(\rho Y_s V_s) + \dot{x}_s W_s, \;\; s = 1, \ldots, n_S \tag{5.95}$$

Conservation of energy:

$$\dot{M}\frac{dT}{dz} = \frac{1}{c_p}\frac{d}{dz}\left(\lambda\frac{dT}{dz}\right) - \frac{1}{c_p}\sum_{s=1}^{n_S}\rho Y_s V_s c_{p_s}\frac{dT}{dz} - \frac{1}{c_p}\sum_{s=1}^{n_S}\dot{u}_s h_s W_s \tag{5.96}$$

State equation:

$$\rho = \frac{p\bar{W}}{RT} \tag{5.97}$$

where z is the spatial coordinate fixed to the flame; $\dot{M}$, the mass flow rate; Y_s, the mass fraction of the sth species; u, the velocity of the fluid mixture; ρ, the mass density; W_s, the molecular weight of the sth species; $\bar{W}$, the mean molecular weight of the mixture; λ, the thermal conductivity of the mixture; and V_s, the diffusion velocity of the sth species. As usual, there is also T, the temperature; p, the pressure; R, the universal gas constant; c_p, the constant pressure heat capacity of the mixture; c_{p_s}, the constant pressure heat capacity of the sth species; $\dot{x}$, the molar rate of production of the sth species per unit volume; and h_s, the specific enthalpy of the sth species.

5.3.2 Freely propagating flame

The governing equations given above apply to both burner-stabilized flames and freely propagating flames. To model the latter, an infinite domain is approximated with a finite domain of length L. This must be sufficiently large so that the flamespeed is not sensitive to the particular value of L. The boundary conditions for the cold boundary are, at $z = 0$:

$$T(0) = T_0, \tag{5.98}$$

$$\epsilon_s(0) = Y_{s_0}, \quad s = 1, \ldots, n_S \tag{5.99}$$

where the mass flux fraction of the sth species is defined as

$$\epsilon_s = Y_s + \frac{\rho Y_s V_s}{\dot{M}}, \quad s = 1, \ldots, n_S. \tag{5.100}$$

The boundary condition at the hot boundary, at $z = L$, is

$$\frac{dT}{dz}(0) = 0, \tag{5.101}$$

$$\frac{dY_s}{dz}(L) = 0, \quad s = 1, \ldots, n_S. \tag{5.102}$$

The mass flow rate, or flamespeed, $\dot{M}$ is an eigenvalue of the system and determined as part of the solution. Thus, either an additional boundary condition is required or a degree of freedom must be removed. A common method is to fix the location of the flame. That is, an extra boundary condition specifies the temperature at an interior point in the domain:

$$T(z_{fix}) = T_{fix}, \tag{5.103}$$

where z_{fix} is a particular interior coordinate in the domain and T_{fix} is a given temperature. The pair (x_{fix}, T_{fix}) must be chosen so that the temperature and species gradients nearly vanish at the cold boundary. Otherwise, $\dot{M}$ will be too low due to heat loss through the cold boundary.

To solve this system and find the flamespeed, we used the software Cantera [27]. The steady state equations are discretized on a non-uniform mesh, in general. The numerical method is a damped modified Newton solver with internal time integration. Convergence of the solution depends on an initial guess of the species profiles, supplied by an equilibrium calculation using the initial temperature and pressure at the inlet. The source terms $\dot{x}$ are provided by the kinetics mechanism. This is described in an input file which contains the reactions and reaction rate coefficients. Thus, to include the stochastic operator as part of the kinetic mechanism, it was

necessary to map the linear operator to a set of reactions. This mapping is described in the following subsection.

5.3.3 Mapping the operator to typical reaction form

The flamespeed of the hydrogen flame was predicted using the case 1 operator. Recall that the operator is of the following form:

$$S = \begin{pmatrix} s_{1,1} & 0 & s_{1,3} & 0 & s_{1,5} & s_{1,6} & s_{1,7} & s_{1,8} \\ 0 & s_{2,2} & 0 & s_{2,4} & s_{2,5} & s_{2,6} & s_{2,7} & s_{2,8} \\ s_{3,1} & 0 & s_{3,3} & 0 & s_{3,5} & s_{3,6} & s_{3,7} & s_{3,8} \\ 0 & s_{4,2} & 0 & s_{4,4} & s_{4,5} & s_{4,6} & s_{4,7} & s_{4,8} \\ 0 & 0 & 0 & 0 & s_{5,5} & s_{5,6} & s_{5,7} & s_{5,8} \\ 0 & 0 & 0 & 0 & s_{6,5} & s_{6,6} & s_{6,7} & s_{6,8} \\ 0 & 0 & 0 & 0 & s_{7,5} & s_{7,6} & s_{7,7} & s_{7,8} \\ 0 & 0 & 0 & 0 & s_{8,5} & s_{8,6} & s_{8,7} & s_{8,8} \end{pmatrix}, \tag{5.104}$$

and $\hat{S} = L^{-1}SL$. Let $s_i = -\hat{s}_{i,i}$. From theorem 3.8.1, the operator reactions are:

$$\mathbb{X}_1 \xrightarrow{s_1} \frac{\hat{s}_{3,1}}{s_1}\mathbb{X}_3 \tag{5.105}$$

$$\mathbb{X}_2 \xrightarrow{s_2} \frac{\hat{s}_{4,2}}{s_2}\mathbb{X}_4 \tag{5.106}$$

$$\mathbb{X}_3 \xrightarrow{s_3} \frac{\hat{s}_{1,3}}{s_3}\mathbb{X}_1 \tag{5.107}$$

$$\mathbb{X}_4 \xrightarrow{s_4} \frac{\hat{s}_{2,4}}{s_4}\mathbb{X}_2 \tag{5.108}$$

$$\mathbb{X}_5 \xrightarrow{s_5} \frac{\hat{s}_{1,5}}{s_5}\mathbb{X}_1 + \frac{\hat{s}_{2,5}}{s_5}\mathbb{X}_2 + \frac{\hat{s}_{3,5}}{s_5}\mathbb{X}_3 + \frac{\hat{s}_{4,5}}{s_5}\mathbb{X}_4 + \frac{\hat{s}_{6,5}}{s_5}\mathbb{X}_6 + \frac{\hat{s}_{7,5}}{s_5}\mathbb{X}_7 + \frac{\hat{s}_{8,5}}{s_5}\mathbb{X}_8 \tag{5.109}$$

$$\mathbb{X}_6 \xrightarrow{s_6} \frac{\hat{s}_{1,6}}{s_6}\mathbb{X}_1 + \frac{\hat{s}_{2,6}}{s_6}\mathbb{X}_2 + \frac{\hat{s}_{3,6}}{s_6}\mathbb{X}_3 + \frac{\hat{s}_{4,6}}{s_6}\mathbb{X}_4 + \frac{\hat{s}_{5,6}}{s_6}\mathbb{X}_5 + \frac{\hat{s}_{7,6}}{s_6}\mathbb{X}_7 + \frac{\hat{s}_{8,6}}{s_6}\mathbb{X}_8 \tag{5.110}$$

$$\mathbb{X}_7 \xrightarrow{s_7} \frac{\hat{s}_{1,7}}{s_7}\mathbb{X}_1 + \frac{\hat{s}_{2,7}}{s_7}\mathbb{X}_2 + \frac{\hat{s}_{3,7}}{s_7}\mathbb{X}_3 + \frac{\hat{s}_{4,7}}{s_7}\mathbb{X}_4 + \frac{\hat{s}_{5,7}}{s_7}\mathbb{X}_5 + \frac{\hat{s}_{6,7}}{s_7}\mathbb{X}_6 + \frac{\hat{s}_{8,7}}{s_7}\mathbb{X}_8 \tag{5.111}$$

$$\mathbb{X}_8 \xrightarrow{s_8} \frac{\hat{s}_{1,8}}{s_8}\mathbb{X}_1 + \frac{\hat{s}_{2,8}}{s_8}\mathbb{X}_2 + \frac{\hat{s}_{3,8}}{s_8}\mathbb{X}_3 + \frac{\hat{s}_{4,8}}{s_8}\mathbb{X}_4 + \frac{\hat{s}_{5,8}}{s_8}\mathbb{X}_5 + \frac{\hat{s}_{6,8}}{s_8}\mathbb{X}_6 + \frac{\hat{s}_{7,8}}{s_8}\mathbb{X}_7. \tag{5.112}$$

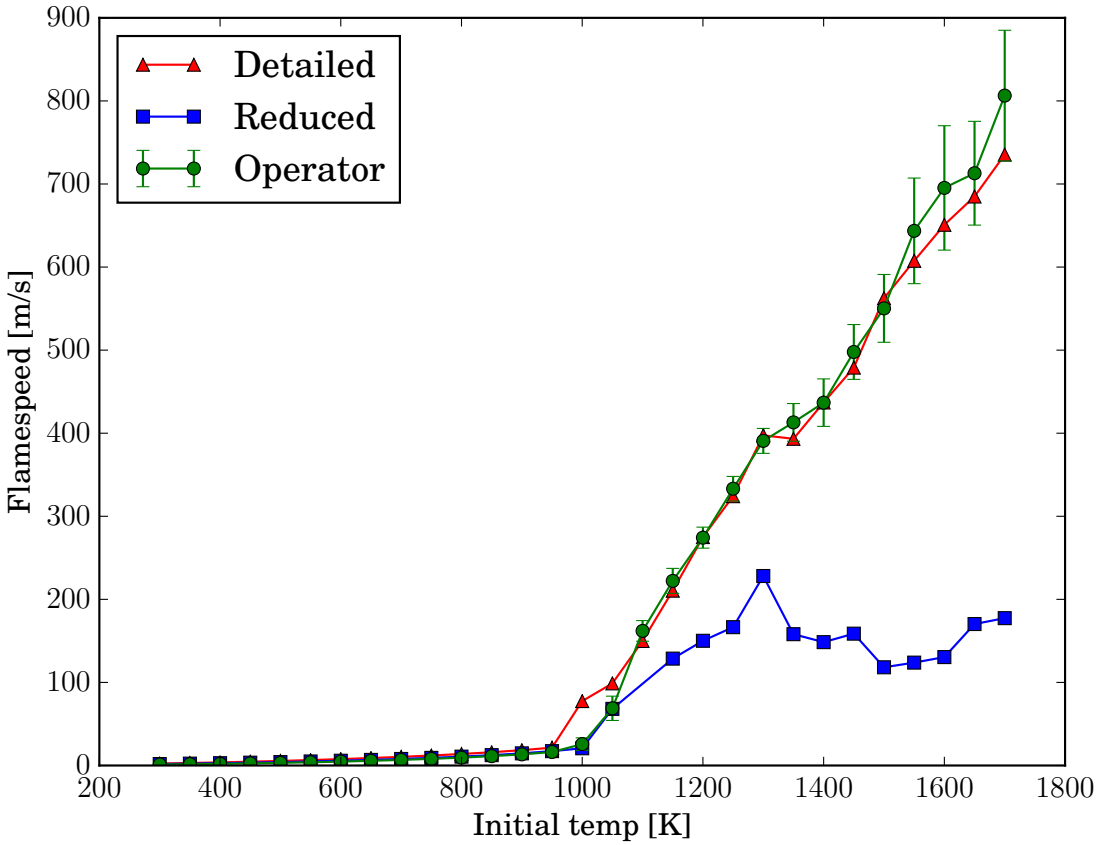

Figure 5.30: Flamespeed of the three models.

5.3.4 Results and analysis

Flamespeed of a 1D hydrogen laminar flame was predicted using the operator model $\mathcal{O}$. In figure 5.30, the flamespeed is shown for increasing values of initial temperature T_0. The operator model prediction is plotted with the mean value and one standard deviation. The reduced model is unusable for $T_0 \geq 1000\,\mathrm{K}$, while the inadequacy model is able to recover the bulk behavior displayed by the detailed model.

Moreover, the standard deviation in the predictions is around 10% of the true value. With this uncertainty, the data is covered by the operator predictions for $T_0 > 1000\,\mathrm{K}$. However, at that single point, the inadequacy representation is not sufficient to make the model consistent with the data. This defines the range of applicability for the operator model. Although it does not extend to all temperatures, it does work in a much wider range than just the scenario for which it was calibrated (1500 K). Presumably, making the inadequacy operator coefficients temperature-dependent would improve this further. This result shows the importance of including a representation of model inadequacy, especially when making predictions of unobserved quantities.

Chapter 6

Conclusions

This study addresses the critical problem of model inadequacy that affects nearly all mathematical models of physical systems. A new approach is developed that combines the flexibility and generality of a probabilistic model with the available deterministic physical information. In the context of predictive models, these two properties are essential: flexibility allows the model to be extended to new scenarios of interest, and respecting physical constraints ensures that the predictions will still be physically meaningful. This inadequacy representation is formulated as a stochastic operator, the bulk of which is described by a random matrix.

The stochastic operator was developed to account for the inadequacy of a reduced chemical mechanism. The mathematical model of a chemical mechanism is a set of ODEs which describe the time derivatives of the species' concentrations and temperature. The stochastic operator modifies these derivatives. Much of the structure of the operator is governed by physical constraints, while the parameteters in the operator are given as distributions whose hyperparameters are calibrated. This is done using data generated by the detailed chemical model. Calibration and validation of the various models relies on a Bayesian framework. In particular, the calibration of the operator model is performed using hierarchical Bayesian modeling

and Delayed Rejection Adaptive Metropolis, a type of Monte Carlo Markov Chain process.

The stochastic operator $\mathcal{S}$ contains three main components: 1) the random matrix S, 2) the nonlinear catchall reactions $\mathcal{A}$, and 3) the energy operator W. The random matrix S contains most of the information in $\mathcal{S}$ and has some interesting properties. Typically, the matrix has many identically zero entries. It always has a negative diagonal, is diagonally dominant, and has non-positive eigenvalues. The reactions in $\mathcal{A}$ allow any species in the reduced model to be the chemical product of the corresponding catchall species (if this is not already possible through S). Both S and $\mathcal{A}$ guarantee conservation of atoms and non-negativity of concentrations. Finally, the energy operator W modifies the time derivative of temperature by endowing the catchall species with thermodynamic properties.

This inadequacy formulation is tested on three major examples. The first is the hydrogen-oxygen reaction, the second is the methane-air reaction, and the third is the flame prediction problem.

The inadequacy operator for the hydrogen-oxygen reaction is first formulated by representing the missing species H_2O_2 exactly: the reduced state vector is augmented with the concentration of H_2O_2. This version of the operator is simpler, but also includes more information a priori, and it in fact performs well: the concentrations of the operator model $\mathcal{O}$ are consistent with the data supplied by the detailed model $\mathcal{D}$. The model output of temperature also matches the data for most points. However, reduced chemical mechansims often exclude many more species, and it is not tractable to account for all of them individually. To address this, catchall species

were introduced as a way to keep track of atoms that, in the detailed model, would exist in the missing species. The random matrix S had to be generalized to include the catchall species as did the energy operator W. Finally the catchall reactions had to be represented in the nonlinear operator $\mathcal{A}$ as discussed below. With the complete operator formulation and a broader calibration dataset, all observations are plausible outcomes of the operator model.

The second main example explored is the methane-air reaction. This is a highly complex reaction: it is more challenging but also more illuminating. After formulating the components S and W, there is an asymmetry problem: carbon atoms can enter the catchall C′ but then can never leave. Moreover, while hydrogen and oxygen atoms can move between H_2 and O_2 and the catchalls, this movement is more limited than implied by the detailed model. Because of this, the cathcall reactions are introduced through the nonlinear operator $\mathcal{A}$. These reactions allow for the catchall species to react with each other to produce any of the reduced model species. This provides a richer representation of the inadequacy.

The stochastic inadequacy operator is able to account for some of the inadequacy of the reduced methane reaction mechanism. The equilibrium concentrations improved and no observation is inconsistent with the operator model. However, there was a major problem that is out of the range of the inadequacy operator as currently formulated: some of the missing physics is highly temperature-dependent. Since there are no temperature-dependent parameters in the inadequacy representation, there is no way to model this behavior. This problem highlighted the importance of understanding the chemistry of the reduced and detailed models. In general, the

more physical (or chemical or biological) information one has about the models at hand, the better the inadequacy representation can be.

The final example problem investigated is the hydrogen laminar flame, which is a prediction problem based on data from the 0D reaction problems. This problem enriches the set of examples by providing a more complex physical problem. That is, the calibrated operator from the 0D reaction is used to describe the kinetics of the hydrogen-oxygen reaction in the flame problem. For the higher range of initial temperatures, the discrepancy between the reduced and detailed models was very large. But, the operator model is able to account for this discrepancy and recover the behavior of the detailed model. Moreover, data from flame calculations with the detailed mechanism are consistent with the calculated uncertainty in the predictions for a broad range of scenarios. Overall, this problem demonstrates the importance of including an inadequacy representation when making predictions with unreliable models.

There are many avenues for extending the work reported here. First, as demonstrated by the methane-air reaction, it appears to be critical to include more physical information into the inadequacy representation such as realistic temperature-dependence, and using stronger priors based on knowledge of the chemical reactions and the physical setup. This leads to the next major opportunity for future work: developing the connection between the stochastic operator and the actual chemistry. Mapping between the random matrix and the typical chemical reactions was a first step in this direction. However, a better understanding of what the stochastic operator means in physical terms is needed. This includes not just the structure, but

also the uncertainty in the calibrated parameters. A future goal is to infer something about the missing chemistry from the calibrated operator. This is important when developing mechanisms based on experimental data, when no detailed mechanism is available.

Another area for future work is to develop variations of the operator. For example, instead of using the random matrix S and the catchall reactions in $\mathcal{A}$, a simplified version is the following: given n_R species in the reduced model, include n_R reversible dissociation reactions where the reactant is one of the original species and the products are the corresponding catchall species. In the reverse combination reaction, the catchall atoms react to form any of the original species. In this fashion, the atoms of any species could move to any other species in two steps. This representation would lose information held in the current formulation; on the other hand, it would decrease the number of random variables and thus would be more tractable in more complex reactions. With a smaller number of additional reactions, the corresponding reaction rates could then be enriched with temperature-dependence.

Another variation could be a more complete set of nonlinear reactions. Instead of only allowing the nonlinear catchall reactions, one could augment the reduced model with all or some subset of all possible nonlinear terms. In contrast to the first variation, this would increase the number of random variables. A formulation like this might only be possible with more informative priors or knowledge about the chemical system.

Finally, it would be very interesting to apply this method to new problems. First, the inadequacy operator could be tested by a more realistic combustion problem.

It may be that doing so requires a more complete thermodynamic description of the catchall species. Another idea is to use the guiding principles of this work (respecting physical constraints, maintaining flexibility, starting with a linearized version) and developing an analogous operator (possibly random matrix) in a different physical context. Crossing into another domain could bring to light many new challenges and common strengths for the stochastic operator approach to representing model inadequacy.

Appendices

Appendix A

Chemical Mechanisms

The 21 reactions in the detailed hydrogen-oxygen mechanism are listed in table A.1 and the five of the reduced mechanism in A.2. The associated reaction rate is $k = AT^b e^{-E/R^\circ T}$.

Next, the four reactions of the reduced model for methane-air combustion are listed in table A.3. The detailed model includes over 300 reactions; for this, please refer to [52].

Reaction	A	b	E
Hydrogen-oxygen chain			
1. $H + O_2 \longrightarrow OH + O$	3.52×10^{16}	-0.7	71.4
2. $H_2 + O \longrightarrow OH + H$	5.06×10^{4}	2.7	26.3
3. $H_2 + OH \longrightarrow H_2O + H$	1.17×10^{9}	1.3	15.2
4. $H_2O + O \longrightarrow OH + OH$	7.60×10^{0}	3.8	53.4
Direct recombination			
5. $H + H + M \longrightarrow H_2 + M$	1.30×10^{18}	-1.0	0.0
6. $H + OH + M \longrightarrow H_2O + M$	4.00×10^{22}	-2.0	0.0
7. $O + O + M \longrightarrow O_2 + M$	6.17×10^{15}	-0.5	0.0
8. $H + O + M \longrightarrow OH + M$	4.71×10^{18}	-1.0	0.0
9. $O + OH + M \longrightarrow HO_2 + M$	8.00×10^{15}	0.0	0.0
Hydroperoxyl reactions			
10. $H + O_2 + M \longrightarrow HO_2 + M$	5.75×10^{19}	-1.4	0.0
11. $HO_2 + H \longrightarrow OH + OH$	7.08×10^{13}	0.0	1.2
12. $HO_2 + H \longrightarrow H_2 + O_2$	1.66×10^{13}	0.0	3.4
13. $HO_2 + H \longrightarrow H_2O + O$	3.10×10^{13}	0.0	7.2
14. $HO_2 + O \longrightarrow OH + O_2$	2.00×10^{13}	0.0	0.0
15. $HO_2 + OH \longrightarrow H_2O + O_2$	2.89×10^{13}	0.0	-2.1
Hydrogen peroxide reactions			
16. $OH + OH + M \longrightarrow H_2O_2 + M$	2.30×10^{18}	-0.9	-7.1
17. $HO_2 + HO_2 \longrightarrow H_2O_2 + O_2$	3.02×10^{12}	0.0	5.8
18. $H_2O_2 + H \longrightarrow HO_2 + H_2$	4.79×10^{13}	0.0	33.3
19. $H_2O_2 + H \longrightarrow H_2O + OH$	1.00×10^{13}	0.0	15.0
20. $H_2O_2 + OH \longrightarrow H_2O + HO_2$	7.08×10^{12}	0.0	6.0
21. $H_2O_2 + O \longrightarrow HO_2 + OH$	9.63×10^{6}	2.0	2.0

Units: mol, cm, s, kJ, K.

Table A.1: The detailed H_2/O_2 reaction mechanism from [62].

Reaction	A	b	E
Hydrogen-oxygen chain			
1. $H + O_2 \longrightarrow OH + O$	3.52×10^{16}	-0.7	71.4
2. $H_2 + O \longrightarrow OH + H$	5.06×10^{4}	2.7	26.3
3. $H_2 + OH \longrightarrow H_2O + H$	1.17×10^{9}	1.3	15.2
Hydroperoxyl reactions			
10. $H + O_2 + M \longrightarrow HO_2 + M$	5.75×10^{19}	-1.4	0.0
12b. $H_2 + O_2 \longrightarrow HO_2 + H$	1.4×10^{14}	0.0	249.5

Units: mol, cm, s, kJ, K.

Table A.2: The reduced H_2/O_2 reaction mechanism from [62].

Reaction	A	b	E
1. $2\,CH_4 + O_2 \longrightarrow 2\,CO + 4\,H_2$	4.4×10^{11}	0	30,000
2. $CH_4 + H_2O \longrightarrow CO + 3\,H_2$	3.0×10^{8}	0	30,000
3. $2\,H_2 + O_2 \rightleftharpoons H_2O$	6.8×10^{15}	-1	40,000
4. $CO + H_2O \rightleftharpoons CO_2 + H_2$	2.75×10^{9}	0	20,000

Units: kmol, m, s, cal, K.

Table A.3: The reduced CH_4/air reaction mechanism from [34].

Bibliography

[1] A New Templated Implementation of Chemistry Hydrodynamics (Antioch). https://github.com/libantioch/antioch. (pages 17, 18).

[2] Cantera User's Guide. http://www.cerfacs.fr/cantera/mechanisms/meth.php. (page 97).

[3] MIT Uncertainty Quantification Library (MUQ). https://bitbucket.org/mituq/muq. (page 58).

[4] J. Andersen, C. L. Rasmussen, T. Giselsson, and P. Glarborg. Global Combustion Mechanisms for Use in CFD Modeling under Oxy-Fuel Conditions. *Energy Fuels*, 23(3):1379–1389, Mar. 2009. (page 99).

[5] I. Babuska, F. Nobile, and R. Tempone. A systematic approach to model validation based on Bayesian updates and prediction related rejection criteria. *Computer Methods in Applied Mechanics and Engineering*, 197:2517–2539, May 2008. (page 1).

[6] M. J. Bayarri, J. O. Berger, R. Paulo, J. Sacks, J. A. Cafeo, J. Cavendish, C.-H. Lin, and J. Tu. A framework for validation of computer models. *Technometrics*, 49(2):138–154, May 2007. (pages 1, 3).

[7] H. E. Bell. Gershgorin's theorem and the zeros of polynomials. *American Mathematical Monthly*, 72:292–295, 1965. (page 37).

[8] M. L. Berliner. Hierarchical Bayesian time series models. In K. M. Hanson and R. N. Silver, editors, *Maximum Entropy and Bayesian Methods*, volume 79 of *Fundamental Theories of Physics*, pages 15–22. Springer Netherlands, 1996. (pages 5, 54).

[9] C. E. Bonferroni. Il calcolo delle assicurazioni su gruppi di teste. In *Studi in Onore del Professore Salvatore Ortu Carboni*, pages 13–60. Rome, 1935. (page 61).

[10] G. E. P. Box and G. C. Tiao. *Bayesian Inference in Statistical Analysis*. Wiley-Interscience, 1 edition, Apr. 1992. (page 60).

[11] M. P. Burke, M. Chaos, Y. Ju, F. L. Dryer, and S. J. Klippenstein. Comprehensive H2/O2 kinetic model for high-pressure combustion. *International Journal of Chemical Kinetics*, 44(7):444–474, Dec. 2011. (page 3).

[12] M. P. Burke, M. Chaos, Y. Ju, F. L. Dryer, and S. J. Klippenstein. Comprehensive H2/O2 kinetic model for high-pressure combustion. *International Journal of Chemical Kinetics*, 44(7):444–474, July 2012. (pages 3, 4).

[13] D. Calvetti and E. Somersalo. An Introduction to Bayesian Scientific Computing: Ten Lectures on Subjective Computing, 2007. (pages 3, 45).

[14] Center for Predictive Engineering and Computational Sciences. *Quantification of Uncertainty for Estimation, Simulation, and Optimization (QUESO) User's Manual*, 2013. (pages 58, 74).

[15] M. O. Conaire, H. J. Curran, J. M. Simmie, W. J. Pitz, and C. K. Westbrook. A comprehensive modeling study of hydrogen oxidation. *International Journal of Chemical Kinetics*, 36(11):603–622, Nov. 2004. (page 3).

[16] M. K. Cowles and B. P. Carlin. Markov chain Monte Carlo convergence diagnostics: A comparative review. *American Statistical Association*, 91(434):883–904, June 1996. (pages 46, 54).

[17] M. H. DeGroot and M. J. Schervish. *Probability and Statistics (4th Edition)*. Pearson, 4 edition, Jan. 2011. (page 57).

[18] A. Edelman and N. R. Rao. Random matrix theory. *Acta Numerica*, 14(-1):233–297, May 2005. (page 5).

[19] R. Ennetta, M. Hamdi, and R. Said. Comparison of different chemical kinetic mechanisms of methane combustion in an internal combustion engine configuration. *Thermal Science*, 12(1):43–51, 2008. (page 97).

[20] M. Feinberg. Lectures on Chemical Reaction Networks. 1979. (page 26).

[21] A. Frassoldati, A. Cuoci, T. Faravelli, E. Ranzi, C. Candusso, and D. Tolazzi. Simplified kinetic schemes for oxy-fuel combustion. In *1st International Conference on Sustainable Fossil Fuels for Future Energy*, 2009. (page 99).

[22] M. Galassi, J. Davies, J. Theiler, B. Gough, G. Jungman, P. Alken, M. Booth, and F. Rossi. *GNU Scientific Library Reference Manual*, third edition. (page 19).

[23] A. Gelman. Exploratory Data Analysis for Complex Models. *Journal of Computational and Graphical Statistics*, 13(4):755–779, Dec. 2004. (page 61).

[24] A. Gelman, X.-l. Meng, and H. Stern. Posterior predictive assessment of model fitness via realized discrepancies. In *Statistica Sinica*, pages 733–807, 1996. (pages 6, 59).

[25] W. R. Gilks, S. Richardson, and D. Spiegelhalter. *Markov Chain Monte Carlo in Practice*. Chapman and Hall/CRC, softcover reprint of the original 1st ed. 1996 edition, Dec. 1996. (pages 46, 54).

[26] P. Glarborg, M. U. Alzueta, K. Dam-Johansen, and J. A. Miller. Kinetic Modeling of Hydrocarbon/Nitric Oxide Interactions in a Flow Reactor. *Combustion and Flame*, 115(1-2):1–27, Oct. 1998. (page 84).

[27] D. G. Goodwin, H. K. Moffat, and R. L. Speth. Cantera: An Object-oriented Software Toolkit for Chemical Kinetics, Thermodynamics, and Transport Processes. http://www.cantera.org, 2015. Version 2.2.0. (pages 19, 118).

[28] P. J. Green and A. Mira. Delayed rejection in reversible jump Metropolis-Hastings. *Biometrika*, 88(4):1035–1053, Dec. 2001. (page 48).

[29] H. Haario, M. Laine, A. Mira, and E. Saksman. DRAM: Efficient adaptive MCMC. *Statistics and Computing*, 16(4):339–354, Dec. 2006. (pages 46, 48, 54, 58, 74).

[30] H. Haario, E. Saksman, and J. Tamminen. An adaptive Metropolis algorithm. *Bernoulli*, 7(2):223–242, 2001. (page 48).

[31] D. Higdon, J. Gattiker, B. Williams, and M. Rightley. Computer model calibration using high-dimensional output. *Journal of the American Statistical Association*, 103(482):570–583, June 2008. (page 3).

[32] D. Higdon, M. Kennedy, J. C. Cavendish, J. A. Cafeo, and R. D. Ryne. Combining field data and computer simulations for calibration and prediction. *SIAM Journal on Scientific Computing*, 26(2):448–466, Jan. 2004. (page 3).

[33] E. T. Jaynes. *Probability Theory: The Logic of Science*. Cambridge University Press, 2003. (pages 2, 3).

[34] W. P. Jones and R. P. Lindstedt. Global reaction schemes for hydrocarbon combustion. *Combustion and Flame*, 73(3):233–249, Sept. 1988. (pages 96, 131).

[35] M. C. Kennedy and A. O'Hagan. Bayesian calibration of computer models. *Journal of the Royal Statistical Society: Series B (Statistical Methodology)*, 63(3):425–464, Jan. 2001. (page 3).

[36] A. A. Konnov. Remaining uncertainties in the kinetic mechanism of hydrogen combustion. *Combustion and Flame*, 152(4):507–528, Mar. 2008. (page 2).

[37] X. Lu and T. Wang. Water-gas shift modeling of coal gasification in an entrained-flow gasifier. In *Proceedings of the 28th International Coal Conference*, Sept. 2011. Paper 45-1. (page 99).

[38] D. Lunn, A. Thomas, N. Best, and D. Spiegelhalter. WinBUGS - A Bayesian modelling framework: Concepts, structure, and extensibility. 10(4):325–337, 2000. (page 58).

[39] O. A. Marzouk and E. D. Huckaby. A Comparative Study of Eight Finite-Rate Chemistry Kinetics for Co/H2 Combustion. *Engineering Applications of Computational Fluid Mechanics*, 4(3):331–356, Jan. 2010. (page 97).

[40] B. J. McBride, S. Gordon, and M. A. Reno. NASA Technical Memorandum 4513: Coefficients for Calculating Thermodynamic and Transport Properties of Individual Species. Technical report, National Aeronautics and Space Administration, 1993. (pages 16, 40).

[41] M. L. Mehta. *Random Matrices, Volume 142, Third Edition (Pure and Applied Mathematics)*. Academic Press, 3 edition, Nov. 2004. (page 5).

[42] K. Miki, S. H. Cheung, E. E. Prudencio, and P. L. Varghese. Bayesian uncertainty quantification of recent shock tube determinations of the rate coefficient of reaction H + O2 OH + O. *International Journal of Chemical Kinetics*, 44(9):586–597, July 2012. (page 2).

[43] R. G. Miller. *Simultaneous Statistical Inference (Springer Series in Statistics)*. Springer, 2nd edition, Mar. 1981. (page 61).

[44] A. Mira. On Metropolis-Hastings algorithms with delayed rejection. *Metron*, 59:3–4, 2001. (page 48).

[45] R. Moser, G. Terejanu, T. A. Oliver, and C. S. Simmons. Validating the prediction of unobserved quantities. Technical report, The Institute for Computational Sciences and Engineering, 2012. (page 1).

[46] M. A. Mueller, T. J. Kim, R. A. Yetter, and F. L. Dryer. Flow reactor studies and kinetic modeling of the H2/O2 reaction. *Int. J. Chem. Kinet.*, 31(2):113–125, Jan. 1999. (page 3).

[47] T. A. Oliver, G. Terejanu, C. S. Simmons, and R. D. Moser. Validating predictions of unobserved quantities. *Elsevier*, submitted. (pages 2, 60, 61).

[48] E. Prudencio and K. Schulz. The Parallel C++ Statistical Library 'QUESO': Quantification of Uncertainty for Estimation, Simulation and Optimization. In M. Alexander, P. D'Ambra, A. Belloum, G. Bosilca, M. Cannataro, M. Danelutto, B. Di Martino, M. Gerndt, E. Jeannot, R. Namyst, J. Roman, S. Scott, J. Traff, G. Vallée, and J. Weidendorfer, editors, *Euro-Par 2011: Parallel Processing Workshops*, volume 7155 of *Lecture Notes in Computer Science*, pages 398–407. Springer Berlin Heidelberg, 2012. (pages 58, 74).

[49] D. B. Rubin. More powerful randomization-based p-values in double-blind trials with non-compliance. *Statist. Med.*, 17(3):371–385, Feb. 1998. (pages 6, 59).

[50] A. Silaen and T. Wang. Comparison of instantaneous, equilibrium, and finite-rate gasification models in an entrained-flow coal gasifier. In *Proceedings of the 26th International Coal Conference*, 2009. (page 99).

[51] D. S. Sivia and J. Skilling. *Data Analysis: A Bayesian Tutorial*. Oxford University Press, 2006. (pages 3, 45).

[52] G. P. Smith, D. M. Golden, M. Frenklach, N. W. Moriarty, B. Eiteneer, M. Goldenberg, C. T. Bowman, R. K. Hanson, S. Song, W. C. Gardiner, V. V. Lissianski, and Q. Zhiwei. GRI-Mech. `http://www.me.berkeley.edu/gri_mech/`. Accessed: 2015-01-15. (pages 2, 18, 96, 129).

[53] C. Soize. Random matrix theory for modeling uncertainties in computational mechanics. *Computer Methods in Applied Mechanics and Engineering*, 194(12-16):1333–1366, Apr. 2005. (page 5).

[54] C. Soize. Generalized probabilistic approach of uncertainties in computational dynamics using random matrices and polynomial chaos decompositions. *Int. J. Numer. Meth. Engng.*, 81(8):939–970, Feb. 2010. (page 5).

[55] J. I. Steinfeld, J. S. Francisco, and W. L. Hase. *Chemical Kinetics and Dynamics*. Prentice Hall, 1998. (pages 2, 7).

[56] L. P. Swiler. Gaussian processes in response surface modeling. Society of Experimental Mechanics Meeting, Jan. 2006. (page 3).

[57] L. Wang, Z. Liu, S. Chen, and C. Zheng. Comparison of Different Global Combustion Mechanisms Under Hot and Diluted Oxidation Conditions. *Combustion Science and Technology*, 184(2):259–276, Feb. 2012. (page 97).

[58] T. Wang, X. Lu, H.-W. Hsu, and C.-H. Shen. Investigation of the performance of a syngas quench cooling design in a downdraft entrained-flow gasifier. In *Proceedings of the 28th International Coal Conference*, 2011. Paper 45-2. (page 99).

[59] P. R. Westmoreland. Reduced kinetic mechanisms for applications in combustion systems. Edited by N. Peters and B. Rogg, Spring-Verlag, New York, Lecture Notes in Physics, Monograph 15, 1993, 360 pp. *AIChE J.*, 40(11):1926–1927, Nov. 1994. (pages 2, 4).

[60] C. K. Wikle, R. F. Milliff, D. Nychka, and L. M. Berliner. Spatiotemporal hierarchical Bayesian modeling: Tropical ocean surface winds. *Journal of the American Statistical Association*, 96(454):382–397, June 2001. (page 54).

[61] F. A. Williams. *Combustion Theory: Second Edition (Combustion Science and Engineering)*. Westview Press, second edition edition, Mar. 1994. (pages 2, 7).

[62] F. A. Williams. Detailed and reduced chemistry for hydrogen autoignition. *Journal of Loss Prevention in the Process Industries*, 21(2):131–135, Mar. 2008. (pages 4, 62, 64, 130, 131).

Vita

Rebecca Morrison was born in San Luis Obispo, California and there attended Mission College Prep High School.

In 2004, Rebecca moved to Claremont, CA to attend Scripps College. There she studied physics, math, and a few languages. She spent several summers doing research: at the Keck Joint Science center in Claremont; at an REU for physics at UC Davis; and at an international math program in Fortaleza, Brazil. She also studied abroad in Seville, Spain. In 2008 she completed her Bachelor's degree in physics with a minor in mathematics. Her thesis, written under Dr. Adam Landsberg, was titled "Combinatorial Games With a Pass: A Geometric Approach."

In 2009 Rebecca started the graduate program at ICES, the Institute for Computational Engineering and Sciences, at the University of Texas at Austin. She worked with Dr. Serge Prudhomme until 2012 and then with Dr. Robert Moser on topics in uncertainty quantification including model uncertainty and inadequacy, Bayesian methods for high-dimensional inverse problems, and reduced-order stochastic modeling. In the spring of 2012 Rebecca received a Master's degree in Computational and Applied Mathematics, and that summer she interned at Sandia National Laboratories in Albuquerque, New Mexico.

Permanent address: `rebeccae.morrison@gmail.com`

This dissertation was typeset with LaTeX[†] by the author.

[†]LaTeX is a document preparation system developed by Leslie Lamport as a special version of Donald Knuth's TeX Program.